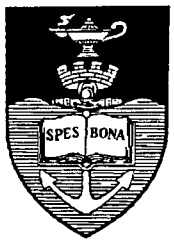

Department of Surveying and Geodetic Engineering.

University of Cape Town.

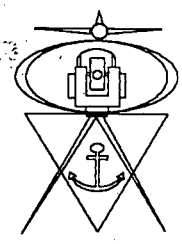

The Development of a Non-Contact Co-ordinate Measurement Machine.

Dirk Hamish Craigie, B.Sc. (Survey), Cape Town

June 1996

Submitted to the University of Cape Town

in fulfilment for the degree of Master of Science in Engineering

Declaration :

I Dirk Craigie, submit this thesis in fulfilment of the requirements for the degree of Master of Science in Engineering. I affirm that this is my original work and that it has not been submitted in this or similar form for a degree at any University.

Synopsis

The Department of Surveying and Geodetic Engineering at the University of Cape Town, in conjunction with the Department of Mechanical Engineering at the University of Cape Town have developed a non-contact co-ordinate measurement machine in a project called *MILLMAP*. The project had the following objectives :

1. To determine unique surface co-ordinates for continuous, complex objects with sub-millimetre accuracy.
2. The representation of the co-ordinates was to be in a format that could be utilised by a computer numerically controlled (CNC) milling machine in a computer aided design/ computer aided manufacture (CADCAM) environment.
3. The device had to use a non-contact method for data capture.

The *MILLMAP* project was undertaken because there is a demand for co-ordinate measurement machines in industry for the inspection of objects for quality control purposes. Conventional Co-ordinate Measurement Machines (CMMs) are expensive and use a contact probe to measure the object. The contact probe measurement technique is unsuitable for the measurement of non-rigid objects such as shoes and automobile seat padding. The *MILLMAP* system provides a non-contact measurement technique that can be applied to non-rigid as well as rigid objects. Additional applications in the archaeological field exist for the non-contact measurement of sensitive, historical artefacts.

A digital photogrammetric system was developed to measure the position of a laser dot projected onto the surface of the measurement object. This measurement system satisfied the criteria of a non-contact measurement method required for the project. The system utilised three digital CCD cameras to capture images of the laser dot projected onto the object. Image processing software, developed from existing software within the Department of Surveying and Geodetic Engineering, was used to photogrammetrically determine the co-ordinates of the laser dot to sub-millimetre accuracy on the surface of the object.

A mechanical device was designed and constructed by the Department of Mechanical Engineering in order to move the laser over the surface of the object, and to rotate the object. The entire surface of the object could be measured by the system using these operations.

The measured co-ordinates obtained from the device are oriented with respect to each other and plotted in *AutoCad (version 12)* to produce a three dimensional mesh representing the surface of the measured object. The mesh is in a format that can be directly utilised by Computer Numerically Controlled (CNC) milling machine in a Computer Aided Design/Computer Aided Manufacturing (CADCAM) environment.

Standardisation tests were made using a prototype device to evaluate the performance of the *MILLMAP* system. It was found that the initial results and measurement of test objects fell short of the sub-millimetre accuracy requirements specified for the project. A hypothesis explaining the poor accuracy achieved by the photogrammetric system was proposed and evaluated. Based on the results of simulation tests, it was recommended that normal case image geometry be maintained between the cameras. In addition, sub-pixel determination of the centre of the target on the reference image would also improve the accuracy of the system. It was anticipated that the *MILLMAP* system would be capable of providing sub-millimetre accuracy in measured co-ordinates based on the simulation test results which yielded RMS values of x=0.17mm y=0.18mm and z=0.42mm for the measured co-ordinates.

The conclusions for the project state that the *MILLMAP* system is an inexpensive, non-contact co-ordinate measurement machine capable of providing sub-millimetre accuracy for the measurement of non-rigid objects. The conclusions indicate that the objectives of the project were satisfied.

The recommendations for the project state that normal case image geometry is essential for the system to provide sub-millimetre accuracy in the measured co-ordinates. The use of sub-pixel accuracy for the determination of the target point centre is another critical factor required for sub-millimetre co-ordinate accuracy. The limitations of the system regarding the complexity of object topography, lighting conditions and surface reflection 'noise' are recommended as characteristics that require further investigation.

The need for automation in defining the edges of discontinuous objects is emphasised and the possibility of fully automatic calibration of the measurement system in an industrial environment are proposed.

Acknowledgements

I am grateful to my supervisor Professor Heinz Rüther for his support and advice throughout this project. The time he afforded me to discuss problems, and his encouragement were greatly appreciated. I am especially indebted to him for reviewing this thesis dissertation.

I wish to thank Julian Smit for all the advice and knowledge he shared with me for the duration of the project.

To Prakash Parbhoo from the Department of Mechanical Engineering at U.C.T., for the long hours he spent developing the mechanical device for the project.

Thanks must also be extended to the staff of the Department of Surveying and Geodetic Engineering at U.C.T. : Dr. Scott Mason, Val Atkinson, Sue Binedell, Michael Haywood and Sidney Smith.

To my fellow post-graduate students in the Department of Surveying : Pierre, Henty, Malcom, Ulrike, Justin, Simon and Siddique, thanks for your help and companionship.

I wish to thank to my parents, without whose love and support I would not have come this far.

Finally I wish to thank my girlfriend Frances for her love and commitment over the last four years. Her support and encouragement were unfailing an served as a major inspiration for my work.

Table of Contents

List of Illustrations

List of Tables

Chapter One

Introduction

In March 1995 the Department of Mechanical Engineering at the University of Cape Town (U.C.T) approached the Department of Surveying and Geodetic Engineering (U.C.T.) for assistance with the development of a non-contact co-ordinate measuring machine. The task was to be undertaken as a joint project between the two departments. The objectives of the project were:

1. To determine unique surface co-ordinates for continuous, complex objects with sub-millimetre accuracy.
2. The representation of the co-ordinates was to be in a format that could be utilised by a computer numerically controlled (CNC) milling machine in a computer aided design/ computer aided manufacture (CADCAM) environment.
3. The device had to use a non-contact method for data capture.

A continuous, complex object is described by *Duncan and Mair (1983:p.vii)* as :

> *"those surface shapes which cannot continuously be generated and have the arbitrary or complex character of forms traditionally modelled by sculptors".*

Examples of such objects are shoes, medical prosthesis, propeller blades and streamlined body work (as found in the automobile and aerospace industry). The need to measure such objects with precision by manufacturers forms an important part of quality control in the manufacturing process.

Conventional co-ordinate measurement machines (CMM) are mechanical devices which probe the surface of the object to be measured. The cost of such devices at present, is of the order R 300 000 and the time taken to measure all the necessary points is dependent upon the speed of the machine in moving the measurement probe over the surface of the measurement object.

A unique feature of the device developed, in contrast to conventional CMMs, was the non-contact method of data capture. This was specified in order that non-rigid (i.e soft or brittle) objects could be measured by the device as well as rigid objects. The ability to measure non-rigid objects gave the system the capability to measuring objects made of plastic, foam rubber, upholstery or thin sheet metal. Objects made from these materials would deform if measured with a contact probe.

Another area in which a non-contact co-ordinate measurement machine can be applied is in the measurement of archaeological artefacts. There is a scientific need for accurate dimensional data of such artefacts for research and the archaeological record. The fragile nature of archaeological artefacts requires that the object be measured without contact to ensure preservation of the artefact in its current condition.

The Department of Surveying and Geodetic Engineering, has a well established Digital Photogrammetry Group (DPG), and elected to use the project as part of ongoing research into the industrial applications of Digital Photogrammetry. A digital photogrammetric measurement system was proposed to satisfy the criteria of a non-contact measurement method. The photogrammetric system had to be capable of measuring the position of a laser dot on the surface of the object, with sub-millimetre accuracy. The system was operate with three cameras (a minimum of two cameras would be needed to solve the photogrammetric problem, the third camera yielded a redundancy for checking purposes).

The Department of Mechanical Engineering was responsible for the development of the mechanical components of the device and data manipulation within a CAD environment. *Parbhoo (1995)* describes this aspect of the project in detail.

The mechanical components of the device comprised of a Laser motion system and an Object positioning system. The Laser motion system positioned the laser at various prespecified points via two orthogonal axes. This arrangement enabled a grid of points to be mapped sequentially on the surface of the object (see ***Figure 1.1*** p.3). In order to map the entire surface of the object it was necessary to rotate the object. This aspect was controlled by the Object positioning system (see ***Figure 1.2*** p 3).

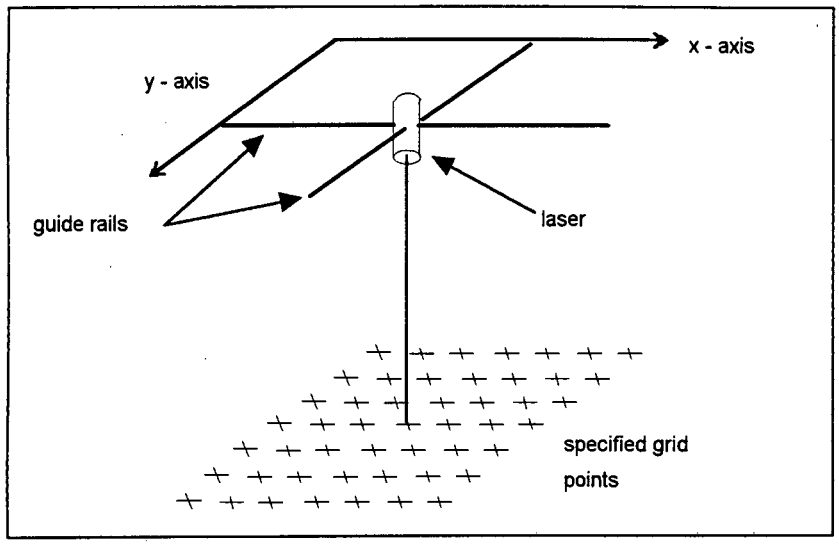

Figure 1.1 - Operation principle of the Laser motion system

By moving the laser along the x and y -axes at specified intervals a grid of specified dimensions is covered by the laser.

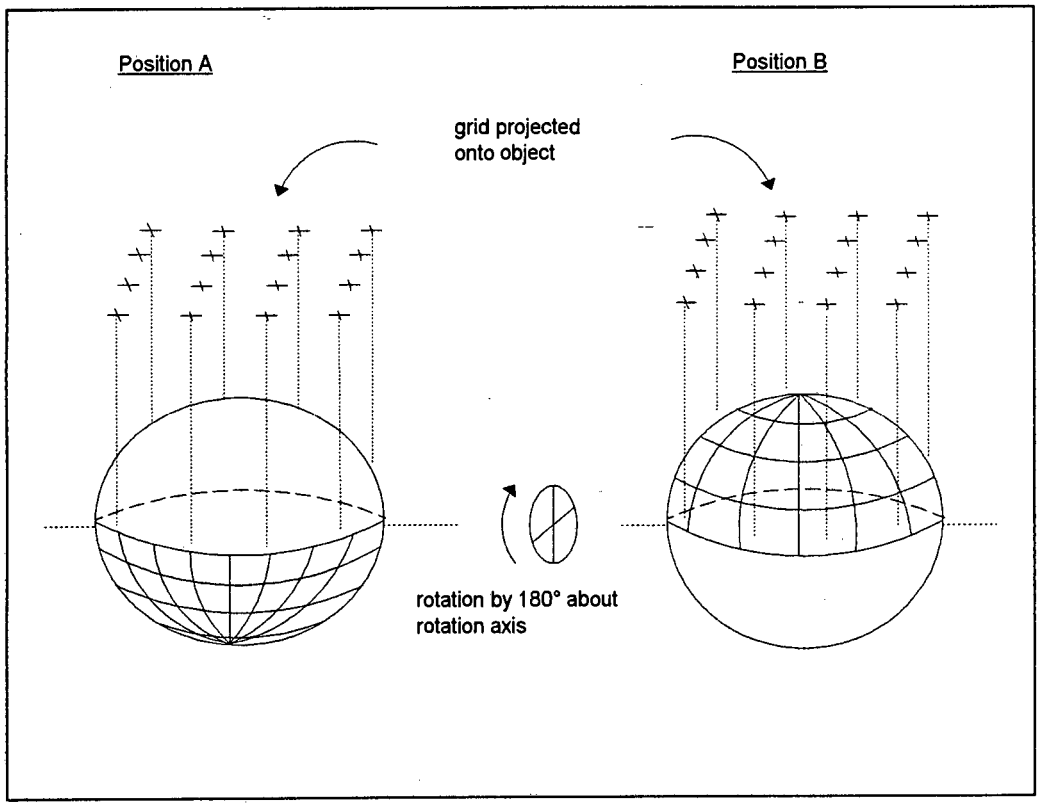

Figure 1.2 - Operation principle of the Object positioning system

By rotating the object about a rotation axis the shaded area can be moved to a position where it can be grid mapped by the laser motion system. The Rotation angle is dependent upon the shape of the object.

The software used for the measurement system was adapted from existing image processing software written within the DPG. The image processing software was developed from the *DIMS* package © *G van der Vlught (1992).* The *PHOTONET (version 2.0)* bundle solution program © *G van der Vlught (1994)* was used to calibrate the cameras. The image processing routines used

in the *DIMS* software operated in a static post processing environment. In order to process the data from the photogrammetric measurement system these routines were modified to operate in a the dynamic measurement environment. Based on previous experience within the DPG it was predicted that the existing software would be capable of meeting the sub-millimetre accuracy requirements for the project.

The output of the non-contact measurement system was a set of three dimensional cartesian co-ordinates (XYZ), which were cross referenced to the position of the object (obtained from the mechanical device). Knowledge of the sequence in which the co-ordinates were measured, and their relationship to the position of the object, enabled a three dimensional mesh describing the surface of the object to be constructed in *AutoCad* (see ***Figure 1.3*** p.4). The *AutoCad* mesh is in a format that can be used in a CADCAM environment to generate the control program for a CNC milling machine to duplicate the measured object.

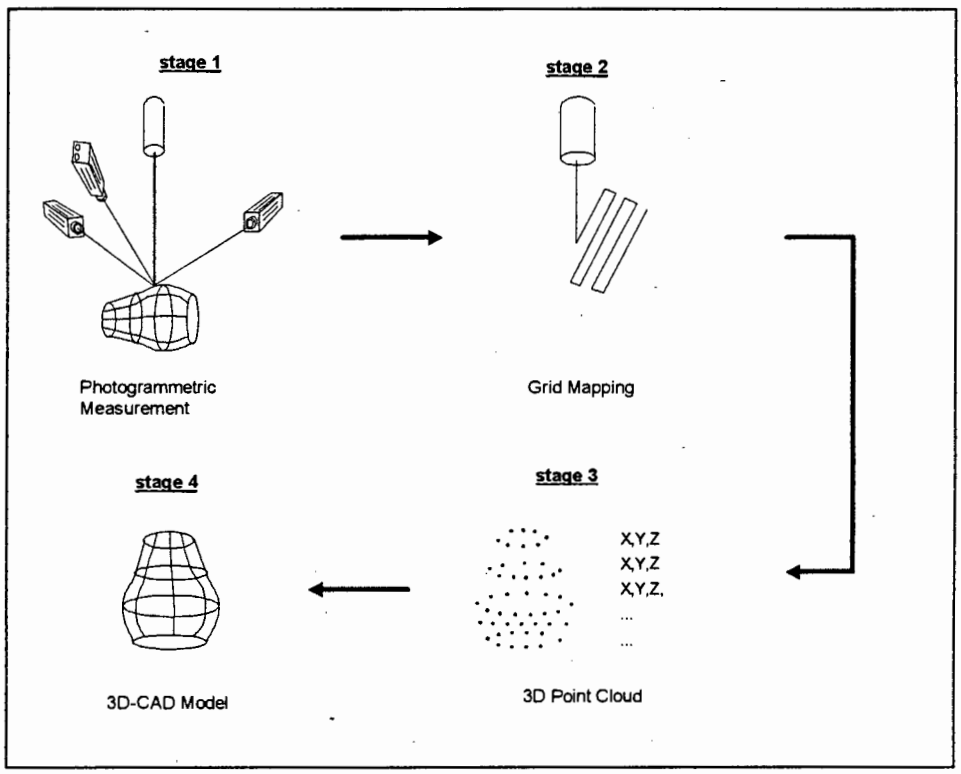

Figure 1.3 - Development sequence of CAD model

Stage 1 of the sequence involves the photogrammetric measurement of the laser dot on the objects surface. Stage 2 moves the laser to a new position and the measurement process is repeated. In this manner the surface is grid mapped. The object is rotated as necessary so that the entire surface can be mapped. This results in a 3D point cloud of XYZ co-ordinates as shown in Stage 3 . By using the sequence of co-ordinate capture the point cloud can be used to create a 3D meshed CAD model as shown in Stage 4.

The entire co-ordinate measurement machine, named *MILLMAP* , consisted of the following components :

A non-contact Measurement system:

The function of this component was to photgrammetrically determine three dimensional co-ordinates for points defined by the laser dot on the objects surface. The measurement system had the following sub-components :

- Three digital photogrammetric cameras.
- One dedicated PC for photogrammetric control.
- Image processing and camera control software.
- A laser projector.

A Motion control system:

The function of this component was to position the laser at prespecified grid points across the surface of the object. The system was also used to control the motion of the object, with respect to rotation, to enable the entire surface to be mapped. The motion control system had the following sub-components :

- Laser motion system (see ***Figure 1.1***, p 3.).
- Object positioning system (see ***Figure 1.2***, p.3).
- One dedicated PC for motion control and final co-ordinate storage.
- Software for the control of all motion systems.

Additional system components :

The photogrammetric control P.C and the motion control P.C. were to control their respective sub-components based upon the status of each component. This required that a communication link between the two computer be established. Additional software to automatically generate the final three dimensional *AutoCad* mesh was also required.

Dissertation outline

Chapter two of this dissertation introduces the principles of photogrammetry. The *MILLMAP* system uses a digital photogrammetric system in order to measure projected laser dots on the surface of the measurement object. The fundamentals of photogrammetry are discussed in order to assist the reader in understanding the measurement procedure.

Chapter three describes the characteristics of co-ordinate measurement. Co-ordinate systems used throughout the dissertation are explained for the benefit of the reader. An introduction to conventional co-ordinate measurement machines and the aspects of numerical control for these devices is presented. CADCAM systems and their advantages over conventional computer numerically controlled (CNC) machines are discussed in the final section of Chapter two.

Chapter four reviews various specialised measurement devices. This section contains the majority of the literature reviewed by the author. Triangulation, structured light techniques and non-photogrammetric techniques are examined.

A detailed description of the methods used for the *MILLMAP* project are presented in Chapter five.

Chapter six examines the software and hardware components of the *MILLMAP* project.

The testing procedure and results attained with the prototype *MILLMAP* device are presented and analysed in Chapter seven. a hypothesis to explain the initial poor results is suggested, tested by simulation and incorporated into the *MILLMAP* system.

Chapter eight draws together the conclusions for the *MILLMAP* project.

Chapter nine reviews the limitations of the prototype device and proposes recommendations for the project. These recommendations are based on experience gained by the author during the construction and testing stages of the project.

Chapter two

Principles of Photogrammetry.

The *MILLMAP* system uses digital photogrammetric techniques during the measurement process. Several digital photogrammetric techniques will be presented in this chapter along with the principles of photogrammetry in order to clarify terminology that will be used throughout this dissertation in describing the *MILLMAP* system. The primary objective of Photogrammetry is to solve the general photogrammetric problem as defined by *McGlone (1989 : p.37) :*

> *"The general photogrammetric problem can be seen as the determination of the camera interior and exterior orientation parameters and the co-ordinates of object space points of interest."*

The process of determining the orientation parameters for cameras in a photogrammetric system is referred to as CALIBRATION. Examining the definition above it is apparent that there are two types of orientation associated with the calibration of a photogrammetric system :

- Interior orientation, and
- Exterior orientation.

The concepts associated with these two components will be discussed in sections 2.2 and 2.3 respectively. Prior to that the principles of image geometry will be presented in section 2.1. Section 2.4 introduces the concepts of digital photogrammetry and some of the image processing techniques used by the *MILLMAP* system. Digital photogrammetry makes use of extensive mathematical modelling in order to solve the calibration problem. The equations used for this modelling and measurement solution will be presented in section 2.5.

2.1 Principles of Image Geometry

A perspective projection can be interpreted as a bundle of light rays which pass through a single point known as the perspective centre. This situation models the characteristics of the camera/ lens component of a photogrammetry system. The film (or in the case of a digital camera - the light sensitive chip) acts as the reference plane on which the image is formed. The focal point of the lens is the perspective centre (the situation is illustrated in ***Figure 2. 1*** p.8). The area between the perspective centre and the image plane is called the image space). The object space is the region in which the object resides.

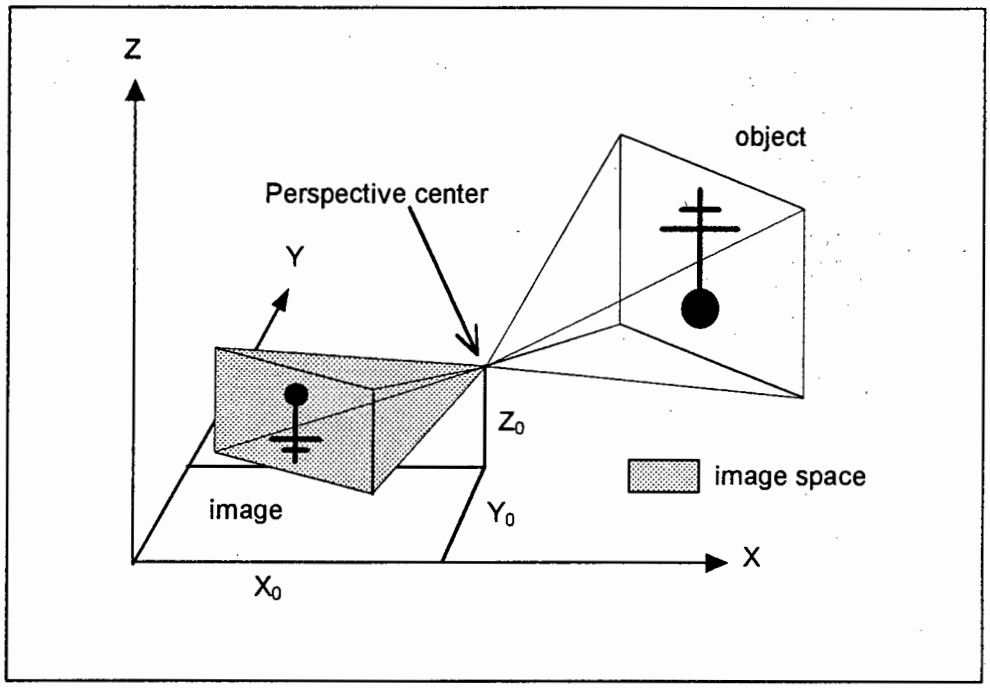

Figure 2. 1 - Perspective Projection

Where :

- *X,Y,Z are the axes of the object space.*
- *X_0 , Y_0 , Z_0 are the object space co-ordinates of the perspective centre.*

The point at which the optical axis intersects the image plane is called the principal point while the distance from the principal point to the perspective centre is called the principal distance . (Note that throughout this dissertation the principle distance will be diagramatically represented by the letter *f*, which refers to the focal length which minimises lens distortion. Physically speaking the focal distance cannot be defined since imperfections of the lens cause the focal length to vary for each incoming ray. The lens distortion parameters described in section 2.2. are applied to the image co-ordinates derived using the value *f* resulting in the correct image co-ordinates for each ray).

The origin of the image space co-ordinate system is located at the perspective centre as illustrated in ***Figure 2. 2*** (p.9).

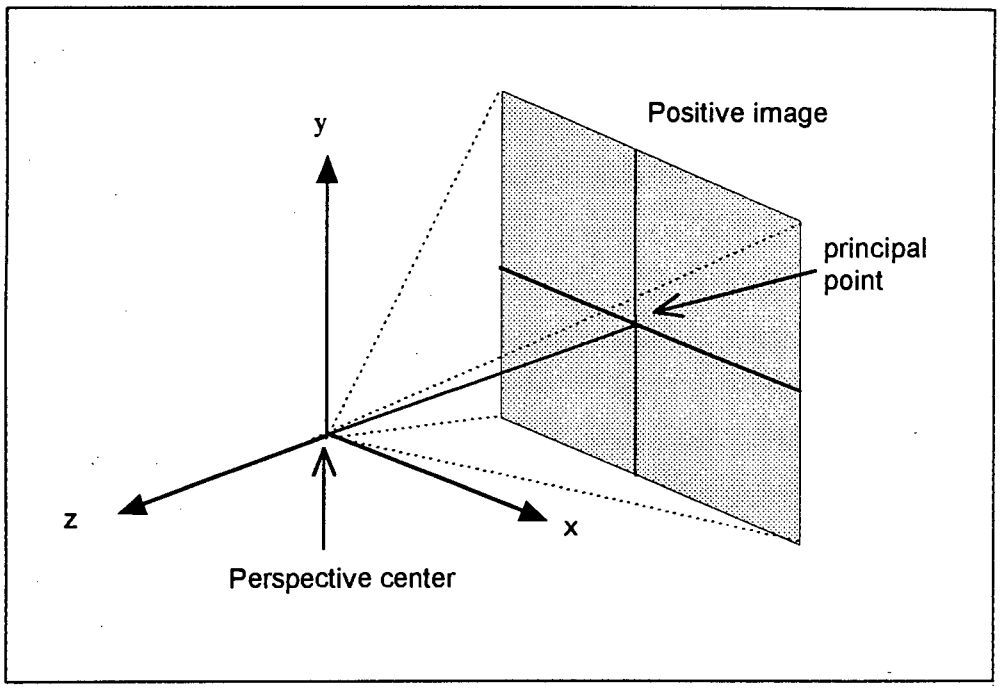

Figure 2. 2 - Elements of Image Space

Where :

- *x,y,z are the axes of the image space.*
- *The origin of the image space is located at Perspective centre.*

Once the calibration procedure has been carried out, and the orientation parameters (see section 2.2 and 2.3) for each camera are known, it is possible to determine object point positions on images captured by the cameras. Since an image comprises a two dimensional representation of a three dimensional object, it is not possible to recover the third dimension from a single image. However, if the interior and exterior orientation parameters of the image have been determined then it is possible to reconstruct the direction of a ray passing through the perspective centre to a selected point on the image. By carrying out this procedure on a second image (captured from a different position but having the same point of interest visible) it is possible to perform an intersection of the two lines which uniquely define the position of the object image point in three dimensions i.e. in the object co-ordinate system (see ***Figure 2. 3*** p.10).

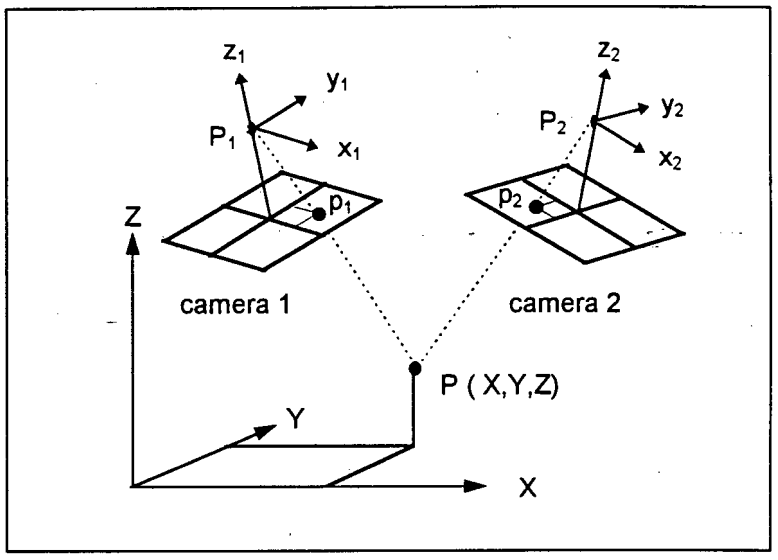

Figure 2. 3 - Dual camera geometry

Where :

- *X, Y, Z are the axes of the object space.*
- *P is the object point with object co-ordinates (X, Y, Z).*
- *P_1 , P_2 are the respective perspective centres for camera 1 and camera 2.*
- *p_1 , p_2 are the respective image points of the object point P (positive image)*
- *x_1, y_1, z_1 ; x_2, y_2, z_2 are the axes of the respective image spaces.*

The point P(X,Y,Z) is projected onto the positive image plane for camera 1 at p_1 in the image space (as shown in ***Figure 2. 3***). The same point is projected onto the positive image plane of camera 2 labelled p_2. By determining the transformation from the object point P(X,Y,Z) to the image points p_1 and p_2 respectively, the transformation from image space to object space, which is the basis for photogrammetric measurement, is achieved. The perspective centres of the respective cameras are labelled P_1 and P_2 . These points form the origins of the respective image space co-ordinate systems (x_1, y_1, z_1) and (x_2, y_2, z_2).

For any camera with perspective centre (X_0,Y_0,Z_0 in object co-ordinate system) principal point (x_p,y_p on image plane) and principal distance (f) the transformation from image space co-ordinates (x,y,f) to object space co-ordinates (X,Y,Z) can be modelled by three translations, three rotations and a scale factor :

$$\begin{pmatrix} x - x_p \\ y - y_p \\ -f \end{pmatrix} = s\, R(\varpi,\varphi,\kappa) \begin{pmatrix} X - X_0 \\ Y - Y_0 \\ Z - Z_0 \end{pmatrix}$$

(2. 1)

The scale, s, is the relative ratio between distances in the object and image space. The rotation matrix , R, describes the attitude of the image plane in the object space co-ordinate system (see section 2.3). The determination of the interior orientation parameters (section 2.2.) deal with principal point and principal distance determination. The elements of the rotation matrix form part of the exterior orientation parameters and are discussed in more detail in section 2.3.

2.2 Elements of Interior Orientation

Interior orientation parameters are associated with the camera itself. They are the geometric properties of the camera : principal distance, principal point co-ordinates and the various systematic errors associated with sensor/lens distortion. The elements of interior orientation are illustrated in ***Figure 2. 4*** (p.11) :

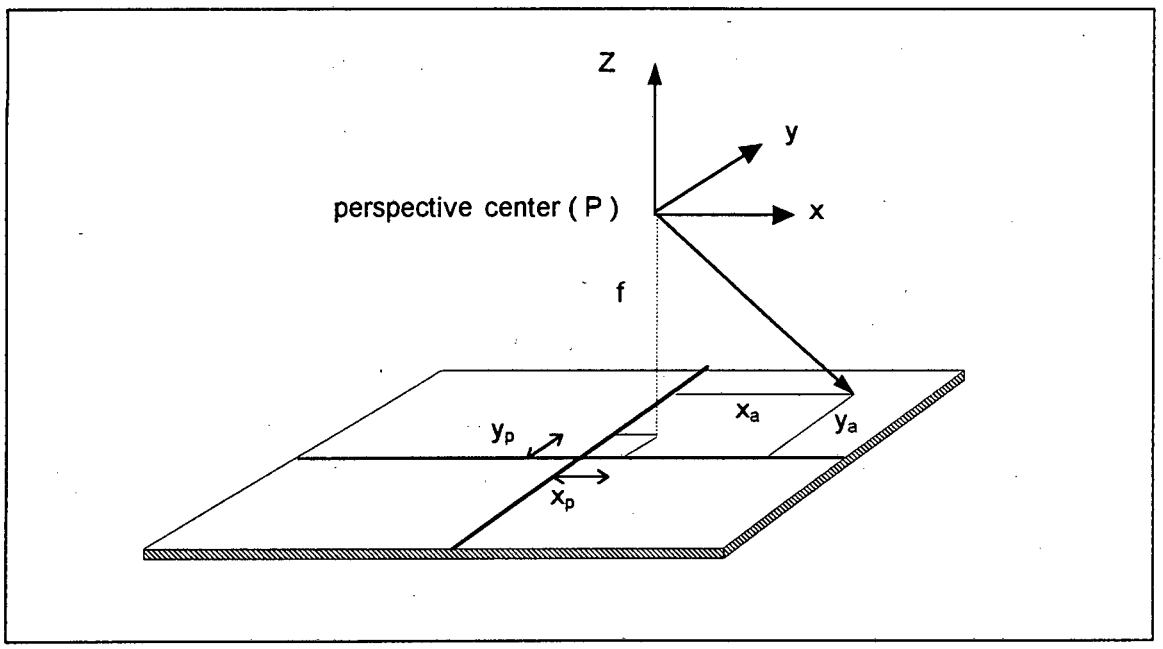

Figure 2. 4 - Elements of Interior orientation

Where :

- *x,y,z are the axes of the image space co-ordinate system.*
- *x_a ,y_a are the image plane co-ordinates of the intersection of a ray of light with the image plane.*
- *x_p , y_p is the location of the principal point on the image plane.*
- *f is the diagrammatic representation of the principle distance.*

From the diagram (***Figure 2. 4***) it can be seen that the principal point does not coincide with the centre of the image plane (as defined by the fiducial marks in analogue photography or the centre of the CCD sensor in the case of digital photography). Due to imperfections in the optical (lens)

system the principal point for any camera will not fall in the centre of the image plane. It is one of the objectives of calibration to determine where the principal point falls (i.e. x_p, y_p). Determination of the principal distance (f) provides the third co-ordinate required to describe the location of the perspective centre in the image co-ordinate system.

The principle distance *f* described refers to the focal distance which minimises the lens distortion to the image co-ordinates. A mathematical model is then used to calculate the distortion parameters required to determine the actual image co-ordinates. The lens distortion parameters calculated for this project, equation 2.2, were based upon the model developed by *Brown (1971)* which uses three radial and two decentering distortion parameters. These parameters are then used to determine the additional parameter corrections (*dx* and *dy*) which are applied to the image co-ordinates :

$$dx = \bar{x}\left(k_1 r^2 + k_2 r^4 + k_3 r^6\right) + \left[P_1\left(r^2 + 2\bar{x}^2\right) + 2P_2(\bar{x}\bar{y})\right]$$

$$dy = \bar{y}\left(k_1 r^2 + k_2 r^4 + k_3 r^6\right) + \left[2P_1\bar{x}\bar{y} + P_2(r^2 + 2\bar{y})^2\right]$$

$$\bar{x} = x_i - x_p \qquad \bar{y} = y_i - y_p \qquad r = \sqrt{\bar{x}^2 + \bar{y}^2}$$

(2.2)

where :

- x_i , y_i *are the image co-ordinates of the object point*
- x_p ,y_p *are the image co-ordinates of the principal point.*
- k_1 *is the 1st term of radial lens distortion.*
- k_2 *is the 2nd term of radial lens distortion.*
- k_3 *is the 3rd term of radial lens distortion.*
- P_1 ,P_2 *are the decentering lens distortion parameters.*

A full description of these terms may be found in *Brown (1971)*. The determination of the elements of interior orientation for this project were attained by the use of the Bundle Adjustment program *PHOTONET©* written by *van der Vlught (1994).*

2.3 Elements of Exterior Orientation

Exterior orientation parameters define the spatial position and attitude of the camera with respect to a reference co-ordinate system. Determination of the position of the image space origin and the orientation of its axes (described by the rotations ω, ϕ, κ about the x, y, z axes) are the elements of exterior orientation which must be determined by calibration.

The first step in recovering the exterior orientation is to define the object space and image space co-ordinate systems. This has already been discussed in section 2.1. The relationship between the two co-ordinate systems is described by the elements of exterior orientation as illustrated in ***Figure 2. 5*** :

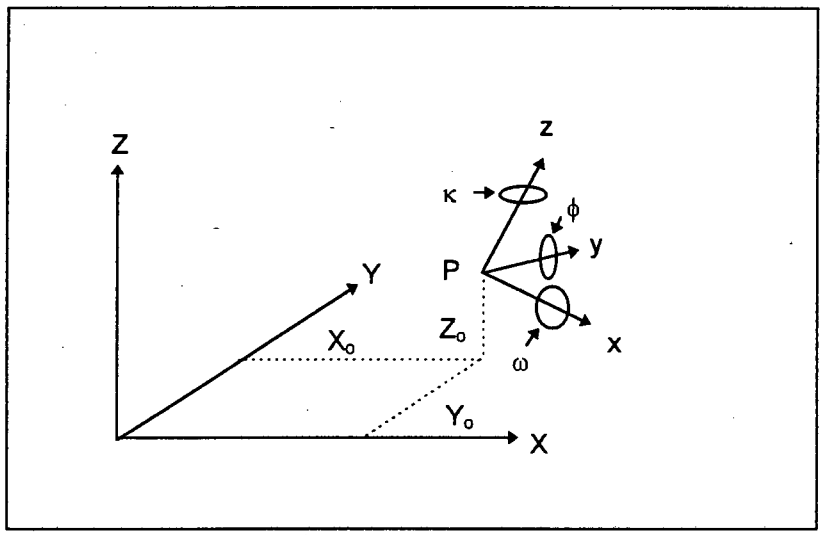

Figure 2. 5 - Elements of Exterior orientation

Where :

- X, Y, Z are the axes of the object space co-ordinate system
- x, y, z are the axes of the image space co-ordinate system
- P is the perspective centre with object space co-ordinates (X_o , Y_o , Z_o)
- ω, ϕ, κ are the orientations of the image space axes.

The angular relationship between the image and object space may be represented by a 3 -by-3 orthogonal rotation matrix ($R_{(\omega\ \phi\ \kappa)}$) given by :

$$R_{(\omega\ \varphi\ \kappa)} = R_{(x)\ \omega}\, R_{(y)\ \phi}\, R_{(z)\ \kappa}$$

where :

$$R_{(x)\ \omega} = \begin{pmatrix} 1 & 0 & 0 \\ 0 & \cos\omega & \sin\omega \\ 0 & -\sin\omega & \cos\omega \end{pmatrix}$$

$$R_{(y)\ \phi} = \begin{pmatrix} \cos\phi & 0 & -\sin\phi \\ 0 & 1 & 0 \\ \sin\phi & 0 & \cos\phi \end{pmatrix}$$

$$R_{(z)\ \kappa} = \begin{pmatrix} \cos\kappa & \sin\kappa & 0 \\ -\sin\kappa & \cos\kappa & 0 \\ 0 & 0 & 1 \end{pmatrix}$$

$$\therefore\ R_{(\omega\ \varphi\ \kappa)} = \begin{pmatrix} \cos\phi\cos\kappa & \sin\omega\sin\phi\cos\kappa + \cos\omega\sin\kappa & -\cos\omega\sin\phi\cos\kappa + \sin\omega\sin\kappa \\ -\cos\phi\sin\kappa & -\sin\omega\sin\phi\sin\kappa + \cos\omega\cos\kappa & \cos\omega\sin\phi\sin\kappa + \sin\omega\cos\kappa \\ \sin\phi & -\sin\omega\cos\phi & \cos\omega\cos\phi \end{pmatrix}$$

(2. 3)

The process of Relative Orientation recreates the orientation between the images in an arbitrary space. Physically the images are oriented relative to each other so that when they are viewed stereoscopically the ray from an object point on one image will intersect with the corresponding ray on the second image thereby recreating a three-dimensional stereomodel of the object within the object space co-ordinate system (see ***Figure 2. 6*** p.15).

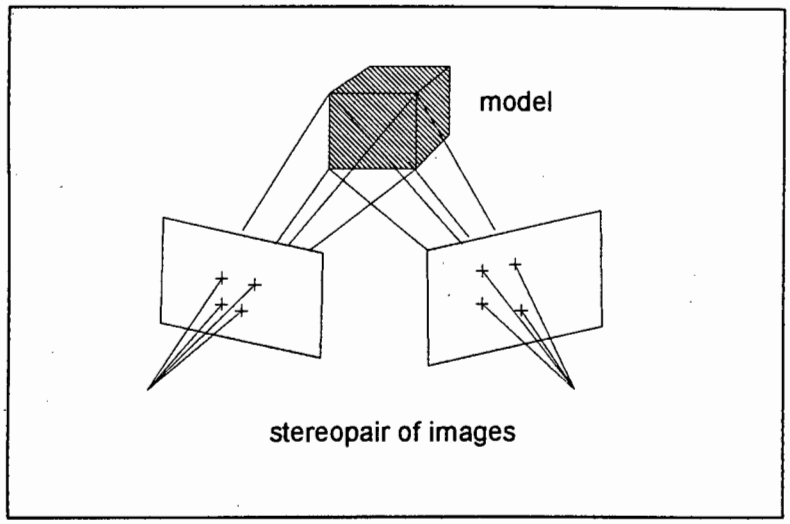

Figure 2. 6 - Physical reconstruction of relative orientation.

Where applicable, the relatively oriented images (in the object co-ordinate system) can be transformed into the reference co-ordinate system via a perspective projective transform in order to obtain co-ordinates of the object within a known system. This procedure is known as *Absolute Orientation.*.

The majority of industrial applications using close range photogrammetry are concerned with the dimensional measurement of objects. The position of the object in a reference co-ordinate system is not required and therefore determination of absolute orientation parameters is generally not performed.

A simultaneous orientation procedure to determine the elements of interior and relative orientation (with a scale factor) may be performed by using any orientation method that uses actual object space co-ordinates of control points in the calibration process (e.g. - *Collinearity Equation, Direct Linear Transform (DLT), Bundle Adjustment* - see section 2.5.). The control point co-ordinates used by such methods define the object space system, and any orientation is determined relative to this co-ordinate system. In this project simultaneous determination of the orientation parameters during calibration was achieved by with the aid of a *Bundle Adjustment* program *PHOTONET©* written by *van der Vlught (1994).* Details regarding the calibration procedure followed in this project may be found in Chapter five.

For further reading concerning the aspects of orientation the reader is referred to *Karara (1989), Slama (1980)* and *van der Merwe (1995).*

2.4 Concepts of Digital Photogrammetry

The current advances in computerisation and image processing techniques have increased the potential of Digital Photogrammetry as a practical tool. The fundamental difference between digital photogrammetry and conventional photogrammetry is the nature of the image. Photogrammetric images are continuous tone, hard-copy images whereas digital images are formed from an array of discrete, very small, finite picture elements or *pixels*. A pixel is a small, square area (typically of the magnitude 25 mm x 25 mm depending upon the device used) and has a uniform photo density. The source of the digital image may be a digital camera or alternatively a digitally scanned conventional image. The fundamental differences between digital and conventional photogrammetry are emphasised in ***Table 2. 1*** (p.16) :

	Conventional Photogrammetry	Digital Photogrammetry
1. Image Acquisition	Conventional camera with film or glass plate	video CCD camera, video chip and frame grabber
2. Image Storage	film or glass plate	frame store IP-board computer RAM (temporary) disk storage (permanent)
3. Image measurement	comparator/analogue plotter or analytical plotter - operator required	automatic detection and measurement of points, grid-intersections, patterns and shapes. - computer software, limited or no operator input
4. Image correlation	by inspection - operator required	automatic image matching
5. Photogrammetric processing	analogue or analytical methods	analytical methods only

Table 2. 1 - Conventional vs. Digital Photogrammetry.

(from Rüther, 1991).

The first sections of this Chapter described the various aspects of Photogrammetry with reference to geometry and orientation of conventional images. This section aims to illustrate some of the factors of digital photogrammetry that are used in solving the photogrammetric problem.

2.4.1. The Digital Image.

As mentioned previously, Digital images are comprised of arrays of discrete pixels. Each pixel is associated with a grey scale value representing the amount of light recorded at that region of the image. The grey scale value typically ranges from 0 (black) to 255 (white) which indicates maximum saturation. ***Figure 2. 7*** (p.17) shows a digital image of a circular target in a 12x12 pixel section (*'window'*) of the original digital image :

80	80	80	81	88	84	83	81	80	80	80	80
80	80	81	85	95	108	116	110	98	80	80	80
80	81	87	110	151	187	202	189	150	106	85	80
80	85	111	149	228	250	253	251	223	151	97	81
81	96	131	228	254	255	255	255	251	193	112	83
98	111	155	255	255	255	255	255	252	190	112	85
85	99	142	251	255	255	255	255	249	189	109	83
84	89	133	230	255	255	255	255	223	147	89	83
84	86	90	150	200	250	254	249	220	111	84	81
80	83	85	101	118	150	150	122	101	89	82	82
80	83	84	96	101	121	130	126	111	86	83	82
81	83	83	83	84	84	84	83	83	83	83	82

Figure 2. 7 - Digital representation of circular target on video image.

Image size and quality is dependent upon the resolution of the sensor used for image capture. The *MILLMAP* system uses three ITC (CCD) cameras each having a resolution of 795 x 596 pixels.

2.4.2. Framegrabbers and Image Storage

The video signal that the CCD sensor outputs is in an analogue form. In order to use digital photogrammetry and image processing techniques a *Digital Image* must be formed from this output signal. The digital image is comprised of a two dimensional array of grey scale values (as described in section 2.4.1.). A separate device or *Analogue-to-Digital Converter (ADC)* is required to sample the video signal and convert it into an 8 bit number for each element (the grey scale value for that element). The output of the ADC is then stored in a Digital *Frame Buffer* capable of accepting the digital signal describing the image at a fast rate.

The Frame Buffer used in the *MILLMAP* system has a 256Kbyte RAM for digital image data storage. This corresponds to the following data requirements for one image :

512 x 512 x 8 = 2097152 bits = 262 144 Kbytes

where :

- 512 x 512 is the ADC resolution in pixels
- 8 is the bits required to store the grey scale value.

The computer has access to the frame buffer via a secondary port. The combination of Frame Buffer and ADC is referred to as *Framegrabber.*

NOTE : camera-to-framegrabber pixel ratio must also be considered with regards to image resolution (see section 2.4.4. p.20).

2.4.3. Pixel To Image Co-ordinate Transformation

It is necessary to make the distinction between pixel co-ordinates and image co-ordinates and establish a relationship between the two. This is because digital photogrammtery measures pixel position based on a pixel co-ordinate system whereas the perspective projection equations refer to the image co-ordinate system (describing the image point position). The origin of the *pixel co-ordinate system* is the top left pixel of the image (with reference to the first pixel of the array being (1,1) based on the bottom right hand co-ordinate of the pixel-see ***Figure 2. 8*** p.19). The x-axis runs from left to right and the y-axis from top to bottom . The pixel co-ordinate system is not necessarily metric i.e. the scales along its axes need not be equal when expressed in a metric unit *(Beyer : 1990)*. The origin of the image co-ordinate system is usually placed close to the principal point as indicated earlier in section 2.2 (see ***Figure 2. 4*** p.11).

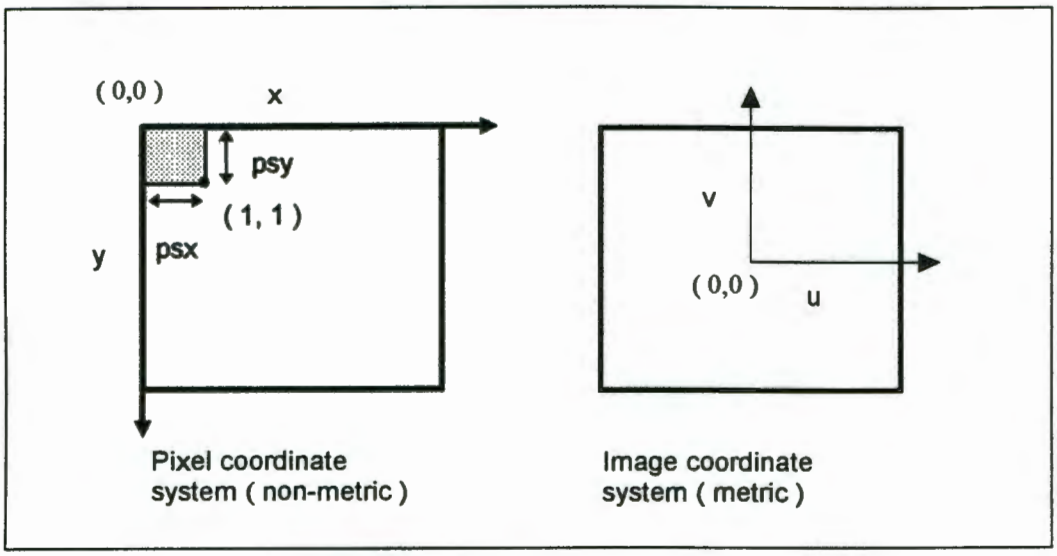

Figure 2. 8 - Pixel and image co-ordinate systems.

Where :

- *x,y are the axes of the pixel co-ordinate system.*
- *u,v are the axes of the image co-ordinate system.*
- *psx, psy are the pixel spacing in the x and y directions.*
- *(1, 1) is the co-ordinate of the first pixel in the array (referenced to the bottom right hand corner of the pixel as illustrated)*

The conversion from pixel co-ordinates to image co-ordinates is performed by the *pixel to image co-ordinate transformation:*

$$x_{im} = psx\,[\,(x_{pix} - 1) - \frac{(numx - 1)}{2}\,]$$

$$y_{im} = psy\,[\,\frac{(numy - 1)}{2} - (y_{pix} - 1)\,]$$

(2. 4)

where :

- x_{im} , y_{im} *are the image co-ordinates.*
- x_{pix} , y_{pix} *are the pixel co-ordinates.*
- *numx, numy are the pixel resolutions in the x and y directions.*
- *psx, psy are the pixel spacing in x and y.*

The pixel spacing in x and y are derived from the manufacturers specifications for the camera (in the case of the cameras used in the *MILLMAP* system the horizontal pixel spacing is 0.01186 mm and the vertical pixel spacing 0.00830 mm). Throughout this dissertation it will be assumed that the term *image co-ordinate* refers to the metric image co-ordinate derived from the *pixel to image co-ordinate transformation.*

2.4.4. Camera-to-Framegrabber Ratio.

An additional complication arises when the camera and frame-grabber resolutions are incompatible. This *camera-to-framegrabber pixel ratio* is described by *Rüther(1991)*. The *MILLMAP* system uses CCD cameras that have a 7.95mm x 6.45mm chip and a nominal pixel array of 795 x 596 pixels recording an image which is then captured by a *MATROX-PIP512B* framegrabber with a resolution of 512 x 512 pixels. It is necessary to resample the analogue signal generated by the 795 pixels of each horizontal line and subdivide it according to the requirements of the framegrabber (i.e 512 pixels). The frame grabber resamples the analogue video signal from the camera at the 512 resolution required requires resulting in the combination of 283 elements (795 - 512 = 283) per row into the sampled values. The vertical elements (corresponding to the rows of the analogue image) are truncated by the frame grabber after the 512 th row, thus the last 84 rows (596 - 512 = 84) of data from the camera are not used during the processing of the image.

2.4.5 Image Processing Techniques

Several Image processing techniques are utilised in the *MILLMAP* software. In order to process the images, image co-ordinates for the centres of targets must be determined from the digital images. These co-ordinates are then used in the photogrammetric equations described in section 2.5.

The *MILLMAP* system performs the following image processing routines in order to find the centre of circular targets :

- Edge detection
- Thresholding
- Feature extraction
- Centroid determination

The procedure followed is similar whether the system is finding the centre of a single laser dot during the measurement process, or the multiple targets on the calibration frame. The individual concepts listed above will be described in the following sections.

Edge Detection and Thresholding.

A digital edge is described by *Haralick and Shapiro (1992 : p.337)* as : *" the boundary between two pixels that appears when their brightness values are significantly different."*. Edges may be "step" with a rapid transition in pixel value (i.e. from a value of 0 to 200) or more typically "ramped" in which the transition is not as fast. Profiles representing greylevel values for step and ramp edges are illustrated in ***Figure 2. 9*** (p.21).

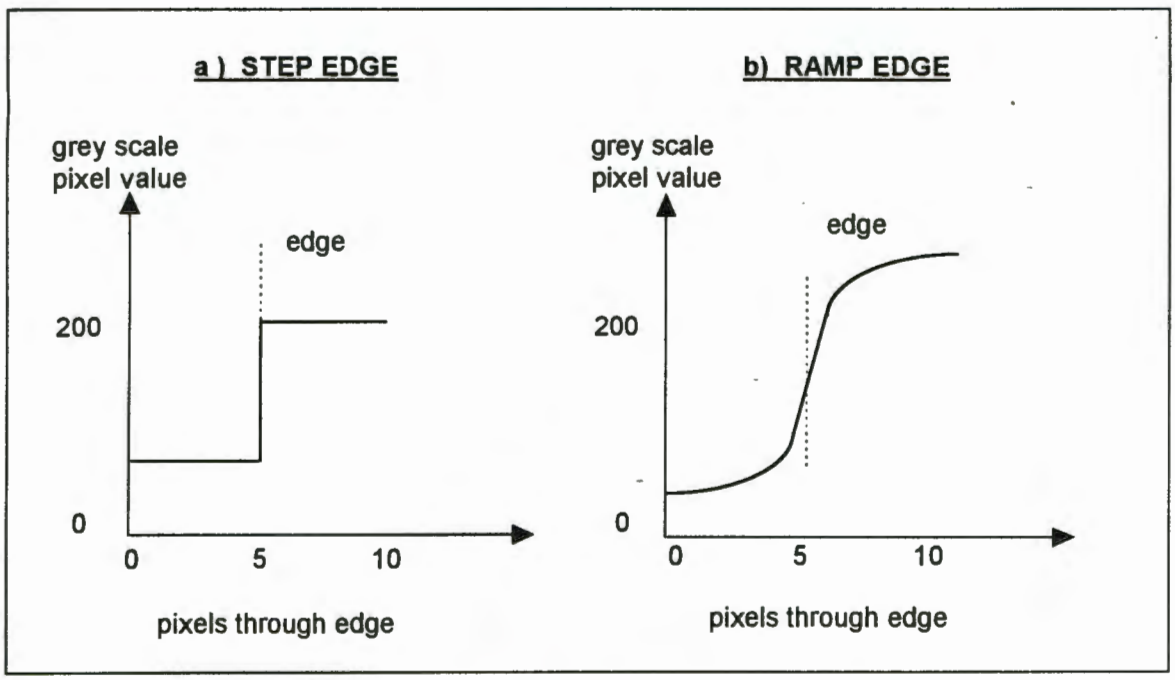

Figure 2. 9 - Profiles of Step and Ramp Edges.

In the case of the ramp edge it is necessary to determine where along the ramp the edge will fall as indicated by the dotted line.

Different edge detection functions have been proposed by *Roberts, Sobel and Prewitt* which are well documented in *Haralick and Shapiro (1992)* . A summary of these edge operators may be found in *van der Merwe (1995)*.

The edge detector used in the *MILLMAP* software calculates the maximum gradient from the four principal directions, for a 3 x 3 window around the current pixel. The average grey scale value for all the maximum gradients (g_m) is calculated as well as the standard deviation (s_g) of the individual maxima. The gradient threshold value (g_t) is defined in equation 2.5 (p.22) according to *van der Vlught and Rüther (1994)*

$$g_t = g_m + c\, s_g \qquad (2.5)$$

where:

- g_m *is the average grey scale for the maximum gradients*
- s_g *is the standard deviation of the individual maxima*
- g_t *is the gradient threshold value*
- *c is a scaling constant (to scale the standard deviation)*

The value of (c) controls the sensitivity of the edge extraction process. *Van der Vlught and Rüther (1994)* suggest that a value of 2-3 for (c) produces good results. The gradient threshold value (g_t) is used as the edge value for the thresholding function in the next stage of image processing by the *MILLMAP* software. All pixels with a maximum gradient greater than the gradient threshold (g_t) are labelled as edges and assigned a grey level value of 255 (maximum saturation) whereas all pixels with a maximum gradient value less than the gradient threshold (g_t) are assigned a value of 0. The result of the gradient edge detector function and the thresholding function is a binarised edge image. The original image and binarised edge image are illustrated in ***Figure 2. 10*** (p.22.)

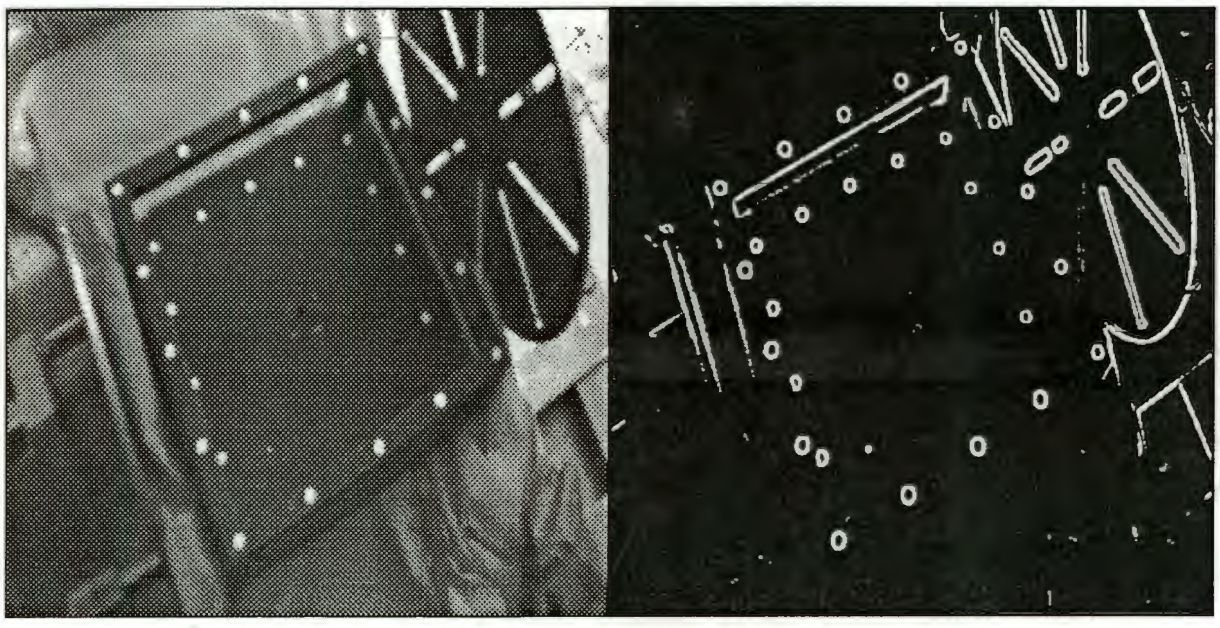

(a) **(b)**

Figure 2. 10 - Edge detection and thresholding.

(a) is the original image and (b) the binarised edge image after application of the gradient operator (edge detection) and thresholding function..

A detailed comparison of alternative edge detection algorithms and techniques may be found in *van der Merwe (1995).*

Feature Extraction.

The binarised edge image contains data from the original image which is used during the automatic processing of the image. The majority of background noise and distracting features have been filtered out. The next stage of image processing requires that the circular targets (or laser dot during the actual measurement phase) be identified on the image. The *MILLMAP* software identifies circular targets based on the *Freeman* pixel search routine illustrated in ***Figure 2. 11*** (p.23).

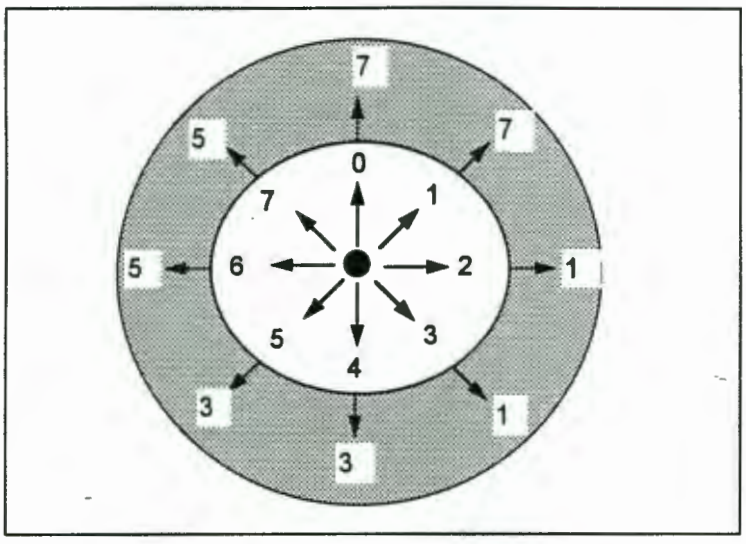

Figure 2. 11 - Initial search direction for Circular search routine.

The inner ring represents the current direction (i.e direction in which the element was found while the outer ring represents the starting direction for the next search - see following example for more detail).

An example *(van der Merwe : 1990)* will be used to describe the operation of this circular search routine.

Consider the following binary edge image (with edge elements labelled 1 and the background labelled 0 - see ***Figure 2. 12)*** *:*

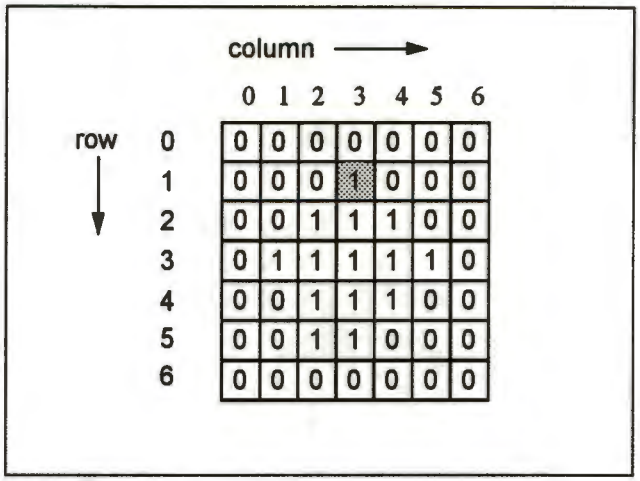

Figure 2. 12 - Binary Edge Image

The image is searched from left to right and top to bottom until the first edge element is found at location (1, 3) shown shaded in ***Figure 2. 12*** *above. The 3x3 window centred at location (1,3) appears as follows:*

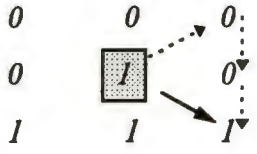

The direction in which the element was found was (2) therefore the clockwise search for the next element begins in direction (1). The progress of the search is indicated by the dotted arrows and the final direction (3) where the next edge is found is indicated by the solid arrow. The edge found at location (2,4) becomes the centre of the next 3 x 3 search window which appears as follows:

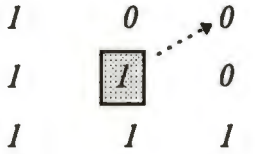

Since the direction in which (2,4 shaded above) was found is (3), the clockwise search for the next element will begin in direction (1)(indicated by the dotted arrow). Continuing the procedure to search for elements until the starting point is reached the search pattern will follow the path indicated in ***Figure 2. 13*** *(p.25) in the process of identifying the circular feature.*

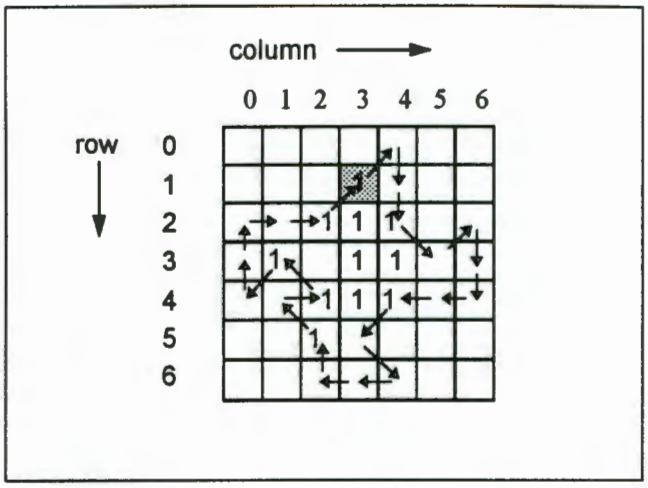

Figure 2. 13 - Direction followed by Circular search routine.

Circular features, once identified, are extracted with all other features being discarded. The centre of these features are calculated using a least squares best fit circle. Note that the values for the circle centres are approximate since they are computed using full pixel values (sub pixel line following of the circular features would permit sub-pixel determination of the circle centres). The size of each circular feature (determined from the radius of the best fit circle) is also calculated to provide the dimensions of a window around the feature. The approximate circle centre and window positions are used in the next stage of image processing which determines the centre of the targets with sub-pixel accuracy as described in the next section (see *Centroid Determination).*

Centroid determination.

In order to obtain optimum accuracy from matching and bundle solutions, accurate image co-ordinates for the centre of the target must be determined. Various methods of determining the centre of the circular features to sub-pixel accuracy can be used :

- weighted centre of gravity.
- weighted intersection of slope elements.
- least squares template matching.
- sub pixel edge determination and best fit ellipse adjustment.

The *MILLMAP* system uses the weighted *centre-of-gravity* approach to determine values for the centres of the targets used in the calibration phase. The equations used to compute the weighted centre of gravity for a grey scale window are shown in equation 2.6 (p.26).

$$x_c = \frac{\sum_{i=1}^{n}\sum_{j=1}^{m} G(X_i,Y_j)X_i}{\sum_{i=1}^{n}\sum_{j=1}^{m} G(X_i,Y_j)}$$

$$y_c = \frac{\sum_{i=1}^{n}\sum_{j=1}^{m} G(X_i,Y_j)Y_i}{\sum_{i=1}^{n}\sum_{j=1}^{m} G(X_i,Y_j)}$$

(2.6)

where :

- *$G(X_i, Y_j)$ is the grey scale value for a pixel located in row i, column j of the digital image.*
- *x_c, y_c are the subpixel image co-ordinates of the target.*

For further reading and examples of the application of this method the reader is referred to *Xue (1992).*

The *MILLMAP* system uses the weighted centre of gravity approach as described previously for the determination of sub-pixel image co-ordinates for target centres on the control frame during the calibration process. During the measurement procedure single pixel coordinates (which are an approximation of the laser dot centre) are used for the target point in the reference image. The target points are matched on subsequent images by a *Multi-Photo Geometrically Constrained (MPGC)* least squares matching routine (see section 2.4.6). The routine was written by *van der Vlught (1992)* and adapted to measure the laser dot for the *MILLMAP* system.

2.4.6 Multi-Photo Geometrically Constrained Matching (MPGC)

The MPGC approach to matching exploits known camera orientation information considerably improving the matching performance *(van der Vlught and Rüther : 1994).* This method solves the space intersection problem while applying constraints to the possible solutions in order to achieve greater accuracy in the determination of object space co-ordinates. The procedure uses a target point (defined with single pixel accuracy) on the reference image and then searches for the location of this same point on the remaining images. The search for conjugate target points is constrained to search the epipolar line in subsequent images.

A definition of the *epipolar line* will be made in order to clarify the term which will be used frequently throughout this dissertation. The epipolar line is defined as the line of intersection

between the image plane and a plane passing through an object point and the perspective centres of two images, as illustrated in ***Figure 2. 14*** (p.27)

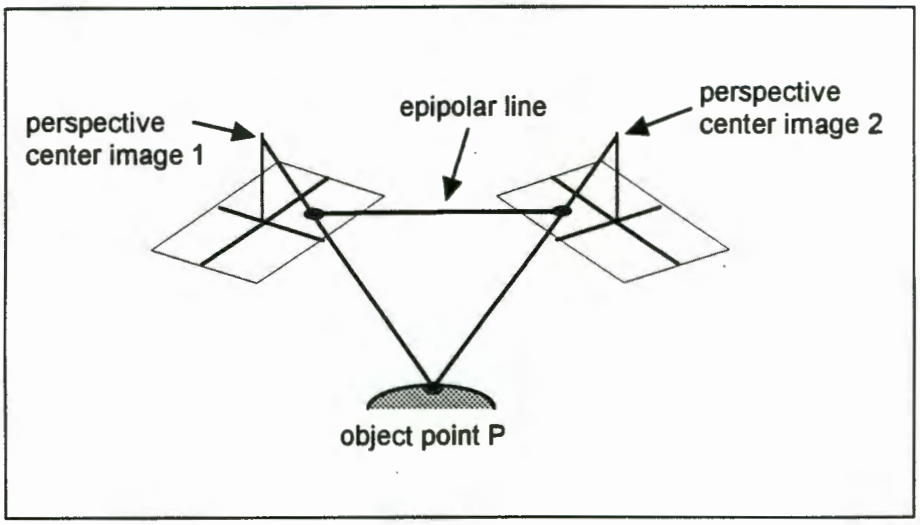

Figure 2. 14 - Definition of the Epipolar Line.

The position of the target point is located to sub-pixel accuracy on the matched target which is shifted, rotated and scaled so that the target window in the search image is matched as closely as possible with the target window on the reference image (thereby constraining the solution by the geometrical shape of the target). A best fit space intersection using the image co-ordinates of the conjugate target points is computed incorporating the matching parameters derived from the matching process. An example illustrating the various constraints imposed during the MPGC matching process is shown in ***Figure 2. 15*** (p.28).

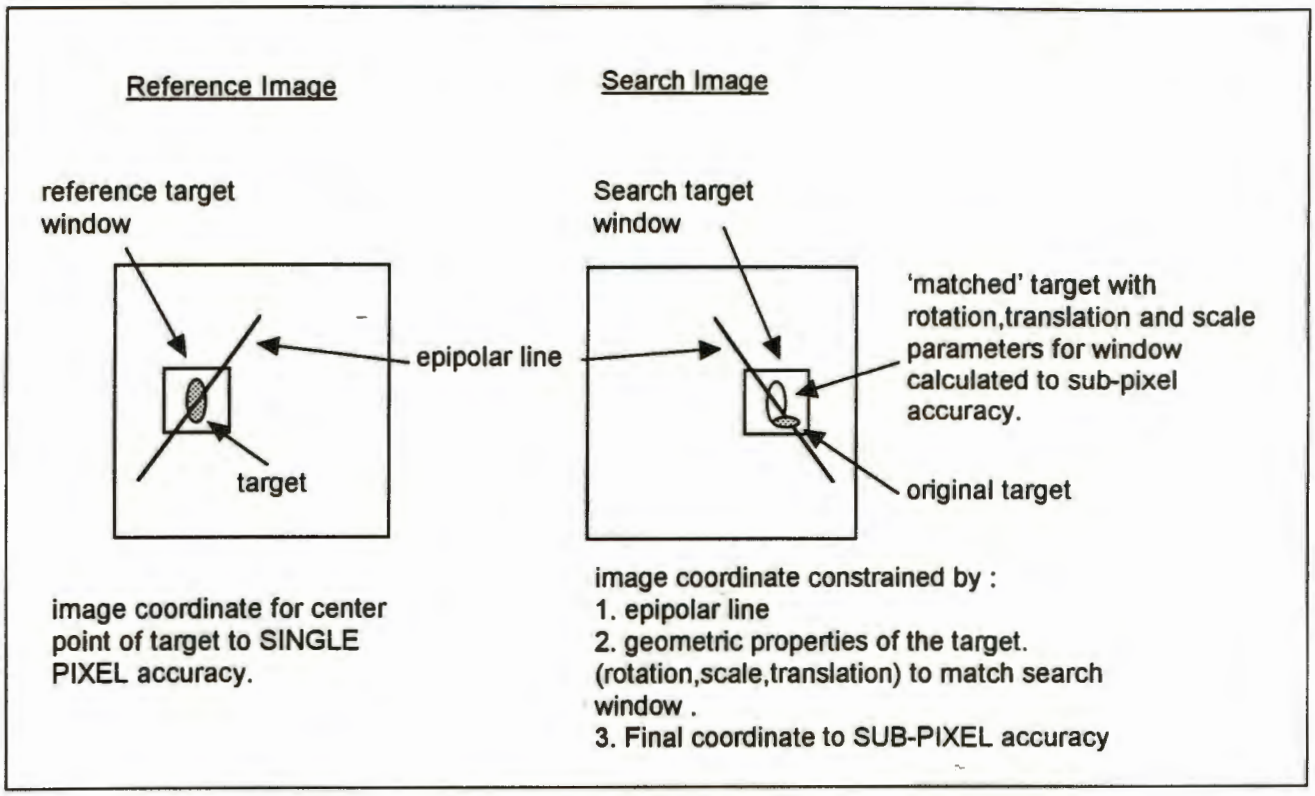

Figure 2. 15 - Diagrammatic representation of the MPGC matching process.

Note that the final solution for the object space co-ordinates is constrained by a best fit least squares space intersection using the image co-ordinates from the reference image and those successfully matched on the search images.

For further details regarding the MPGC procedure the reader is referred to *van der Vlught and Rüther (1994)* and *Gruen and Baltsavias (1988 b)*.

2.5 Photogrammetric Equations

There are several equations that are fundamental to the solutions of the various photogrammetric tasks described in the preceding sections. This section will provide the mathematical equations referred to throughout this dissertation. A description of the application of the following equations will be provided :

- *The Collinearity Equation.*
- *The Bundle Adjustment*
- *The Direct Linear Transformation (DLT)*

2.5.1 The Collinearity Equation.

The *Collinearity Equation* is a mathematical model based on the assumption that the object point, perspective centre and image point lie on an idealised line i.e. *they are collinear.* These conditions represent the *perspective projection*, which was introduced earlier (see equation 2.1, p.10) as :

$$\begin{pmatrix} x - x_p \\ y - y_p \\ -f \end{pmatrix} = s\, R(\varpi,\varphi,\kappa) \begin{pmatrix} X - X_0 \\ Y - Y_0 \\ Z - Z_0 \end{pmatrix}$$

where :

- *X, Y, Z object space co-ordinates of the object point.*
- *X_o, Y_o, Z_o object space co-ordinates of the perspective centre.*
- *x_p , y_p image space co-ordinates of the principal point.*
- *x , y are the image co-ordinates of the object point.*
- *f is the principal distance.*
- *s is a scale factor.*
- *R (ϖ ϕ κ) is the rotation matrix describing the orientation between the image and object space co-ordinate systems.*

After determining the interior and exterior orientation parameters from calibration, and measuring the image point, the object point co-ordinates may be calculated from the above equation. If the first and second rows of the equation system are divided by the third row then the scale factor is eliminated. The resulting equations may be rearranged to yield the more practical form of the perspective projection which are called the *Collinearity Equations* (equation 2.7, p.29).

$$\frac{x - x_p}{-f} = \frac{r_{11}(X - X_0) + r_{12}(Y - Y_0) + r_{13}(Z - Z_0)}{r_{31}(X - X_0) + r_{32}(Y - Y_0) + r_{33}(Z - Z_0)}$$

$$\frac{y - y_p}{-f} = \frac{r_{11}(X - X_0) + r_{12}(Y - Y_0) + r_{13}(Z - Z_0)}{r_{31}(X - X_0) + r_{32}(Y - Y_0) + r_{33}(Z - Z_0)}$$

(2. 7)

where :

- *r_{11} - r_{33} are the individual elements of the rotation matrix.*

The elements of the rotation matrix are given by equation 2.3 (p.14). The image co-ordinates used in the collinearity equations will be modified by the distortion parameters previously described in

equation 2.2 (p.12). The collinearity equations form the basis from which other mathematical models of the photogrammetric situation are derived (see 2.5.2 and 2.5.3).

2.5.2 The Bundle Adjustment

The *Bundle Adjustment* uses the collinearity equation 2.7 (p.29), for each ground or control point, and from multiple camera stations combined into a simultaneous solution for the unknown parameters using a least squares adjustment. The procedure is the same as that used for standard block adjustment in aerial triangulation. The physical situation for three camera stations and four control points is illustrated in ***Figure 2. 16*** (p.30) .

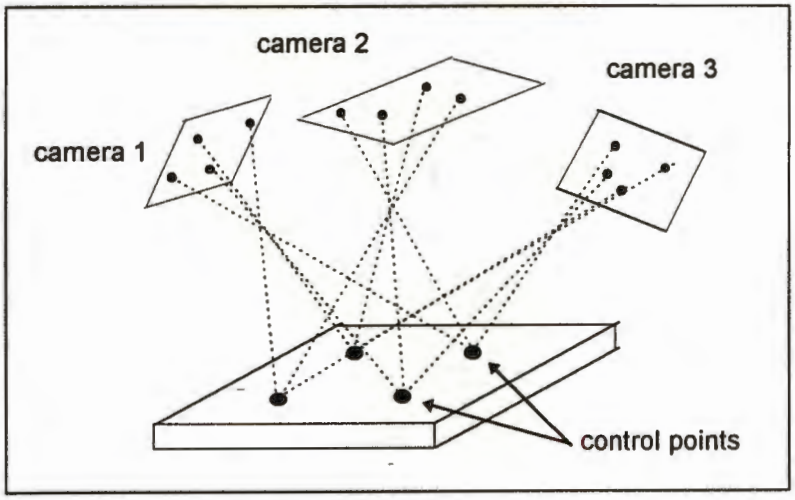

Figure 2. 16 - Multi station bundle configuration.

The observation equations formed from the collinearity equations must be linearised before they can be used in a least squares adjustment. Details on the linerisation and formation of the observation equations may be found in chapter two of *Slama (1980).* Only the linearised equations in matrix form will be presented. The matrix notation for the observation equation is shown in equation 2.8 (p.31).

$$\begin{bmatrix} V_{x_{ij}} \\ V_{y_{ij}} \end{bmatrix} + \begin{bmatrix} b_{11} & b_{12} & b_{13} & b_{14} & b_{15} & b_{16} \\ b_{21} & b_{22} & b_{23} & b_{24} & b_{25} & b_{26} \end{bmatrix} \begin{bmatrix} \Delta\omega_i \\ \Delta\phi_i \\ \Delta\kappa_i \\ \Delta X_i^c \\ \Delta Y_i^c \\ \Delta Z_i^c \end{bmatrix} + \begin{bmatrix} b_{17} & b_{18} & b_{14} \\ b_{27} & b_{28} & b_{29} \end{bmatrix} \begin{bmatrix} \Delta X_j \\ \Delta Y_j \\ \Delta Z_j \end{bmatrix} = \begin{bmatrix} -f_x^0 \\ -f_y^0 \end{bmatrix} \tag{2.8}$$

where :

- V_{xij} V_{yij} *are the corrections to the image co-ordinates of the jth point at the ith station.*
- b_{11} ..b_{19} *are the coefficients of the linearised collinearity equations with respect to the x image co-ordinate.*
- b_{21} .. b_{29} *are the coefficients of the linearised collinearity equations with respect to the y image co-ordinate.*
- $\Delta\omega_i\ \Delta\ \phi_i\ \Delta\ \kappa_i$ *are the corrections to the orientation angles at station i*
- $\Delta X_j\ \Delta Y_j\ \Delta Z_j$ *are the corrections to the perspective centre object co-ordinates at station i.*
- $-f_x^0$ - f_y^0 *are the provisional values for the collinearity equations.*

The solution is iterated with the provisional values being continually updated by the corrections to the unknowns until the correction reaches a prespecified tolerance. *Karara (1989)* notes that in using the bundle solution various parameters may be treated as known or unknown by manipulating their weights in the adjustment. For high accuracy applications the camera orientation parameters and point co-ordinates are treated as unknown (i.e. a free net adjustment) with distance measurements used to eliminate the datum defect.

2.5.3 The Direct Linear Transformation (DLT)

The *Direct Linear Transformation (DLT)* is an alternative method for solving the analytical orientation of images for photogrammetry. The major advantage of this method is that it does not require initial provisional values in order to solve for the orientation parameters (as with the *Bundle Solution* described previously). The method solves for the object space co-ordinates directly in terms of the image co-ordinates by means of an affine transformation.

The equation for the DLT solution is given in equation 2.9. Derivation of this equation is not shown but may be found in *Karara (1989).*

$$x_i + \Delta x_i = \frac{b_{11}X_i + b_{12}Y_i + b_{13}Z_i + b_{14}}{b_{31}X_i + b_{32}Y_i + b_{33}Z_i + 1}$$

$$y_i + \Delta y_i = \frac{b_{21}X_i + b_{22}Y_i + b_{23}Z_i + b_{24}}{b_{31}X_i + b_{32}Y_i + b_{33}Z_i + 1}$$

(2.9)

where :

- x_i, y_i *are the image co-ordinates of point i.*
- Δx_i, Δy_i *are the systematic errors of the image co-ordinates of the point i.*
- X_i, Y_i, Z_i *are the object space co-ordinates of point I.*
- b_{11} .. b_{33} *are the unknown transformation parameters.*

The transformation parameters determined from the DLT (b_{11} ..b_{33}) are used to calculate the elements of interior and relative orientation. These elements are then used as provisional values for the orientation parameters of the cameras in the *MILLMAP* system. A bundle solution is performed to calculate the final orientation parameters for the cameras which are used during the measurement phase.

Chapter Three

Characteristics of Co-ordinate Measurement.

The first section of this Chapter (3.1) introduces the co-ordinate systems used throughout the project. References to the object space co-ordinate system and machine co-ordinate system are made throughout this dissertation and require an introduction. The second section of this Chapter (3.2) aims to present the reader with an overview of the characteristics of conventional co-ordinate measurement machines (CMMs). In discussing the principles and concepts of co-ordinate measurement the problems associated with the subject will be considered in the remaining sections of this chapter (3.3 - 3.5). Discussion of non-contact measurement systems and related problems will be covered in Chapter four. A description of the project methods and procedure followed can be found in Chapter five.

3.1 Co-ordinate Systems used in the Project

Before a description of co-ordinate machines is presented a brief introduction to the co-ordinate systems used in this project will be made.

Conventional co-ordinate measurement machines (CMMs) have two co-ordinate systems : the **machine co-ordinate system** and **object co-ordinate system.** The co-ordinates in the object co-ordinate system are the physical points on the surface of the object. It is these points that the co-ordinate measurement machine measures in order to produce a replica of the object being measured. The machine co-ordinate system defines the position of the CMM probe. When the probe is positioned at various points on the object's surface the position is recorded by the CMM in the machine co-ordinate system. These co-ordinates are dimensionally consistent with the object and are used as measurement data.

The *MILLMAP* system uses the machine co-ordinate system as a delivery system for the laser probe. Measurement of the object is not determined from the machine co-ordinate system. The measurement of the object is made by recording the position of a laser dot at points on the object's surface. This measurement is made by a digital photographic system which is defined by the **object space co-ordinate system** during the calibration of the digital cameras (see Chapter

two). The relationship of the object, machine and object space co-ordinate systems is illustrated in ***Figure 3. 1*** (p.34).

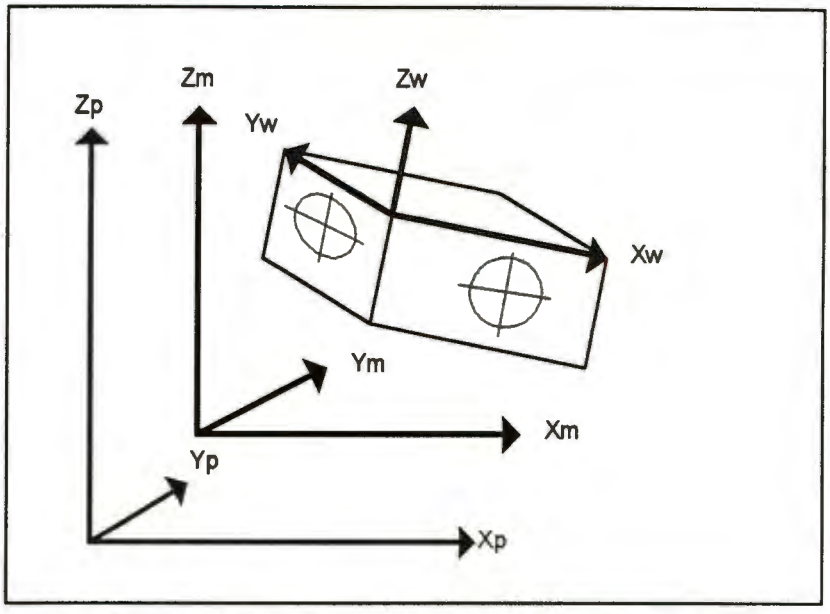

Figure 3. 1 - Relationship of Co-ordinate Systems.

The axes of the Machine co-ordinate system are labelled (Xm,Ym,Zm) ,the axes of the Object co-ordinate system (Xw,Yw,Zw) and the axes of the object space co-ordinate system (Xp,Yp,Zp).

3.2 Co-ordinate Measurement Machines

> *"Manufacturers are required to inspect the parts they produce with increasing precision, especially parts supplied to the automotive and aerospace industries. The need for such accuracy has driven the evolution of measuring tools from hand held devices such as callipers and scales to sophisticated co-ordinate measuring machines (CMMs). CMMs are now widely used by manufacturers and part suppliers to document the physical attributes and overall quality of parts".*
>
> *Computer Graphics (1995(a): p.36).*

The above statement indicates the importance of CMMs in the manufacturing industry at present. The principal application of these machines is in the area of quality control inspection. An example of quality control is given by *Herzog (1982)* describing the surface accuracy of a television screen as one of the factors responsible for the colour and contrast qualities of the television image. By measuring the curvature of the screen with a CMM designers can gauge how true to design the manufacturing process is.

The basic co-ordinate measurement machine has a **controller** which sends a set of instructions to the **motion system** which moves the **probe** and/or object. The probe is a contact measurement device which usually has several measurement heads. Upon contact with the object, the

measurement head will trigger the machine to measure its position. Details regarding the operation of a contact probe may be found in *Zeiss (1982, 1990b)*. The co-ordinates measured in this manner are automatically compensated for probe **position offset,** and probe head **size offset** (see ***Figure 3. 2*** p.35). The position offset is the co-ordinate difference between the head position and the **reference point**. The individual probe head size offset must also be determined and compensated for since this may vary depending upon the probe head options available. The reader is referred to *Zeiss (1995)* for details regarding probe head configurations and options.

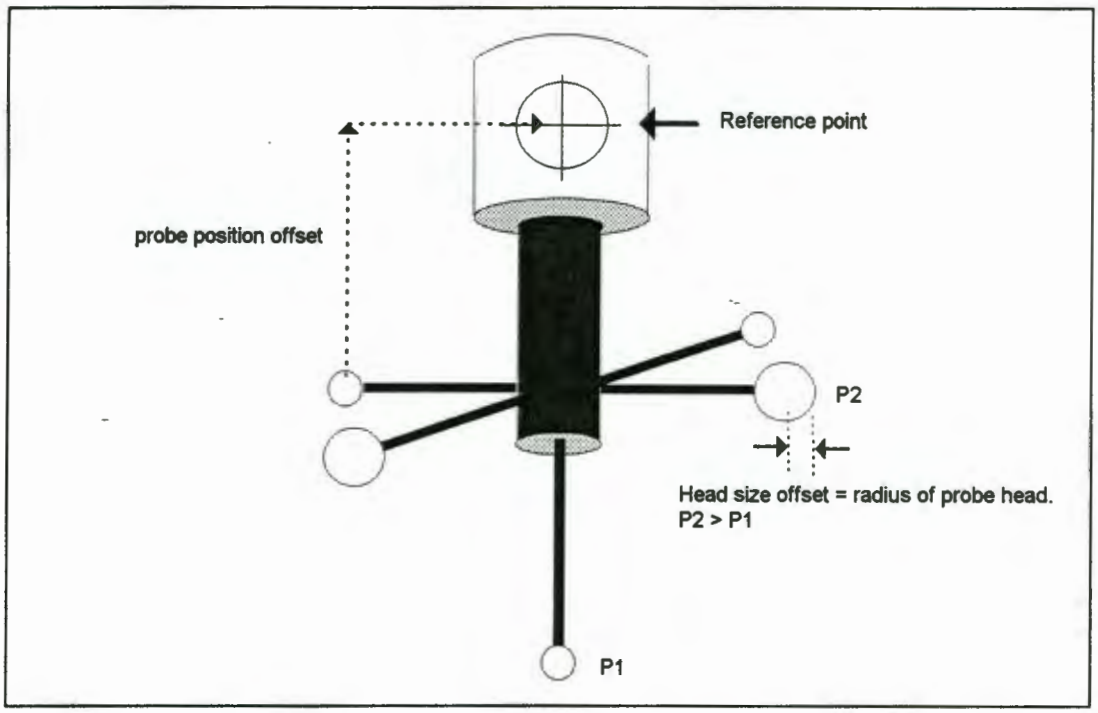

Figure 3. 2 - Probe Offset Measurements.

*Note : throughout this dissertation the **probe** will be used to describe the arrangement shown in **Figure 3. 2. The probe head** will be used to describe the individual measurement heads attached to the probe.*

Both the position offset and probe head size offset are determined by calibration of the probe. The calibration procedure requires that the various probe heads are used to measure a specially designed calibration sphere (whose dimensions are accurately known). The resulting measurements are used to calculate the co-ordinate offset for each probe head and the probe head size. The final co-ordinates obtained from the probe, irrespective of probe position or size, will then be correctly adjusted with respect to the reference point. The different probe heads act as one common mathematical point, which is defined as the reference point.

3.3. Fundamentals of Numerical Control.

The actual operation of CMMs is based on numerically controlled processes. These processes form the basis of operation for milling machines, lathes and CMMs . There is hardly an aspect of discrete-part manufacture that has not been strongly influenced by numerical control processes *(McMahon : 1993)*. By introducing some of the concepts associated with numerical control it is hoped that the reader will gain an understanding of the programming considerations necessary for machine control.

A typical numerically controlled machine will consist of a **controller** capable of processing a **stored program** in order to control the actual machinery via an **actuation device** (for a CMM this is the motion system for the probe). In the case of a **closed loop control** system the control of the actuation device is modified according to information received from feedback sensors monitoring the position of the actuation devices. An alternative to closed loop control is an **open loop** system in which instructions are passed to the actuation system without the controller receiving feedback on the response of the system. The CMM developed in this project can be considered an open loop system. Implementation of a closed loop system would have required additional sensors to check the position of the laser probe and correct this position to the required position. The addition of these sensors would have caused the budget for the project to be exceeded. A discussion of the limitations of the open loop system are presented in Chapter nine.

The numerical control of the machine is determined by the stored program which is executed by the controller. This program is known as the **part program**. The part program represents the geometry of the object, and the motion capabilities of the probe as a set of instructions which will enable the probe to follow a path on the surface of the object (in the case of a milling machine the path of the head will actually define the surface of the object). Traditionally these programs were prepared by the part programmer who would prepare the part program from a set of engineering plans of the object and knowledge of the probe motion capabilities. Knowledge of basic object geometry is necessary for CMMs in order to specify where the probe is to measure. For example the probe will have to be positioned in the bore of a hole before it can be programmed to measure the bore.

Selection of the probe head will depend on the accessibility of the object itself. A smaller head will allow improved access to smaller bores in the case of CMMs. The choice of cutter head size and shape will reduce the cusping and gouging affects on a milling machine (see ***Figure 3. 3*** p.37). Typical numerical control will require that various aspects of machine control and object geometry be considered before programming the device.

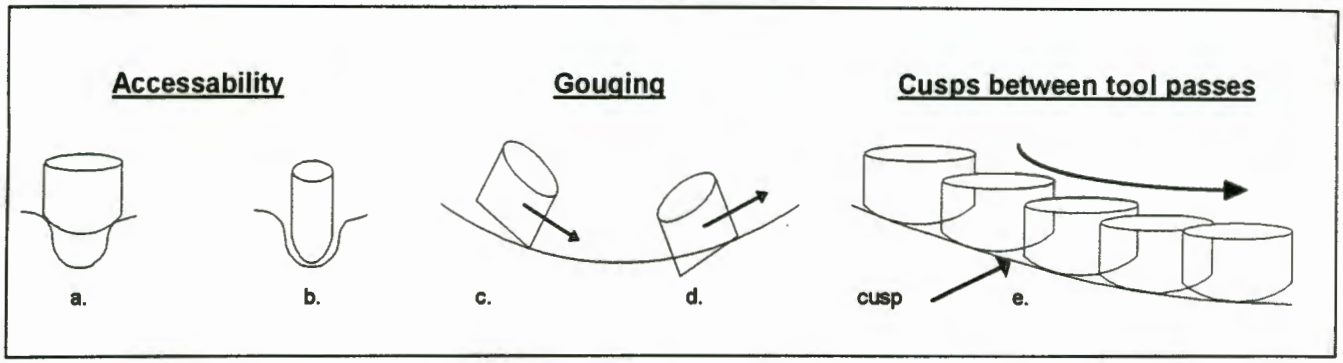

Figure 3. 3 - Machine Head Conditions.

Position (a) shows the probe head is too large to access a region on the objects surface.
Position (b) shows that a smaller probe head will be able to access the same region as in (a).
Position (c) shows a square edge cutting tool on the leading edge of a concave curve. In this position the object surface is unaffected by the tool.
Position (d) shows the same square edge interfering with the concave curve by gouging.
Position (e) shows the region where a cusp is formed between passes of a circular cutting tool.

Machine tools typically fall into various categories defined by the motion axes of the probe. A greater number of motion axes will increase the mobility of the probe, thereby increasing the accessibility of the object. But the complexity of commands required to operate multiple motion axes will also increase. *McMahon (1993:296-7)* reviews multiple axis machines and gives examples of applications of each :

- 2-Axis motion , generally two orthogonal directions in a plane, which applies to most lathes as well as punch-presses, flame and plasma-arc and cloth cutting machines, electronic component insertion and some drilling machines.
- 3-Axis motion along the three principle directions (x, y and z of the cartesian co-ordinate system). Motion along two (x,y) axes coupled with a rotation axis may also be considered in this category. Typical applications include milling, boring, drilling and CMMs.

- 4-Axis motion involving three linear and one rotation axis, or two x-y motions for example in some lathes fitted with supplementary milling heads.
- 5-Axis motion normally consist of three linear (x,y and z) axes, with rotation about two of these (normally the x and y axes) generally applicable to milling machines.

The device developed in this project has two orthogonal axes and one rotation axis. As such it falls under the classification of a 3-axis machine. The rotation axis is required to increase the accessibility of the object, but there are several factors that must be considered when rotating the object. Section 3.5. deals with this topic in more detail.

Once the probe has been selected and the motion of the probe has been defined, the path the probe is to follow must be confirmed to be free of obstructions by the machine and the object itself. When all the aspects of the part program have been considered, the part program is coded into a digital format, representing the sequence of commands required, for direct control of the machine. This final format is the **machine control data**. The program is then tested and modified where necessary. Modifications to the program include the variation of the speed at which the object is rotated or **spindle speed** (in the case of a lathe) depending on the material which is to be machined. The periodic addition of coolant for the cutter head and the speed at which the cutter moves, in the case of a milling machine, are also examples of modifications to the machine control data.

To summarise, numerical control of part programming comprises the following stages:

- Identification of the part geometry, probe head selection and probe motion.
- Coding of probe motion and general machine instructions.
- Checking the probe path for any obstructions from either the machine or the object itself.
- Coding the instructions as machine control data and testing the program to evaluate the performance of the instructions.
- Modifying the machine code according to the material to be machined (in the case of milling and lathe operations).

The production of machine control data, considering the factors imposed by part geometry and probe motion, directly from CAD drawings is the principle behind CADCAM systems (Computer Aided Design and Computer Aided Manufacture). CADCAM systems have eliminated the need

for part programming by automating the production of machine control data from digital CAD representations of the object geometry and a database of machine control commands. The concepts associated with part programming assist in understanding the factors of numerical control (NC) that are automated by CADCAM processes. A more detailed analysis of CADCAM is presented in section 3.4.

3.4. CADCAM Approach to numerical control.

> *"An industry that routinely takes four years or more to bring a product to market and spends several billion to do so, has seemingly done the impossible. Chrysler has developed the Neon in only 31 months at a cost of less than $1.3 billion. The company readily acknowledges that its use of CAD/CAM/CAE tools ... has played a critical role in getting the Neon out of the door in record time and at minimal cost."*
>
> *van Niekerk (1995 : 9)*

The most important advantage of CADCAM is that it eliminates the need for a part program. Object geometry and probe path motion are automatically assessed to produce the machine control code. Without having to evaluate part geometry and define the probe motion in the NC process greatly reduces the time required to program a machine as described in *Computer Graphics (1995b)*

Additional benefits include interactive graphic displays which allow the motion of the machine to be displayed and easily edited. An approach to programming in a CADCAM environment may be outlined as follows (*McMahon: 1993)*:

- Aspects of part geometry important for machining purposes are identified. Geometry is edited and additional geometry may be added to define boundaries for the probe path.
- Probe motion and geometry is defined (from a prespecified library of probes/tools).
- The desired sequence of operations and major probe paths are defined interactively.
- The probe motion is displayed and may be edited to refine motion.
- Upon completion the machine control data is output by the system for direct operation of the machine.

CADCAM yields faster solutions for the machine control programs along with an easier environment for the operator to work. All the aspects of numerical control described are automatically integrated by the CADCAM system eliminating repetitive calculations traditionally performed by the part programmer. The prevalent approach to computer assisted

programming today is to prepare the machine control code directly from the CAD part geometry, either by using NC programming commands included in the CADCAM system or by passing the CAD geometry into a dedicated CAM program *(McMahon : 1993)*. The reader is referred to *Gold (1991)* and *Zeiss (1994)* for examples of CADCAM numerical control.

3.5 Application of Rotary tables to co-ordinate measurement machines

The orthogonal arrangement of the axes on 3-axis CMMs allows access to any point within the measuring volume (as opposed to all points on the object's surface which may require the use of a specialised probe head). The addition of a rotation axis would then appear to be unnecessary. In the case of symmetrical objects and solids of revolution, a rotation axis reduces the probe path travel distance and hence the time spent in moving the probe. For highly twisted profiles, such as impellers, probing is practically impossible without a rotary table (*Neumann : 1985)*. The application of rotary tables to objects with more irregular geometry also has advantages. *Neumann (1985 : p.5)* lists some of these advantages :

- Increase in the effective measurement volume.
- Simplification of probe configuration.
- Extension of probing options.
- Improvement of visibility/ accessibility of objects.
- Reduction of temperature influence due to shorter travel paths.

The probe configuration is simplified since the measurement of an object will always proceed from one side of the CMM (see ***Figure 3. 4*** p.41). The object is then rotated to allow the probe access to other regions of the object. The rotary table increases the capabilities of a 3-axis machine to those of a 4-axis machine by introducing an extra axis. The additional axis allows greater accessibility to the object while at the same time increasing probe head options. The reduction of temperature effects due to shorter time periods for shorter probe paths is obvious.
A comparison of probe path travel areas is illustrated in ***Figure 3. 4*** (p.41). The increase in effective measuring volume is derived from the area comparison but requires further explanation.

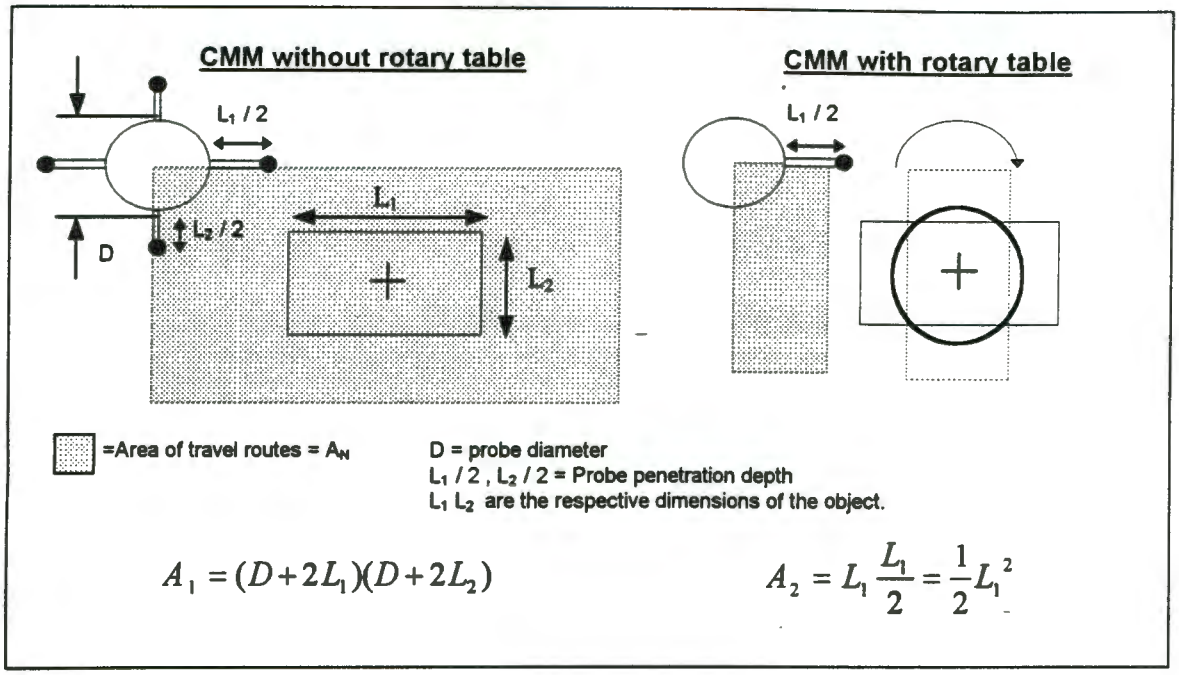

Figure 3. 4 - Comparison of Probe Travel Areas : with and without a rotary table.

Note the simplification of the probe required for measurement with a rotary table (one probe head vs. four probe heads for measurement without the rotary table) from Neumann(1985 : p.6).

If the area ratio $V = \frac{A_1}{A_2}$ then the following ratios of the area covered by the probe in ***Figure 3. 4*** may be determined:

$$D = \frac{L_2}{2},\ L_2 = \frac{2}{3}L_1 : V = 7.8 \quad (\textit{as illustrated})$$

$$D = \frac{L_2}{2},\ L_2 = L_1 : V = 12.5 \quad (\textit{for square object})$$

$$D = 0,\ L_2 = L_1 : V = 8 \quad (\textit{for low object height})$$

$$D = 0,\ L_2 = 0.1L_1 : V = 0.8 \quad (\textit{for long, narrow object})$$

The relationship between the area traced by the probe path and the measuring volume is discussed in section 3.5.1.

3.5.1. Increase in effective measuring Volume.

The comparative area of the probe path route is smaller when a rotary table is used (see ***Figure 3. 4*** p.41). ***Figure 3. 4*** represents the relative motion of the probe along two axes. By introducing a third axis the volume of the probe path may be defined. However the probe path in the third axis will be identical in both cases. Thus the ratios calculated previously (relating to area comparison) represent the ratios between measuring volumes of the two probes. A single probe head using a rotary table will be capable of measuring an object with volume 7.8 times greater than a four headed probe and no rotary table (using an object with dimension ratio of 2:3 as illustrated). The volume advantage created by the rotary table is further increased with square geometry (ratio = 12.5), but diminishes for long narrow objects (ratio = 0.8).

The use of a rotary table does require additional calculations to be introduced to the measurements in order to obtain corrected co-ordinates. The relationship between the machine co-ordinate system (in the case of a conventional CMM), rotation axis and the object must be established (see ***Figure 3. 5*** p.42) in order to make these calculations.

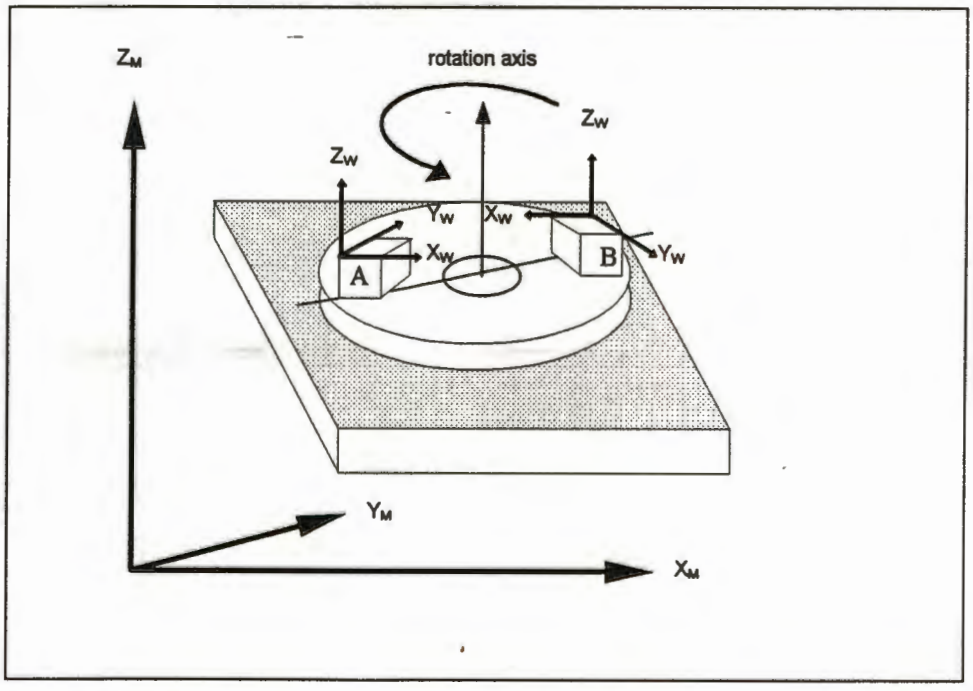

Figure 3. 5 - Relationship of Rotation Axis and Machine Co-ordinate System.

where :

- *X_M Y_M Z_M are the axes of the machine co-ordinate system*
- *X_W Y_W Z_W are the axes of the object co-ordinate system*
- *A and B are 180° apart.*

The object need not be centred with respect to the rotary table. The object co-ordinate system is defined in two positions, A and B . The axis of symmetry between the two z-axes is defined as the rotation axis. After calibration of the rotary table in this fashion the controller automatically calculates the correct co-ordinate as defined in the machine co-ordinate system, taking the rotation into account (see ***Figure 3. 6*** p.43). A similar calculation is performed to orient the object space co-ordinates measured by the *MILLMAP* system when applying a rotation. Discussion of the method used for the *MILLMAP* system is given in Chapter five (section 5.4).

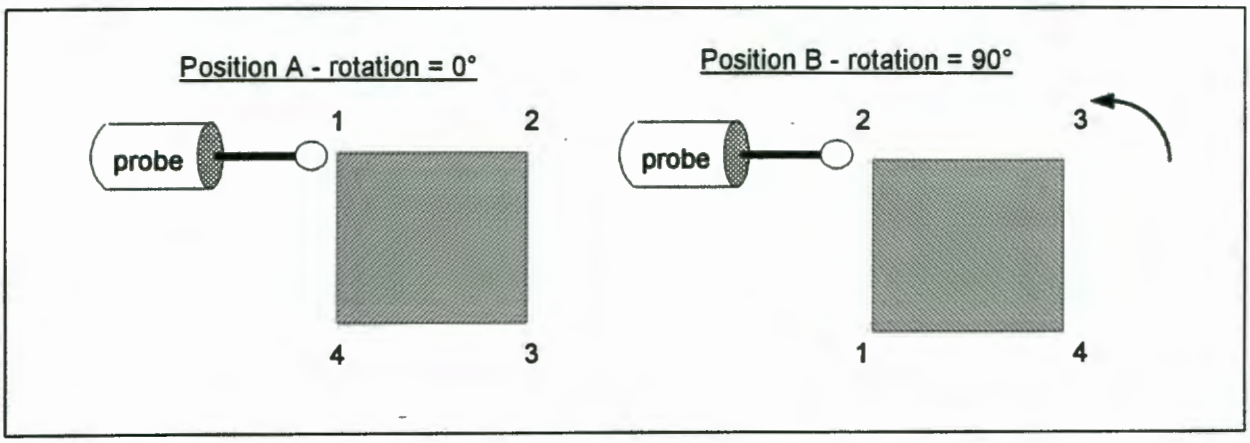

Figure 3. 6 - Nature of Rotation Correction to Probe Co-ordinate.

Consider the 2D case illustrated for a block of unit dimensions 2 X 2. In position A the probe has co-ordinates (0, 0) and rotation = 0°. In position B the probe has co-ordinates (0, 0) and rotation = 90°. The co-ordinate measured in position B is for point 2, therefore the probe co-ordinate must be corrected for rotation (90 °) to give the correct reading of (0, 2) for position B (point 2).

There are several factors introduced by the rotary system that must be determined to assess the impact of errors associated with the rotary table on the accuracy of the measurement system. *Neumann (1985)* lists the following :

- Angle position uncertainty
- Angle position reproducibility
- Axial runout
- Radial runout
- Wobble
- Permissible load

The rotation axis may be horizontal or vertical depending upon the CMM application. The concept of the rotary table is used in this project for the Object positioning system. A horizontal rotation axis has been chosen to maximise the orthogonality of the object surface to the laser beam (which is projected vertically). A detailed discussion of the rotation system used for this project may be found in Chapter five.

Chapter Four

Review of Specialised Measurement Systems.

The literature review by the author has revealed numerous technologies dedicated to solving specific measurement problems. The specific nature of these systems involves the development of specialised equipment and/or application in a controlled environment. This Chapter reviews several systems investigated by the author. Some of the systems are not photogrammetric systems but are described to illustrate the various solutions and techniques used to solve measurement problems. The systems will be discussed under the following headings :

4.1. Triangulation - Intersection Techniques

4.2. Structured Light Techniques, and

4.3. Further Measurement Techniques.

In all cases it will be assumed that the orientation parameters for the sensors have been predetermined by calibration.

4.1. Triangulation - Intersection Techniques

Haggren (1986) describes a system developed at the Technical Research Centre of Finland known as MAPVISION. The system uses four solid state (CCD) cameras to capture images of the object. Targets are then projected onto the object (using a laser) and a second set of images captured. The first set of images (object only) are subtracted from the second set (object + target) resulting in an image consisting of the target only. This resultant image eliminates the need for complex target recognition algorithms since the image is comprised of the target only. The image co-ordinates for the centre of the target in each image are computed and the object co-ordinates calculated using the orientation parameters for each image in a space intersection.

The system is non-contact using photogrammetric principles but requires active targeting of points on the object. Once a point has been measured the target can be moved to the next point. A relative accuracy of 1:5000 is reported *(Haggren : 1986)* with approximately 1 second required to process each point.

El-Hakim (1986) describes a system developed at the Photogrammetric Research Section of the National Research Council of Canada. The approach is similar to that of the MAPVISION system described earlier, however only a single set of images is captured (the target points are attached to the object prior to image capture). These images contain the object as well as attached targets. Feature extraction routines (based on a choice of up to 50 linear and non-linear convolution operations) are used to identify targets and then the centres of these targets are computed using the centroid method (see Chapter two). This provides image co-ordinates for the space intersection to proceed as in the MAPVISION system. The results from the measurement of different objects with the system range from RMS accuracy estimates of x=0.014mm y=0.015 z=0.022mm (for an image scale of 1:3 and a high contrast object) to x=0.112mm y=0.121mm z=0.255mm (for an image scale of 1:40 and a poor contrast object) *(El-Hakim : 1986).*

The Zeiss laser triangulation system LTP 60 *(Zeiss : 1990a, 1990b)* while not a photogrammetric system, relies on the triangulation principle with optical sensing. The system is mounted on the probe of a CMM replacing the conventional contact probe head. The measurement principle relies on the projection of a laser beam onto the object, an optical sensor at a specified oblique angle records the position of the laser spot. The optical sensor consists of the imaging optics (lens system) and a diode array for the actual recording of the image. Grey scale image processing techniques are used to determine the position of the spot based on the measuring range. The probe is moved in the z-direction by the CMM to determine the convergence of the beam with the optical plane, thus determining the range from the laser probe to the object. Knowledge of the CMM z-co-ordinate plus the range determined from the laser probe provide the final z-co-ordinate for the measured point. The x-y co-ordinates are determined directly from the CMM which acts as a delivery device for the laser probe. The principle of the laser triangulation technique is illustrated in ***Figure 4. 1*** (p.47).

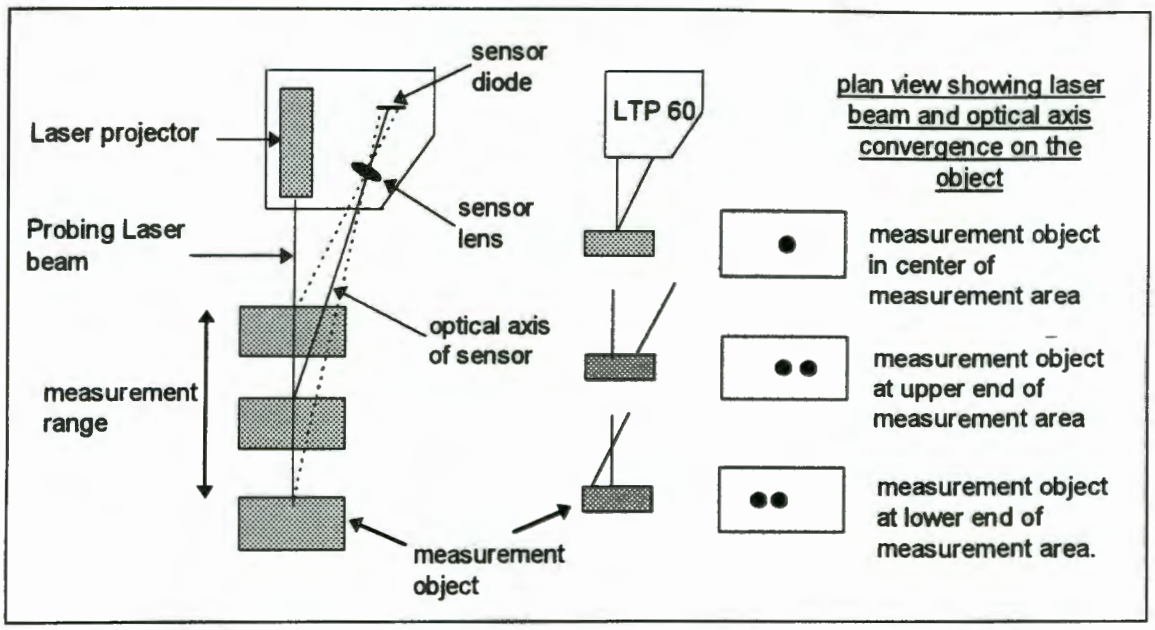

Figure 4. 1 - Measurement principle of Laser Triangulation Probe.

Zeiss (1990b).

Examples of applications of the laser probe in the automobile industry include the measurement of seat surfaces and clay models (both non-rigid surfaces that will deform if a contact probe is used). The accuracy of the system is not discussed.

4.2 Structured Light Techniques.

The measurement of surfaces in photogrammetry (as opposed to discrete points) causes two basic problems for solutions using photogrammetric techniques *(Karara : 1989).* The first is that the resolution of measured points must be increased for complex features or reduced for those features with uniform topography. In particular irregularly shaped objects (as found in medicine) require careful consideration of the density of measurement points in order to define the surface of the object. The second problem is that the surfaces that have to be measured are generally homogeneous. This complicates the identification of conjugate points on stereopairs of images. Structured light techniques rely on artificial light conditions to assist in solving the two problems previously described. The nature of these conditions may be passive (as in the case of digital image correlation where the lighting is used merely for targeting purposes) or active (as in the case of Moiré topography and rastereography where the light patterns form part of the actual measurement). Digital Image correlation techniques using structured light will be reviewed in section 4.2.1 while Rastereography and Moiré techniques will be discussed in section 4.2.2.

4.2.1 Digital Image Correlation Techniques

Digital Image correlation techniques are used extensively for the measurement of homogeneous, low contrast objects. In the case where the application of targets to the object is difficult or impractical, structured lighting techniques provide an alternative solution. A control frame with targets is frequently placed around the untargeted object during the calibration phase to determine the orientation parameters of the sensors. The relative co-ordinates of the control points on the frame are known to a high degree of accuracy, and used to calculate the orientation parameters of the sensors by a three dimensional space resection. Digital image correlation uses corresponding pixel arrays of overlapping digital images to match the images *(Wildschek :1989).* Once conjugate arrays on the images have been matched then the precise location of the centre of the array or patch is determined for the space intersection to be computed.

Wong and Ho (1986) describe a system developed at the University of Illinois which uses epipolar geometry to search for conjugate points on a pair of images. An arbitrary object point on the left hand image is selected and the epipolar line for this point on the right hand image is calculated. By applying the coplanarity equations a conjugate point is searched for along the corresponding epipolar line on the right image. The image points obtained from this process are then used to compute the object space co-ordinates via a space intersection. A relative accuracy of 1:2000 is reported *(Wong and Ho : 1986).*

InduSURF is a system developed by Carl Zeiss for the three dimensional measurement of surface shapes in order to produce a CAD "wire model" representation of the surface. The system was developed by Zeiss in collaboration with Volkswagon AG in 1986 for measurement of styling models in the production of automobiles. *Claus (1988)* describes the function of the styling model during the development of a new car. The manually created styling model will be reshaped, and functional parts redesigned up to 100 times during the development phase. Each alteration has to be remeasured and recorded on the CAD model.

The InduSURF system uses metric or réseau cameras to capture stereometric images of the object, which is specially prepared for correlation by applying a texture which is either sprayed or projected onto the object's surface *(Claus : 1988).* The images are digitised by two CCD cameras specially fitted to a C100 Planicomp to enable automatic measurement of the targets on the object.

A host computer matches the images based on a priori approximations of the image co-ordinates of the various target points derived from a feature-based matching algorithm. No details regarding this algorithm are published. An operator is required to position the floating mark (viewed through the Planicomp) on the object's surface.

The image acquisition phase of the system is not real time (since the images require development before digitisation) but the processing time required by the system is quoted as approximately 1 second per point. At an image scale of 1:15 object co-ordinates with accuracy of 0.2mm are measured *(Claus : 1988)*.

The Programmable Optical 3D Measurement system (POM) is a multi-sensor, non-contact, optical measurement system that uses digital image processing and close-range photogrammetric techniques. *Loser and Luhmann (1992)* report that the system was initially developed for use in the automobile industry by Leica in conjunction with Volkswagen. The system allows data capture using réseau-scanning cameras, CCD cameras and video theodolites with future plans for the inclusion of data from motorised theodolites and laser pointers. The system also uses a rotary table which improves the flexibility of the system for the photogrammetric measurement of complex shapes (*Godding and Luhmann : 1992)*. Object points may be targeted using either retro-reflective targets or laser pointing devices. Feature extraction algorithms to identify elliptical targets are used. The three dimensional point determination of object co-ordinates is calculated using a multi-image space intersection, the camera orientation elements being predetermined by a calibration process. The determination of the system accuracy is dealt with in *Godding and Luhmann (1992)* and quoted at ±0.1mm for an object space of 2.0 x 2.0 x 0.6 m at a rate of 1 point per 30 seconds. Practical examples of the systems application to measure speaker mountings in car dashboards, vehicle cooling tubes and edges of car doors are given in *Loser and Luhmann (1992)*.

Petterson (1992a) describes the Metrology Norway System (MNS) which like the POM system previously has been developed for the Automobile (and in this case Aerospace) industry. The MNS is a non-contact, photogrammetric system that uses high resolution CCD cameras to measure image targets produced by Light Emitting Diodes (LEDs) or laser spots. An additional device described as "The Light Pen" (see ***Figure 4. 2*** p.50) may be used to give the system the capability of a "Hand Held Co-ordinate Measurement Machine".

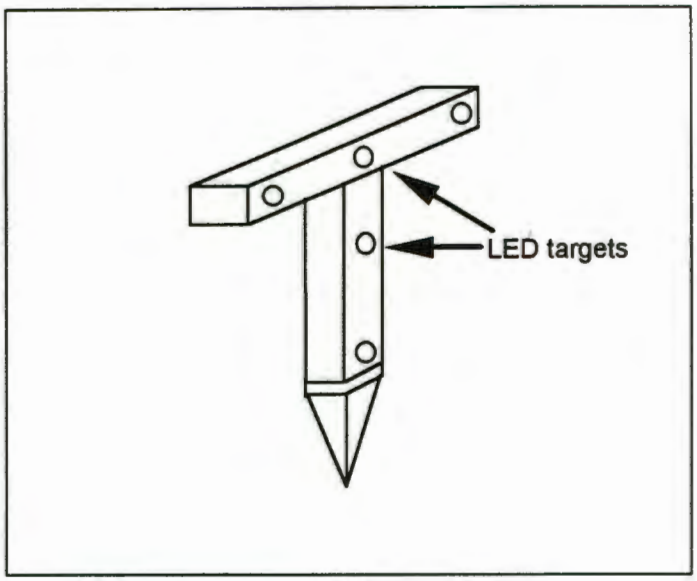

Figure 4. 2 - Metronor "Light Pen" pointing device.

Petterson (1992a) notes that a specially patented factory calibration technique is used by Metronor to establish high accuracy values for the interior orientation elements of the CCD cameras. No details of this technique are made available. The exterior orientation parameters are determined from a Reference bar constructed of Invar with control points illuminated by LEDs. Bundle adjustment is used for calibration of the overall system. Practical application of the system to measure manufactured surfaces at Saab, Volvo and Fiat are given by *Petterson (1992a).* A general system accuracy of 0.1mm for car body measurements is quoted *(Petterson : 1992a)* at a rate of 2 measurements per second. A detailed discussion of the accuracy of the system may be found in *Petterson (1992b).* A specialised Single camera version of the MNS system is described later in section 4.3.3 -Single Camera System (SCS).

Gruen and Baltsavias (1988a) describe a system using Multiphoto Geometrically Constrained Matching (MPGC) to correlate images used to measure the shape and size of a human face. Details of MPGC matching may be found in *Gruen and Baltsavias (1988b).* Due to the lack of contrast on images of the face a vertical line pattern is projected onto the face to provide sufficient contrast. The average image scale used was 1:43 with the control point targets measured to an accuracy of 0.2mm. The processing time is given as approximately 1 second per point, with relative accuracy of 0.09mm in the z-axis. Due to the nature of the measurements, (on the human face) a qualitative estimate of the accuracy of the system is given : *"The accuracy as checked visually was very satisfactory" (Gruen and Baltsavias, 1988a : 116)* .

Van der Vlught and Rüther (1994) developed a system using MPGC matching techniques to correlate object images in a similar procedure to that of *Gruen and Baltsavias (1988a).* As with the system developed by *Gruen and Baltsavias (1988a)* when texture on the object surface is absent, a pattern is projected onto the surface to artificially create texture. The system has two approaches to identifying image points. Circular features may be extracted (target approach) or, alternatively, patches of interest determined from interest operator functions *(Forstner : 1987)* and thresholding techniques are extracted. Various methods for determination of the centre of these features to sub pixel accuracy are described by *Van der Vlught and Rüther (1994).* The centres of these features are used as image co-ordinates to solve the collinearity equations, geometrically constrained as described by *Gruen and Baltsavias (1988b). Van der Vlught and Rüther (1994)* report an accuracy of 0.11mm in x, 0.14mm in y and 0.37mm in z using this method to measure an outboard motor propeller.

Maas (1992) describes a system which follows similar principles to those of *van der Vlught and Rüther (1994).* Two to four CCD cameras are used to capture images of an object. A slide projector is used to project a regular grid of dots (800 - 8000 for a 300 x 500 mm area) onto the surface of the object. Epipolar geometry is then used to correlate these targets on the different images, and the centres are determined to sub pixel accuracy. These target centres are then incorporated into a spatial intersection with camera calibration data in a single bundle adjustment. The method has been used to create contour plots of a carbon panel under stress, a model car and a bust of Beethoven. No indication of accuracy or time limits are given.

Further examples of systems using projected targets onto the object followed by some form of correlation between images prior to intersection may be found in and *Keefe and Riley (1986)* and *Rüther(1989).* The PHOENICS system described by *Rüther(1989)* has the option of circular target recognition, or a grid following routine to identify conjugate grid intersection points for the correlation of images. *Wildschek (1989)* describes the grid following routine of the PHOENICS system to measure sculptured objects.

4.2.2. Rastereography and Moiré topography.

Digital Image correlation techniques (described previously) depend on the brightness and intensity between images remaining constant. Due to the nature of some surfaces this may be difficult to achieve. The methods described in section 4.2.1 use structured light in a *passive* sense. The lighting is used merely as an aid to creating contrasting targets or texture on the surface of the object in order to measure the surface. Rastereography and Moiré topography are *active*

structured light techniques in that the light patterns projected onto the surface of the object are used directly to measure the object.

Rastereography

Karara (1989) describes Rastereography as being quite similar to conventional stereophotography except that one of the cameras is replaced by a projector with some form of raster diapositive. The raster may be a grid pattern or a line pattern *(Frobin and Hierholzer : 1982b)* depending on the identification routine preferred. The following diagram (***Figure 4. 3*** p.52) illustrates the geometric similarity between Stereophotogrammetry and Rastereography

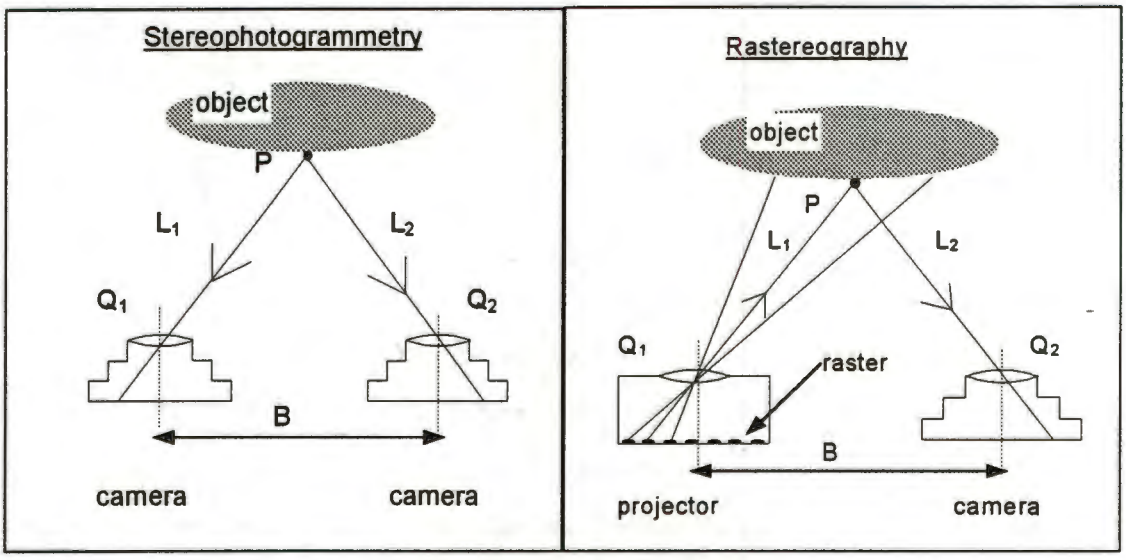

Figure 4. 3 - Stereophotogrammetry vs. Rastereography.

In the sterophotogrammetric case the location of an object point P is determined by spatial intersection of the light rays L_1 and L_2 , which are in turn, determined from the geometry of the stereo-camera pair and from the image co-ordinates of the surface point P in the image planes of both cameras. The geometric parameters (or orientation elements), include the locations of the nodal points Q_1 and Q_2 (stereo base - B), the angular orientation of the two optical axes, and the principle distances (focal lengths) of the cameras (*Karara : 1989).*

According to the principles of geometric optics, the directions of all light rays may be reversed without changing the geometry of the light paths. Thus if one of the two cameras in the stereophotgrammetric case is replaced by a projector with raster diapositive, the direction of light ray L_1 is reversed, but the new arrangement is optically equivalent to a stereo-camera pair. This arrangement captures the same three dimensional data of a stereophotographic system but only one image is required (since the 'image' co-ordinates of the raster are known a priori).(*Karara : 1989*).

Once the geometry of the camera - projection system has been established (via calibration) the computation of three dimensional object co-ordinates of the raster points as projected onto the object may be solved by applying the same perspective geometry equations used in stereophotogrammetry. For detailed explanation of computations and equations for solving the Rastereograph the reader is referred to *Frobin and Hierholzer (1982a).*

El-Hakim (1985) describes a system that uses a line rastereographic approach. A single line is projected onto the object (this reduces the problems associated with line identification and location on the rastereograph) in various positions, thus scanning the surface of the object (see ***Figure 4. 4*** p.54.). A similar identification technique to that used by *Haggren (1986)* (see p.45.) is used. First an image of the object without the line is taken and stored by the system, then a line is projected onto the object and an image captured. The stored image (object only) is subtracted from the second image (object + line), resulting in an image for processing in which only the line is present. The line location, in the resultant image, is found by analysing the grey levels along vertical profiles spaced at intervals specified by the resolution required for the project. Sub-pixel line point location is determined along the peak of the profile. This provides x, y-image co-ordinates of a point. Knowing the co-ordinate of this point on the projector plane, the orientation of projector and sensor (from calibration), collinearity equations can be formed and solved to determine object point co-ordinates. The system described by *El-Hakim (1985)* is used to recognise shapes and positions of objects in near real time for robot manipulation.

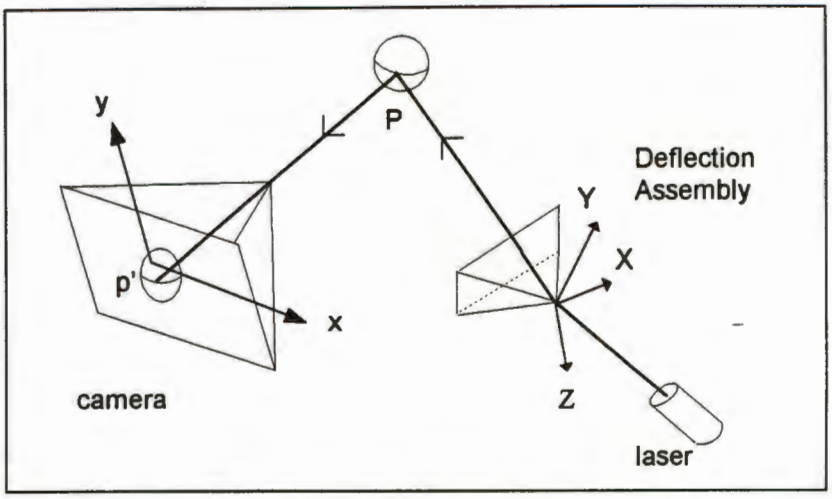

Figure 4. 4 - Camera-Laser scanning device configuration.

(El-Hakim :1985 p.549)

Where :

- *XYZ are the axes of the Laser deflection system.*
- *P is the object point on the scan line.*
- *x,y are the axes of the image plane.*
- *p' is the image of P.*

The Reverse Engineering System developed by *Kreon Industrie (1995)* uses a laser line projector and two CCD cameras to triangulate by laser section (see ***Figure 4. 5*** p.54). This non-contact measurement system may be fitted to a conventional CMM, CNC machine, robot arm or fixed scanning platform. *Kreon Industrie (1995)* report that the system can acquire 600 points per section, at a rate of 10 points per second and with an error estimate after filtering of 20-60µm.

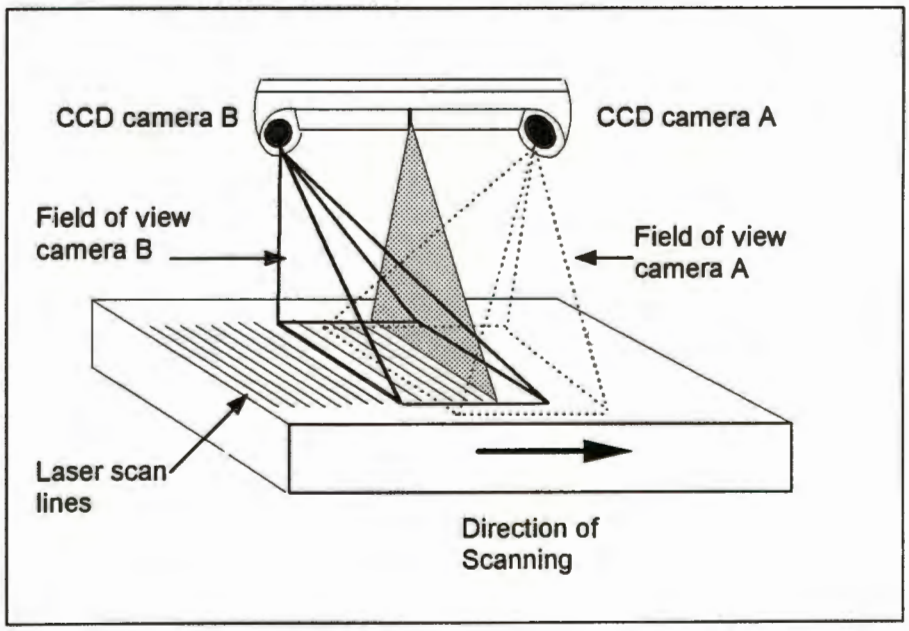

Figure 4. 5 - Kreon Laser Scanning Device.

Kreon Industrie (1995 : 3)

The dual camera system used in the Kreon system is not used for stereometric measurement although stereoscopic vision is a possible option. The system relies on dual rastereographic scanners, using the same projected laser line, operating in conjunction with each other. The purpose of the arrangement is to prevent occlusions of the scanning line in certain conditions (see ***Figure 4. 6*** p.55). The cameras are calibrated together with the laser scanner prior to measurement. The line may be sampled at a maximum of 600 points along its length (25-75mm). Where the line is visible from both cameras the redundant camera solution is included in the measurement calculation. The Kreon system uses a non-contact, rastereographic measurement technique which has been used in the following industrial applications :

- Reverse Engineering.
- Copying / Reproduction.
- Inspection and on-line control.
- Backup copies for accurate reproduction of dies and moulds.
- Backup copies of parts no longer in production.

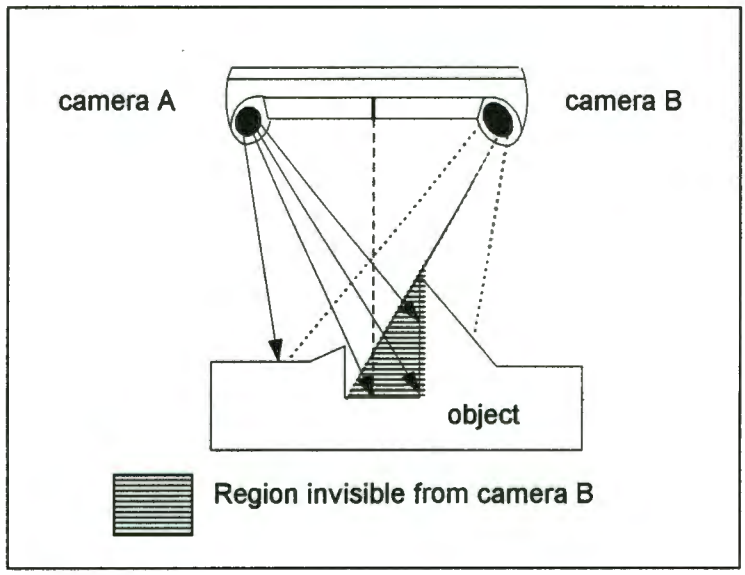

Figure 4. 6 - Occlusion of Camera due to Object shape

Kreon Industrie (1995 : 18)

Moiré Topography.

The Moiré phenomenon is produced when two sets of identical parallel lines (denser than the line raster used in rastereography) are superimposed approximately parallel to each other. The principle of Moiré topography requires that a raster pattern be projected onto the object to be measured. The object scene is then captured by the sensor which observes the object through a second raster. The second raster is undistorted by the object and reconstructed from "optical computing" *(Frobin and Hierholzer : 1982b).* The first (projected) raster will be distorted by the

object geometry resulting in Moiré interference patterns being recorded by the sensor. By measuring these fringes the geometry of the object can be determined. The reader is referred to *Karara (1989)* for a full explanation of Moiré topography measurement techniques.

An alternative approach is to use a shadow Moiré technique (see ***Figure 4. 7*** p.56.). This consists of projection and superimposition of rasterlines from the same grid. The procedure requires that the surface be illuminated by a light source projected through the raster grid. The image is then captured through the same grid resulting in the Moiré interference pattern on the image.

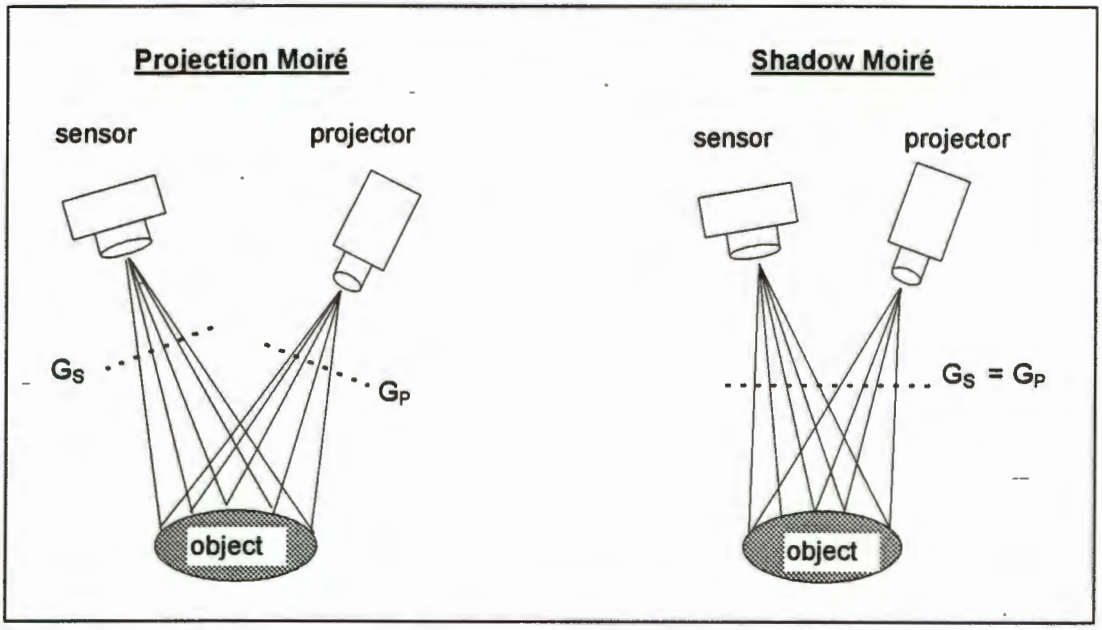

Figure 4. 7 - Shadow vs. Projection Moiré.

The projection Moiré situation uses a separate raster grid for the sensor (G_S) and the projector (G_P). The shadow Moiré technique uses a single grid for both projection and sensor ($G_P = G_S$). Note that in the case of Shadow Moiré the angle of incidence between projector and sensor will tend to be less than in the projection case.

Unlike the techniques described in previous sections the interference pattern created by Moiré techniques relate directly to the geometry of the object. The Moiré fringes represent isolines on the surface of the object (see ***Figure 4. 8*** p.57). The height difference between fringes may be calculated, however distinction between "hill" and "valley" features (i.e. the sign of the height differences) is a restriction due to ambiguity in fringe order *(Keefe and Riley : 1986).* The major use of Moiré topography lies in Biomedical applications and structural deformation analysis. The reader is referred to *Karara (1989)* for further reading.

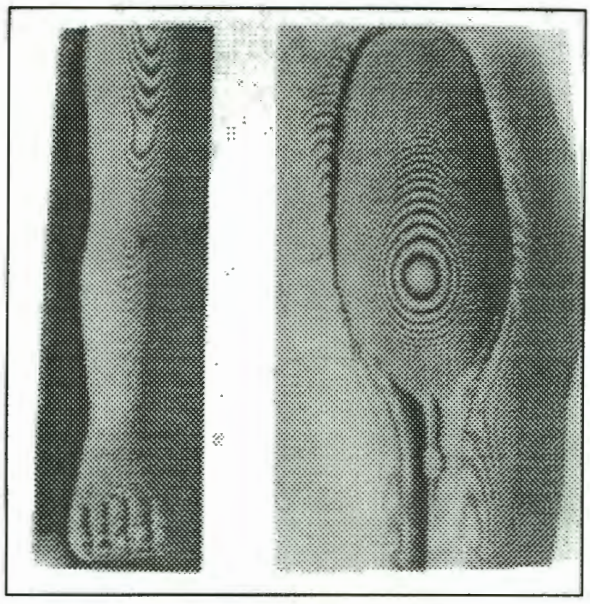

Figure 4. 8 - Examples of Isolines formed by Moiré interference Fringes.

4.3 Further Measurement Techniques.

This section aims to review those systems investigated by the author in the literature search that do not fall into the categories previously listed (Sections 4.1 and 4.2). These systems are used to capture three dimensional data from objects and will be described to illustrate the wide variety of techniques available in the metrology field. The following systems will be presented :

- Optical Probing system - *Zeiss (1985).*
- A Vision Based Co-ordinate Measurement Machine - *El-Hakim (1989).*
- Single Camera System (SCS) - Metronor AS *(Åmdal : 1992)*
- 4D Laser Scanning System - *Hartl, Wehr, Pritschow and Iannides (1992).*
- Line scanner sensors - *Godber, Robinson and Evans (1992).*

4.3.1. Optical Probing system.

The Optical Probing system by *Zeiss (1985)* is a non-contact, single sensor device, designed to work in conjunction with a conventional co-ordinate measurement machine (CMM) previously described in Chapter three. The probe head of the CMM is replaced by a video camera with a Newvicon video tube. Applications of the system are described by *Zeiss (1985 :1)* as follows :

> *"for measuring of parts which could not be measured (or at least at great expense) by conventional mechanical probing. This applies, for example , to flat parts without edges (such as films, foils, circuit boards, vacuum deposited layers etc). Other typical fields of application can be found in the inspection of soft parts which evade mechanical contact."*

The system has Image Processing functions which perform the following :

- Thresholding the grey image to create a binary image for measurement.
- Centroid function (to find the centre of given targets).
- Erosion, dilation, opening and closing to improve the quality of the digital image.

The x and y co-ordinates are measured directly from the CMM which is positioned according to a prespecified grid used to map the object. The z-axis measurement is determined by the focus of the image. The focus of the video camera remains at a fixed distance (pre -calibrated) therefore the distance to the object's surface is adjusted by moving the video camera, in the z-axis direction of the CMM, until a sharp, focused image is achieved. The focal distance is added to the z-co-ordinate of the CMM to provide a z-co-ordinate for the measured point. The x,y co-ordinates of the measured point are determined directly from the CMM. From the information supplied *(Zeiss:1985),* it appears that the system has the capability to track edges around the object. The system can also be numerically controlled in a CADCAM environment to approximately follow edges, or features based on working drawings. Accurate measurements are then made by positioning the probe with the optical positioning system. The accuracy of the system is quoted at 2-10μm depending on the lens used and lighting conditions and the minimum measurement time of 40ms for 512 x 512 image points *(Zeiss : 1985).* The system description appears to be near real time but information regarding detailed tests was not available.

4.3.2 A Vision Based Co-ordinate Measurement Machine.

This system was developed by *El-Hakim and Barakat (1989)* in order to present an attractive solution to increasing the accuracy of low standard Co-ordinate measurement machines (CMMs). The system uses a conventional low accuracy CMM as a delivery system, while measurement of the object is achieved by a four camera vision system. *El-Hakim and Barakat (1989)* describe the advantages and disadvantages of both optical techniques and CMMs in the measurement of objects. CMMs are listed as excellent for the measuring of sculptured surfaces and inside "difficult to see areas." Vision systems are described as less costly, mainly passive systems with flexible volume capacities. The system developed by *El-Hakim and Barakat (1989)* aims to combine the advantages of both systems providing a hybrid solution.

The principle of the device relies on a low cost CMM to deliver a contact probe with no measurement capabilities to the point of interest on the objects surface. The vision system tracks the motion of the CMM by means of a high contrast target fixed to the probe itself. The vision system comprises of two pairs of CCD cameras stereometrically arranged. The second pair of cameras have their baseline perpendicular to the depth direction of the first pair. By this arrangement the first pair provide X and Z co-ordinates while the second pair provide the Y co-ordinate (see ***Figure 4. 9*** p.59). *El-Hakim and Barakat (1989)* report that test results yield an accuracy of 1 : 35 000 . The time to acquire object measurement will be dependent upon the speed of the CMM delivery system and the complexity of the object itself.

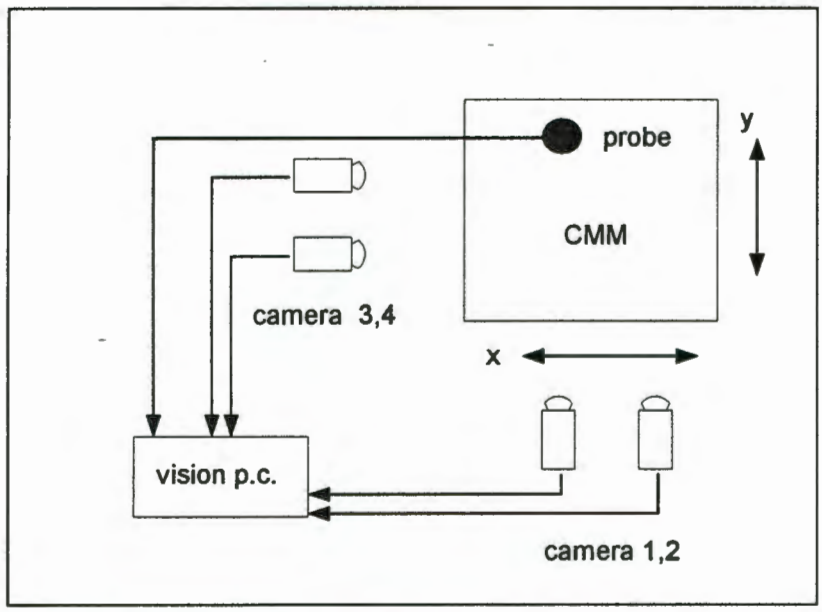

Figure 4. 9 - Block diagram of Vision Based Co-ordinate Measurement Machine.

(El-Hakim :1989 p.218)

4.3.3 Single Camera System (SCS)

This system has been developed as an alternative to the Multi-camera Metronor Norway System (MNS) previously described in section 4.2.1 Digital Image Correlation Techniques. The standard photogrammetric application uses a minimum of two camera stations, with the orientation elements of the cameras determined by calibration. The Single Camera System (SCS), as the name implies, uses a single camera in conjunction with a special "Light Pen" (see ***Figure 4. 2*** p.50) to determine 3D co-ordinates of measurement objects. *Åmdal (1992)* states that the idea of the SCS system was initiated at SAAB Scania Aircraft Division in Linköping, Sweden and developed by Metronor AS. The reasons for developing the SCS system are given by *Åmdal (1992):*

- To have a system capable of being used on large constructions in the aircraft industry.
- To have a system that has fast operation. The SCS does not require system calibration since there is no relative orientation with another sensor.
- To have a system that is capable of reaching inaccessible regions where dual or multi-camera set-ups are not possible due to physical restrictions.
- To have a system capable of measuring hidden points (i.e. not visible from the camera). For example, the Light Pen may be inserted into a bore to measure the depth. The top of the pen which is measured, will still be visible, while the tip of the pen, measuring the depth of the bore, is invisible to the camera.

The pre-calibrated light pen is a fundamental component of the system and acts in a similar capacity as the calibration frame for conventional photogrammetry. Different pen tips allow flexibility to different types of objects. The SCS software uses a bundle solution to calculate 3D object point co-ordinates in an on-line solution, or alternatively post processing of multiple measurements for improved accuracy. *"The accuracy characteristics are quite different for the SCS compared to a dual or multi-camera system. Higher accuracy is achieved in the XY plane (lateral and vertical axes which are parallel to the sensor inside the camera) than in the z-direction (along the depth axis which is perpendicular to the CCD sensor in side the camera)"*

Åmdal (1992 : 230).

Practical applications of the SCS include :

- Measurement of the straightness of aeroplane fuselages.Measurement of wing contour.
- Measurement of flush and gap on nacelle (aircraft engine cover).
- Measurement of collision tested cars.

4.3.4 - 4D Laser Scanning System.

A 4D laser mapper has been developed at the Institute of Navigation (University of Stuttgart) by *Hartl, et al (1992).* The system measures objects by a two dimensional scanning laser beam, and records the intensity of the laser spot (diameter 2mm) at a particular location on the objects surface. The data acquired is thus four dimensional, comprising of the XYZ co-ordinate and the fourth element, the intensity (I) of the point. All the data is stored on disc for the subsequent reconstruction of a computer model for the measured object. The laser beam is moved across the

objects surface by the Opto-Mechanical Deflection unit (see ***Figure 4. 10*** p.61) which consists of two galvanometer scanners. If the deflection angles of the two scanners are known and the range to the object, then the three dimensional co-ordinate for the object point may be calculated. The deflection angles are derived directly from the galvanometers and the range is deduced by modulating the optical power of the laser with a high frequency signal. A photodiode measures the phase difference of the laser and the range is computed (the reader is referred to *Hartl, et al (1992)* for a complete description of the equations used to compute the range from phase difference of the laser signal).

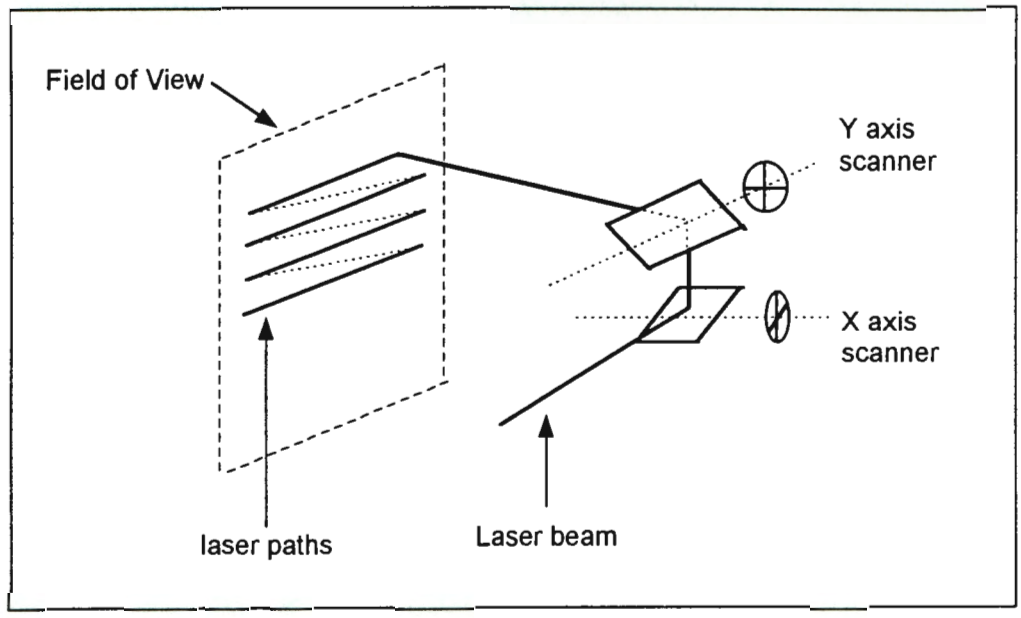

Figure 4. 10 - Opto-Mechanical Deflection Unit.

Hartl, et al (1992 : 524)

The accuracy of the 4D laser scanning system is reported as 0.1mm at a range of 1m (maximum range is 2m) and a scanning time of 20sec is given for 200 x 200 pixels. No practical applications of the system are given.

Chapter Five

Project Methodology and Procedure

This Chapter describes the methodology used by the *MILLMAP* system. Description of the operation procedure with regards to software used will also be presented. The following sections will be discussed :

- 5.1 System Design Overview.
- 5.2 Calibration of the Photogrammetric system.
- 5.3 Measurement of the rotation axis.
- 5.4 Orientation of Rotated points in *AutoCad* - Surface of Revolution.
- 5.5 Measurement of discontinuous objects.

5.1 System Design Overview.

This section deals with a review of the various components that comprise the *MILLMAP* system and discussion of an alternative configuration considered for the project. As previously introduced in Chapter one the system has three major components :

- The Measurement system;
- The Motion Control system; and
- System control, data manipulation, system communication.

The links between these components are schematically represented in ***Figure 5. 1*** (p.64). Each of the components listed above will be reviewed in detail in the proceeding sections

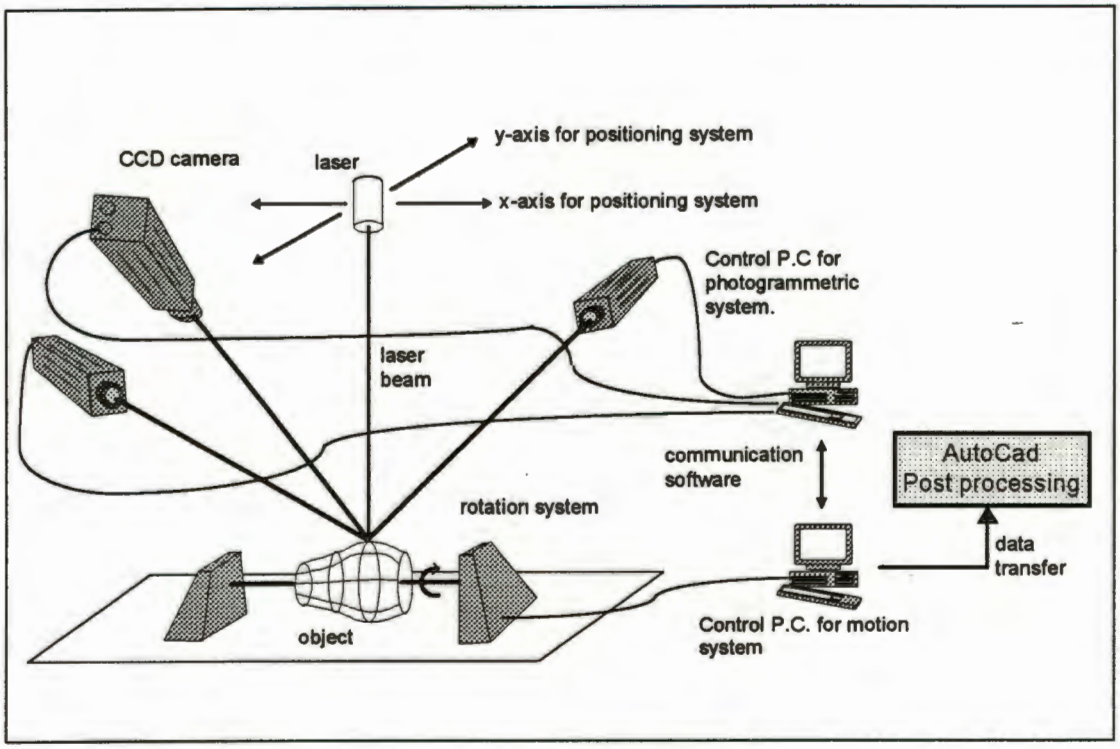

Figure 5. 1 - Components of the MILLMAP system.

- *The Measurement system is comprised of the three CCD cameras, the photogrammetric control P.C. and the laser.*
- *The Motion Control system is comprised of the Object positioning system (rotation system), the Laser Positioning system and the P.C. for the Motion Control system.*
- *The communication software provides a link between the Measurement and Motion systems. Data processing is performed using AutoCad (v.12) in a post-processing environment.*

5.1.1 Measurement system

The Measurement system selected for the *MILLMAP* project had to be capable of providing sub-millimetre accuracy in the measured co-ordinates by using a non-contact measurement technique. It was anticipated that a digital photogrammetric system measuring the position of a laser dot projected onto the surface of an object would satisfy this criteria. The Measurement system consists of the following components :

- Three CCD digital photogrammetric cameras.
- Framegrabber card
- One dedicated PC for photogrammetric control.
- Image processing and camera control software.
- Laser (for target projection).

In order to make photogrammetric measurements, a minimum of two images, photographed from differing positions with a common overlap, of the measurement area must be captured. In the *MILLMAP* system three cameras were used in order to provide a redundancy check for each measured point. The framegrabber card provided the interface between the cameras and the photogrammetric computer. The CCD camera control software and photogrammetric software were maintained by a dedicated photogrammetric P.C. The hard drive of the photogrammetric P.C also provided a backup medium on which the measured co-ordinates could be stored in the form of a text file.

The photogrammetric software consisted of a control program *MILL*, which provided facilities to capture images for calibration and calculate provisional orientation parameters for the three cameras using the *Direct Linear Transformation (DLT)* solution. The *MILL* program also controlled the automatic measurement of the laser target projected on to the surface of the object using the *Multiphoto Geometrically Constrained Matching (MPGCM)* method. The *MILL* software was developed from the *DIMS©* program written by *van der Vlught and Rüther(1992)*.

The DLT parameters for camera calibration were used in a Bundle Adjustment program *PHOTONET©* written by *van der Vlught (1994)*. The orientation elements for each camera obtained from the Bundle Adjustment were used as the final parameters in the *MILL* program during the measurement of objects. Details regarding the procedure followed to calibrate the cameras are given in section 5.2.

The sequence of operations carried out by the *MILL* software during the automatic measurement of the laser dot projected onto the surface of the object are listed as follows :

1. Images from the three CCD cameras are captured by the framegrabber and transferred to a *RAMDRIVE* created on the Photogrammetric P.C. (the use of the Ramdrive significantly speeds up the process of transferring the images from the framegrabber)

2. Edges on the image from the first camera are extracted and binarised.

3. The circular feature representing the laser dot is extracted and the centre of the best fit circle stored to single pixel accuracy Note : the laser dot should be the only feature present on the

image since the entire system is veiled after calibration to prevent illumination of the object which would generate 'noise' in the images.

In subsequent measurements a window 100x100 pixels centred on the image co-ordinates of the previous laser dot is used. This reduces the processing time required by the photogrammetric P.C. to extract the edges of the laser target. (The window size was chosen to allow for all possible movements of the laser dot within a radius of 5cm from the previous point measured on the objects surface. It was assumed that the grid resolution selected for the Laser Positioning system would never be greater than 5cm.)

4. The circle centre pixel recorded in step 3 is used as the target pixel on the reference image for *Multi Photo Geometrically Constrained Matching.*

The initial epipolar line, calculated for the target search in the matching procedure, considered a z-range of values that allow for an object height of 30cm. In subsequent searches the parameter defining the length of this line is set so that a z-range of 2cm either side of the last height value is calculated. It was assumed that the topography of the object is continuous and that the grid resolution specified prevents the z-value recorded for adjacent points falling outside the 2cm range of the previous value. The shortening of the epipolar search line reduced the time required by the Photogrammetry P.C. to process the images. A window size of 11x11 pixels centred on the circular target located on the epipolar line was used during the sub-pixel grey -scale matching of the targets in the additional two images.

5. Once the matching of the targets on the images has been completed the x,y,z object space co-ordinates of the laser dot are transmitted via the communications software to the Motion Control P.C. where they are cross referenced with the laser position and Object Motion parameters. A record of the x,y,z measured points is also stored on the hard drive of the Photogrammetric P.C. for backup purposes.

6. If the grid defined by the software on the Motion Control P.C. has not been completed then the laser and object are positioned as required and the Measurement procedure proceeds as from step 1. When the system has completed the measurement grid defined it will give the user the option to quit.

5.1.2 Motion Control System

The Motion Control system controls the mechanical movement aspects of the *MILLMAP* system and has two components :

- The Laser Positioning System.
- The Object Motion (Rotation) System.

The software to control these two components was developed by *Parbhoo (1995)* using Borland C++. The configuration of the Motion Control system is illustrated in ***Figure 5. 2*** (p.67)

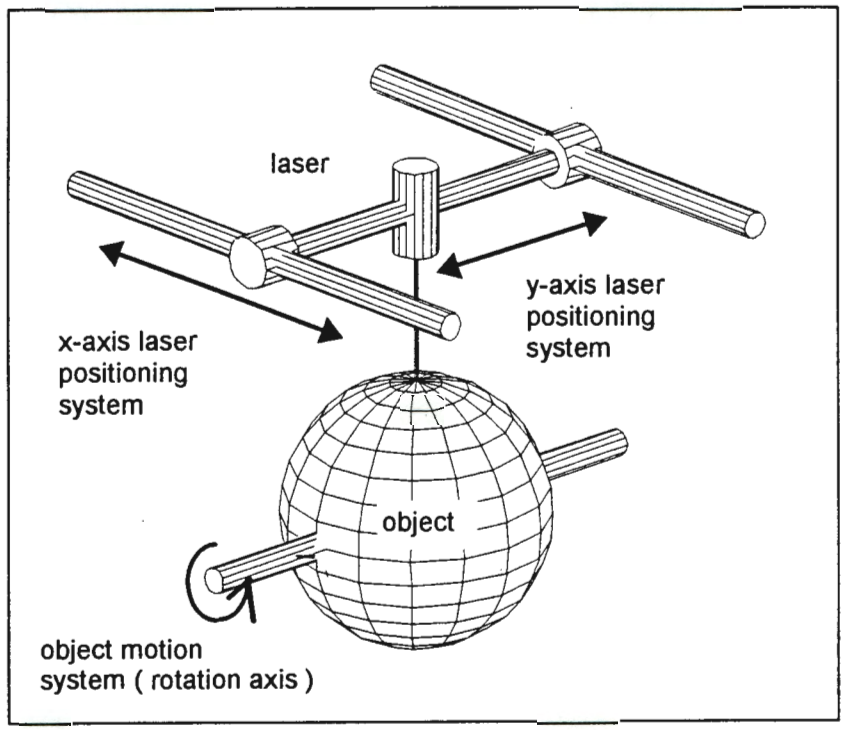

Figure 5. 2 - Motion Control System.

The function of the Laser Positioning system is to translate the laser along dual axes, as illustrated in ***Figure 5. 2***, in order to provide complete two dimensional coverage of the object. The laser provides a target 'dot' on the surface of the object which is measured by the Measurement system. The laser positioning system can be programmed to position the laser at systematic grid points in order that a regular mesh of grid points describing the surface of the object can be measured. This method of controlling the Laser Positing system will be referred to as the *grid scanning* method throughout this dissertation.

The function of the Object positioning system is to rotate the object in order that the Measurement system can capture data over the entire surface of the object. Without a rotation, the system can only

operate as a grid scanner. A dedicated Motion Control P.C is used to control both the Laser Positioning system and the Object positioning system. The x,y machine co-ordinates of the Laser Positioning system and the angle of rotation applied by the Object positioning system are recorded in a text file on the hard-drive of the Motion Control P.C. The x,y,z object space co-ordinates from the Measurement system are transferred from the Photogrammetric Control P.C. (via communication software) and cross referenced with the Motion Control data. A complete record of the position and measurement conditions for each point measured is thus built up as the result file. It is this file that is used as the raw data for the generation of three dimensional mesh representations of the object in *AutoCad.*

Alternative Configuration.

An alternative configuration for the Motion Control system was considered. The configuration had to satisfy the criteria that the entire surface of the object be accessible to the Measurement system. The configuration differs from the Motion Control system shown in ***Figure 5. 1*** (p.64) in that the laser is fixed in a stationary position. The object is translated and rotated in order to provide the access required by the Measurement system. This configuration is illustrated in ***Figure 5. 3*** (p.68).

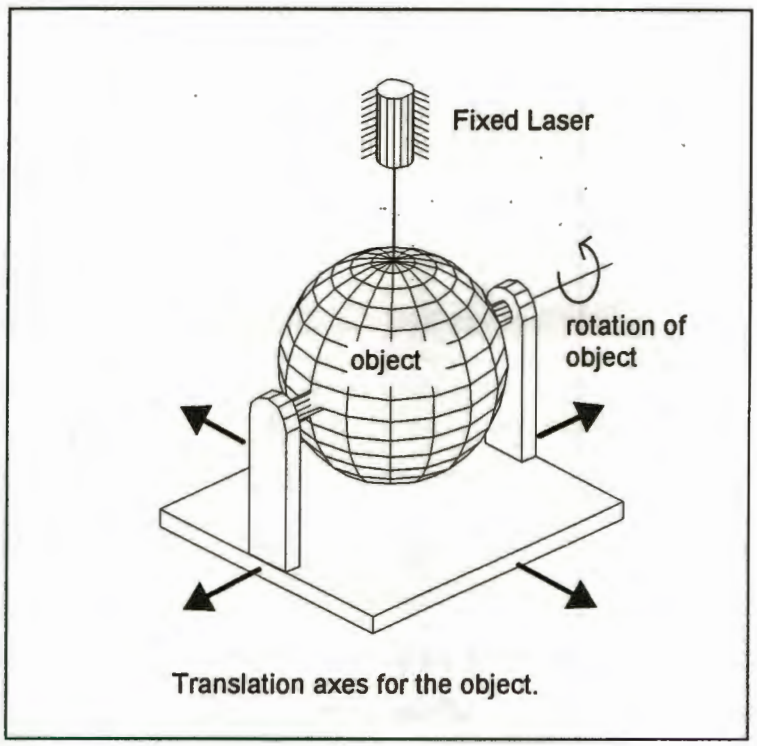

Figure 5. 3 - Alternative Motion Control Configuration.

The advantages of this configuration are that the laser can be any size. It need not be mounted on the device itself, the laser beam can be deflected via a series of mirrors onto the surface of the object.

The stationary laser would allow the field of view of the photogrammetry system to be reduced to a window in which the laser will always be positioned (since the laser is not moving over the entire object). This reduction in the field of view reduces the image scale which improves the resolution of the laser target thus increasing the accuracy of the co-ordinates measured by the photogrammetry system. The image processing required to extract the target would be minimal since the target would be the only feature in the image.

The disadvantages of this configuration are that in order to provide the Measurement system access to the entire surface of the object, the translation axes for the object must operate over an area four times the area of the object (i.e double the dimensions of the object =2x2=4 x area). The mechanical complications with supporting a device this size and ensuring the stability of the object motion table are limiting. Discussion of the mechanical complications associated with this configuration may be found in *Parbhoo (1995).*

5.1.3 System Control Data Manipulation and Communications

Two computers are used to control the *MILLMAP* device during operation. A sequence of operations is carried out by each computer which are dependent upon each other as illustrated by the flowchart in ***Figure 5. 4*** (p.70). In order for the two computers to be able to execute their respective operations some form of control link between them is necessary. The two computers were linked via a standard RS232 communication port. Communications software on each computer provided the system with the interface to exchange data. Details regarding the Communication software may be found in *Parbhoo (1995).*

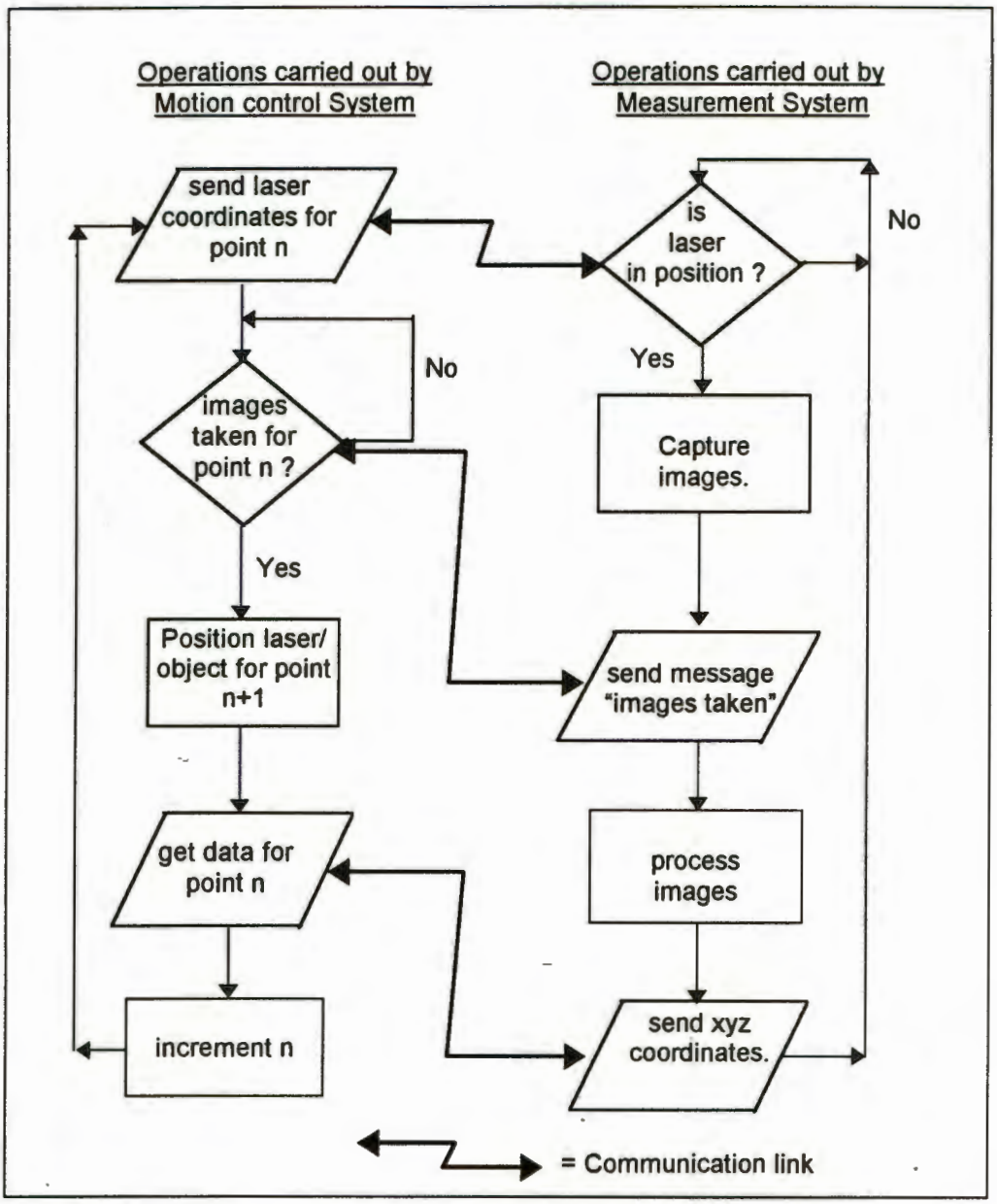

Figure 5. 4 - Flowchart showing Communication links during measurement.

from Parbhoo (1995)

Once the measurement data had been collected for the object it was processed using *AutoCad.* Various macro functions were written in C++ code by *Parbhoo (1995)* to produce the final three dimensional meshed surfaces which describe the surface of the measured object in *AutoCad.* Examples of the result meshes may be found in Chapter seven of this dissertation.

5.2 Calibration of the Photogrammetric system.

Prior to executing the measurement procedure described in section 5.1.1 the Photogrammetric system must be calibrated. As described in Chapter two, calibration determines the orientation parameters of the cameras, which are required to carry out the photogrammetric measurement of object points. The orientation parameters are determined by the measurement of control points with known (x,y,z) object space co-ordinates. The control points used to calibrate the *MILLMAP* system were located on a control frame (see ***Figure 5. 5*** p.71) which was positioned in the measurement region, where the object would be mounted, prior to measurement. Images of the control frame were captured by the three CCD cameras and processed to extract the image co-ordinates for the centre of the control points to sub-pixel accuracy. By solving the collinearity equations for the image and target points in a Bundle Adjustment the orientation parameters for each camera are solved for. This section describes the sequence of events executed by the *MILL* software in order to calibrate the three CCD cameras. Definition of the orientation elements may be found in Chapter two.

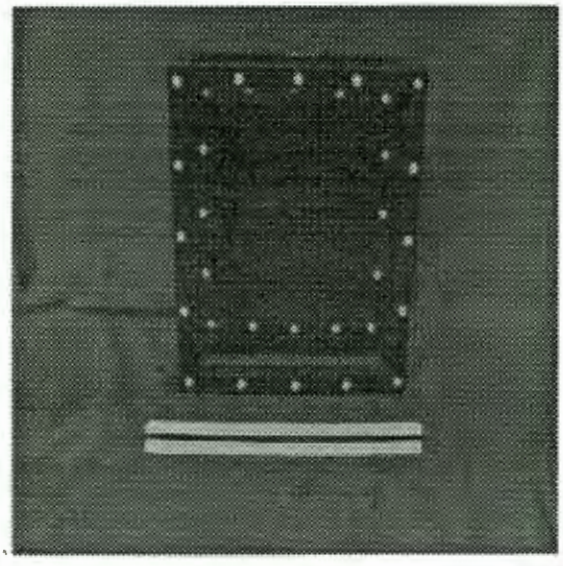

Figure 5. 5 - Control frame used for calibration of the CCD cameras.

The ruler in the foreground has length 30cm.

When the *MILL* software is executed in order to run the *MILLMAP* system the user is given the option to calibrate the system, commence measurement or perform manual measurement. The calibration procedure measures the control targets using the same method described for the laser dot (see section 5.1.1.). Upon selection of the calibration option the following steps are carried out by the *MILL* software (it is assumed that the control frame is positioned in the measurement region of the device and is visible from all three cameras):

1. Three images of the control frame are captured. One from each camera station.

2. Edges on the first image are detected and binarised (later this process will be repeated for images two and three).

3. The binarised edge image has circular features extracted (i.e. the control point locations).

4. The image co-ordinates for the control point centres and radii (determined in step 3) are used to define a window around each control point. The grey scale centre of gravity for each control point is automatically calculated from this window and written to a file representing the image co-ordinates. The user is asked to manually identify 8 control points on the original image to compute the DLT, which automatically identifies and labels the remaining control points. All of the image co-ordinates (automatically identified by the DLT) are stored in a file for input to the Bundle Adjustment program. Provisional values for the orientation parameters of the camera are automatically calculated during the DLT and stored in a file for input to the Bundle Adjustment program.

5. The process is repeated for cameras two and three (from step 2 onwards) until provisional orientation parameters have been calculated and image co-ordinates measured for each camera station.

6. The provisional orientation parameters and the image co-ordinates for each camera are input into the Bundle Adjustment program *PHOTONET©*. The final orientation parameters for each CCD camera are calculated and the results stored on file.

With the calibration parameters of each CCD camera determined, the control frame may be removed, an object mounted for measurement and the measure option of the *MILL* software selected to commence automatic measurement of the object as described in section 5.1.1.

Note : it is essential that the camera positions and attitude are fixed during the measurement phase. Any movement of the cameras will alter the respective orientation parameters causing the software to calculate erroneous image space co-ordinates for points measured. Re-calibration in the case of disturbed cameras is required in this situation.

5.3 Measurement of the rotation axis.

For the *MILLMAP* system to measure the entire surface of an object it must be rotated. This is controlled by a dedicated Motion Control computer which operates the Object positioning system as described in section 5.1.2. The definition of the rotation axis of the Object positioning system in the object space co-ordinate system is a problem which must be solved to orient the points measured by the system (see section 5.4). This section describes the sequence of events used to measure points on the rotation disc in order to define the rotation axis in the object space co-ordinate system. It is assumed that the system has been calibrated as described in section 5.2.

A spherical probe was attached to the rotation disc to provide a target for the three CCD cameras to measure (see ***Figure 5. 6*** p.73).

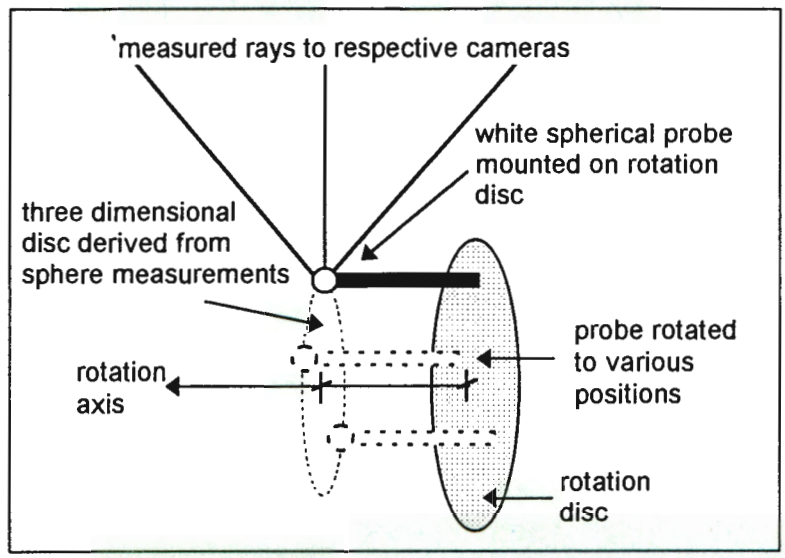

Figure 5. 6 - Probe measurement for definition of rotation axis.

The probe consisted of a white sphere mounted at the end of a thread. The sphere appears as a dot on the images captured by the three CCD cameras. It was assumed that the centre of this dot, from the respective images, would represent the position of a ray passing through the centre of the sphere, and that these rays would intersect as illustrated in ***Figure 5. 6*** (p.73). Measurement with the *MILLMAP* system to obtain object space co-ordinates of this point are then used for the axis determination as described in step 4 of the following procedure.

The procedure used to measure the probe in order to determine the axis of rotation is described in the following steps :

1. Images of the target sphere are captured by the three pre-calibrated CCD cameras. Images are captured in multiple angular positions as illustrated in ***Figure 5. 6*** (p.73).

2. The images of the sphere are processed and the centre of the target extracted with sub-pixel accuracy.

3. The target centres extracted in step 2 are used in a space intersection to determine the object space co-ordinates for the measured positions of the sphere.

4. The object space co-ordinates of the measured probe positions are used to define a best fit three dimensional disc in *AutoCad,* with the rotation axis being defined as the line perpendicular to the plane containing the disc and passing through the centre of the disc (as shown in ***Figure 5. 6*** : p.73).

This method provides a provisional definition of the rotation axis in the object space co-ordinate system. It does not take mechanical imperfections (as described previously in Chapter three) of the rotation disc into account. Due to accuracy limitations discovered in the first design of the Measurement system (see Chapter seven) the provisional definition of the rotation axis using only three measured points, (i.e. no redundancy) was used for the *MILLMAP* project. An alternative method to define the rotation axis (using redundant observations) was considered, in anticipation of more accurate results from the Measurement system. The reader is referred to Chapter seven for discussion of this alternative method.

5.4 Orientation of Rotated points in AutoCad - Surface of Revolution.

When the three dimensional object space co-ordinates for each measurement point are captured by the *MILLMAP* system they are cross referenced to their respective co-ordinates describing the position of the laser (in the Machine co-ordinate system), and the rotation angle applied by the Object positioning system to the rotation disc. The co-ordinates recorded for the position of the laser serve as a check so that the laser can be repositioned manually in the event of a breakdown in the automatic measurement process. The object space co-ordinates are used to generate the mesh in

AutoCad which describes the surface of the object being measured. This section describes the procedure used to orient the object space co-ordinates in the *AutoCad* system by using the angular measurement from the Object positioning system in order to generate a surface of revolution.

1. The first stage requires that the object space co-ordinate system be defined in *AutoCad* .This is achieved automatically by importing the object space co-ordinates describing the rotation disc (as measured in section 5.3) into *AutoCad.*

2. A three dimensional disc is fitted through these points and a line is plotted perpendicular to the disc through the centre of the disc as described in section 5.3. The rotation axis is defined by this line.
3. Any object points measured with zero rotation can be plotted directly in the *AutoCad* system defined up to this point.

4. Assuming the next set of object points is captured by the Measurement system, but have a rotation of α degrees applied by the Object positioning system the following method is used :

- The first set of data points (plotted when the rotation angle = 0) is rotated about the rotation axis (defined in the object space co-ordinate system using the procedure described in section 5.3) by an amount α in the same direction as defined by the physical rotation of the Object Motion disc.
- The data points from the second measurement set is plotted normally as if no rotation had been applied. They are plotted with their respective object space co-ordinates as measured by the *MILLMAP* system. The second set of data points will be relatively positioned correctly with respect to the first set of data points since the same rotation angle, α, has been applied about the same rotation axis (as defined within the accuracy of the Measurement system) to the data set.
  The reader is referred to ***Figure 5. 7*** (p.76) which illustrates the steps outlined in stage 4 above.

5. The entire data set plotted thus far, will be rotated, as described in stage 4, for each new set of rotated data until the entire data set surface of the object has been oriented in *AutoCad.* The resulting three dimensional point cloud in *AutoCad* will contain the correct orientation between the measured points, with the neighbourhood links required to generate a mesh .

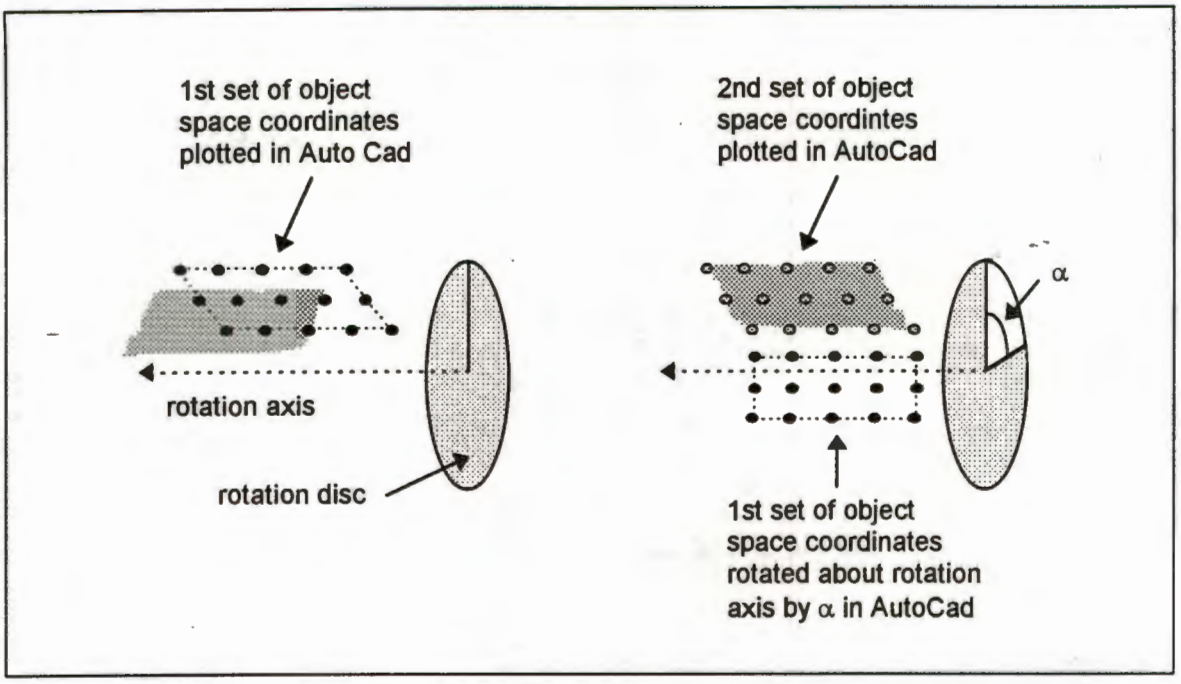

Figure 5. 7 - Orientation of rotated object space co-ordinates.

AutoCad automatically computes the transformation matrices required to rotate the point clouds about a defined axis as described in steps 1-5 above. *AutoCad* allows the implementation of C++ coded routines to automatically read in the data and perform the transformations as described. The C++ routines used to control the orientation and plotting of data points in the object space co-ordinate system were written by *Parbhoo (1995)* .

In order to recreate the surface of the object the oriented point cloud described must be linked together by a mesh to form a surface of revolution. With a record of the sequence in which the data was captured, the neighbourhood relationship between adjacent data points is known and a mesh can be generated in *AutoCad.* A C++ routine to automatically generate a mesh in *AutoCad* from the oriented point cloud was written by *Parbhoo (1995).*

The success of the method described in this section to orient the data points in the object space co-ordinate system and generate the surface mesh in *AutoCad* is reviewed in Chapter seven. The surface mesh is the final product of the *MILLMAP* system, and can be used as input data for CADCAM controlled Milling machines to reproduce a measured object.

5.5 Measurement of Discontinuous objects.

This section describes the method used to measure a discontinuous object. A discontinuous object is defined for this dissertation as "an object that has a disjointed and irregular shape". The grid scanning procedure (see section 5.1.2) and the Surface of revolution method (section 5.4) rely on regular grid spacing between laser positions used to measure object points as well as a regularly defined boundary region. The start point, end point and grid resolution are specified (in the machine co-ordinate system) using the Motion Control software prior to commencement of measuring an object. The choice of values for the grid parameters will depend on the physical properties of the object and the detail required to duplicate the surface of the object These choices are made by the user after inspection of the object.

In the case of a discontinuous object (the test case used was an outboard motor propeller) it is necessary to prepare a customised grid of positions on the surface of the object to control the Laser Positioning system. This grid ensures that the points measured fall on the object. The procedure for preparing the customised grid is listed in the following stages and diagrammatically illustrated in ***Figure 5. 8*** (p.78) :

1. The Laser Positioning system is manually located to points that define the outline of the object. A plot of this outline is then prepared in *AutoCad* using the Machine co-ordinate system to define the working environment.

2. A conventional scanning grid described by a starting co-ordinate, finishing co-ordinate and resolution (in the Machine co-ordinate system) is defined in *AutoCad.*

3. A customised grid is defined by stretching the scanning grid to fit the outline of the object in *AutoCad.* This grid defines measurement points along the edge of the object and uses a known number of points to generate the grid (i.e. it has n x m grid points, where n and m are the number of rows and columns from the conventional rectangular grid stretched to create the customised grid). It is necessary to have a known number of grid points in order to generate a surface mesh in *AutoCad* which represents the physical surface of the object.

4. The co-ordinates of the intersections of the grid points (in the Machine co-ordinate system) are placed in sequence to define the path that the Laser Positioning system will follow. This path is then used as the 'grid' during the measurement of the object.

In the test case of the propeller it was necessary to prepare a path for the laser for each blade of the propeller. Discussion of the time requirements to prepare these paths and the potential for increased automation in this region are presented in Chapter eight.

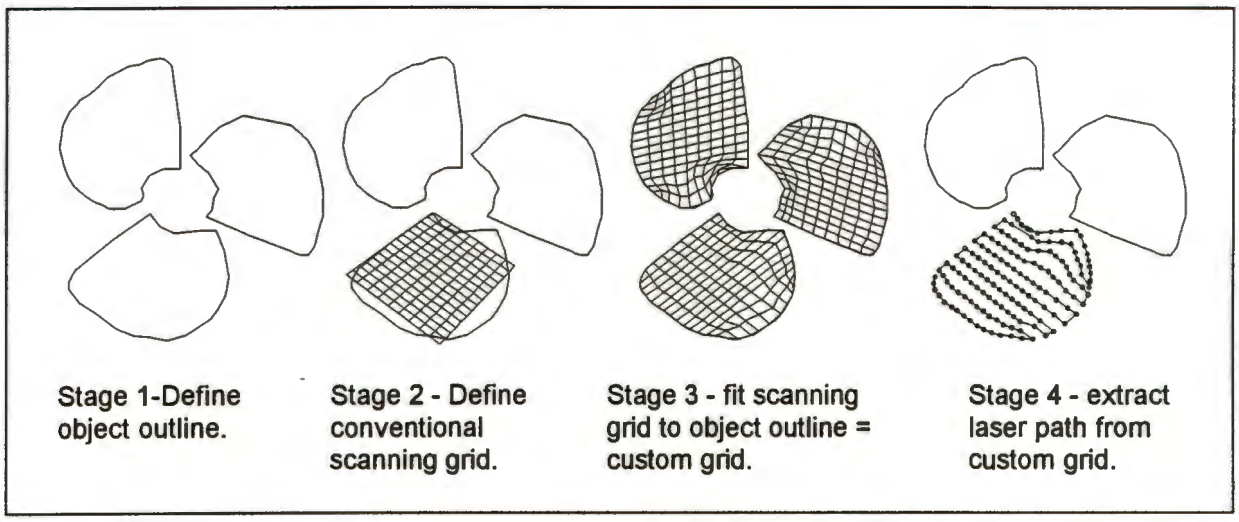

Figure 5. 8 - Stage preparation of a custom grid for a discontinuous object.

The procedure described in stages 1-4 previously and illustrated in ***Figure 5. 8*** (p.78) results in the preparation of a part program (see Chapter three) in a CAD environment. The data prepared by this method considers the geometry of the object (defined by the outline of the object) and the motion of the Laser Positioning system (Machine control) to define the measurement path. Once the measurement path has been defined, measurement of a discontinuous object can proceed as described in section 5.5.1.

Chapter Six

Software and Hardware Components

This Chapter presents a list of the Software and Hardware components of the *MILLMAP* system. ***Table 6. 1*** lists the Software used and the respective authors. A brief description of the software functions within the *MILLMAP* system is also made. ***Table 6. 2*** lists the Hardware components of the *MILLMAP* system.

Software Name	Author/Distributor	Function Description
MILL	D.Craigie	General control of the Photogrammetric system. Calibration, DLT, MPGCM routines. This program was adapted from the *DIMS©* software written by G.van der Vlught and H.Rüther.
PHOTONET©	G van der Vlught	Bundle adjustment program to calculate the final orientation parameters for the Photogrammetric system.
CAMCONT1/2/3	D.Craigie	External camera routines called by *MILL*. Used to control the framegrabber in order to snap images from the three CCD cameras during the measurement procedure.
CALLBN	D. Craigie	External camera routine called by *MILL*. Used to control the framegrabber in order to snap images from the three CCD cameras for Calibration of the Photogrammetric system.
COMIN	P.Parbhoo	Communication software used to link Photogrammetric and Motion Control systems. Interprets messages sent by *COMOUT*.

CONTINUED OVER PAGE...

CONTINUED FROM PREVIOUS PAGE

Software Name	Author/Distributor	Function Description
COMOUT	P. Parbhoo	Communication software used to link Photogrammetric and Motion Control systems. Sends messages which are interpreted by *COMIN.*
STEPCOMM	P. Parbhoo	Motion Control system software. Controls the position of the laser positioning system using grid scanning options to define the grid mapped. Controls the Object positioning system - rotation of the object, prespecified prior to measurement.
AutoCad (v.12)	Autodesk, Inc.	Commercial software used to define the rotation axis, define laser path for discontinuous objects and generate three dimensional meshes from object space co-ordinates.

Table 6. 1 - MILLMAP Software components.

It should be noted that various macro functions were programmed by *Parbhoo (1995)* in Borland C to automatically process data in *AutoCad* as described in Chapter five.

The list of Hardware components will include the technical specifications and a description of the function for each component:

Hardware Component	Technical Specifications / Function
Photogrammetric Control Computer	80386 processor with 80387 coprocessor. 8Mb RAM. For the control of the CCD cameras and all software associated with the photogrammetric measurement system.
Motion Control System Computer	80386 processor. 1Mb RAM. For the control of the Laser positioning system and Object positioning system and all software associated with these systems

CONTINUED OVER PAGE...

CONTINUED FROM PREVIOUS PAGE

Hardware Component	Technical Description / Function
External Video Monitor	Phillips RGB CM 8833 To monitor the video images being captured by the CCD cameras.
Sensors	3 x ITC black and white CCD cameras. Chip size 7.95mm(H) x 6.45mm (V). Pixel resolution 795 (H) 596 (V). Pixel dimensions 0.01186mm (H) 0.00830mm (V). 2 x 8.0mm lenses. 1 x 8.5mm lens. The sensors for the Digital Photogrammetric measurement system.
Framegrabber	Matrox PIP- 512B. 512 x 512 elements. Single image storage. For camera control and the analogue-to-digital conversion of the images captured by the CCD cameras.
Laser Positioning System / Object positioning system	Designed by *Parbhoo (1995)* and built by the Department of Mechanical Engineering. University of Cape Town. Illustrated in ***Figure 6. 1*** (p.82). For the movement of the laser targeting device and rotation of the object for complete surface accessibility.
Communications Link	Standard RS232 cable to fit serial communications port at both ends. To provide a control link between the photogrammetric and motion control computers.

Table 6. 2 - MILLMAP Hardware components.

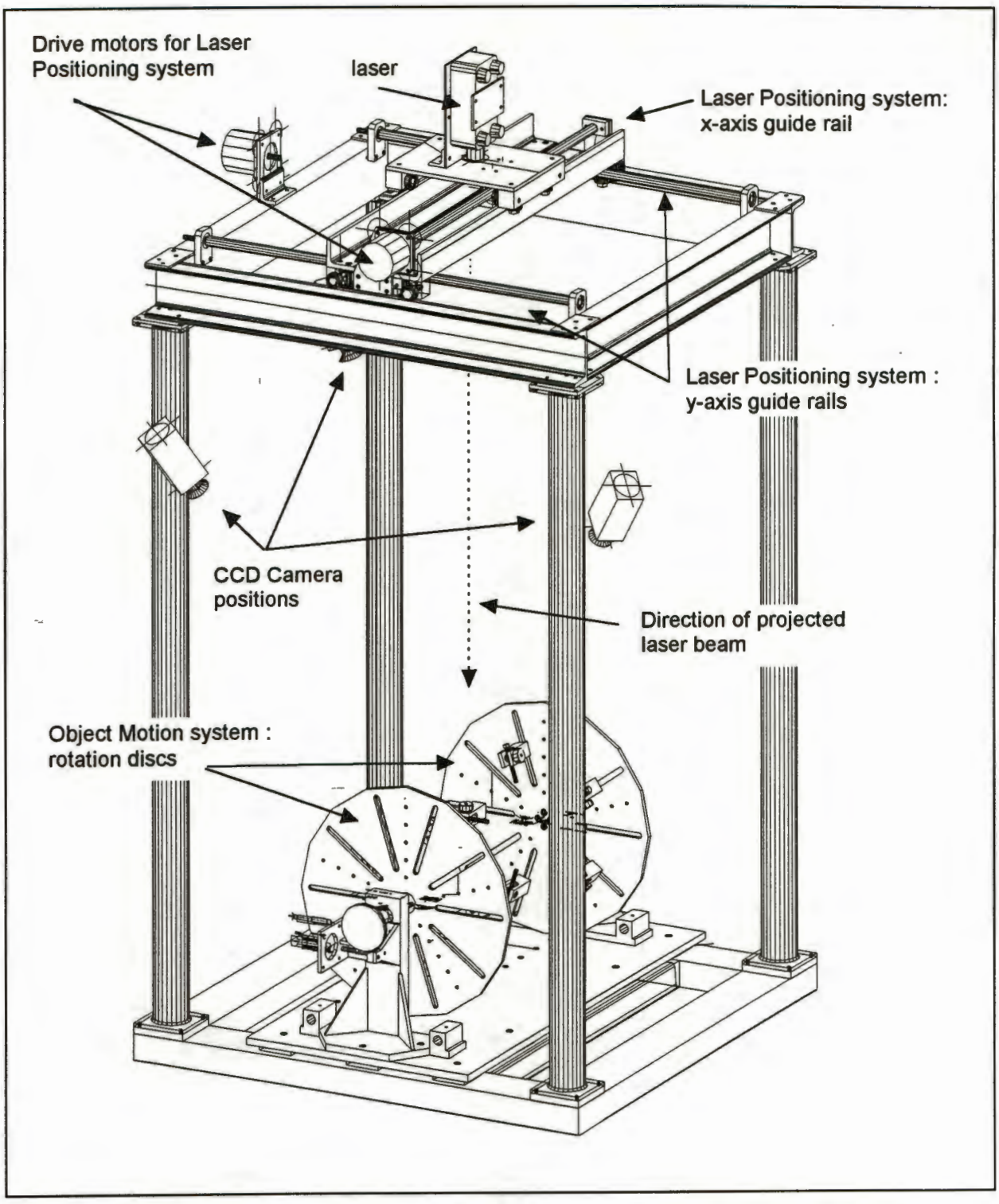

Figure 6. 1 - Laser Positioning System and Object positioning system Hardware.

Chapter Seven

Test Results and Analysis.

This Chapter presents the results obtained from testing the *MILLMAP* system. The tests fall into two categories :

- System testing, and
- Test Cases.

The System testing was used to determine the precision and accuracy of the Measurement system used in the *MILLMAP* system. The Test Cases provide a basis to evaluate the performance of the *MILLMAP* system in measuring three different test objects. These objects, with a variation of properties, were selected to provide a range of conditions under which the system could operate. An analysis is made for each individual set of results.

The resolution of the Laser Positioning system was 0.01mm (with a backlash=0.02mm) The resolution of the of the Object positioning system was 0.042° (with a backlash=0.01°). The determination of these accuracy parameters for the Motion system are described in detail by *Parbhoo (1995)*, and will not be discussed further in this dissertation.

7.1 System Testing

The precision of the Measurement system was determined by testing as described in section 7.1.1. below. The results of the test to determine the accuracy of the object space co-ordinates obtained from the Measurement system are presented in section 7.1.2. Section 7.1.3 analyses the problem associated with the inaccuracy obtained from the Measurement system. Finally the effect of the Object positioning system on the accuracy of the Measurement system is discussed in section 7.1.4.

7.1.1 Precision of the Measurement System.

The precision of the Measurement system was evaluated by taking repeated measurements of the laser dot in a fixed position on a flat surface. This test provides an indication of the 'noise' associated with the laser beam when projecting a dot onto the surface of an object. The noise

could affect the CCD sensors and the image processing algorithms which would subsequently affect the precision of the Measurement system. The measured dot position should remain constant from one measurement to the next, assuming that the projected laser dot is noise free. Should the laser dot be contaminated with noise, the measured position of the dot will vary from one measurement to the next. The results from the test to evaluate the precision of the Measurement system are listed in ***Table 7. 1*** (p.84).

	X	Y	Z
Mean (mm)	214.74	327.85	192.94
Range (mm)	0.05	0.06	0.10
RMS (mm)	0.01	0.02	0.03

Table 7. 1 - Precision Test results for Measurement System.

Analysis :

From ***Table 7. 1*** it can be seen that the Measurement system has a high level of precision with RMS values of 0.01mm for X, 0.02 mm for Y and 0.03mm for the Z co-ordinate. These results also indicate that the laser dot is a stable target with no noticeable noise affecting the precision of the Measurement system

7.1.2. Accuracy of the Measurement System

In order to assess the overall accuracy of the system a number of points with known object space co-ordinates were measured by the Measurement system. The known points were the targets on the control frame used to calibrate the system. The object space co-ordinates of the targets were determined by a free network least squares adjustment with scaling factor, the initial estimates for the co-ordinates being derived by photogrammetric methods. The results obtained from using the measurement system to measure the 32 points on the control frame are presented in ***Table 7. 2*** (p.84).

	X	Y	Z
RMS (mm)	0.120	0.157	0.644
Max.deviation(mm)	0.33	0.51	1.85
Range (mm)	0.44	0.69	2.28

Table 7. 2 - Deviation of Co-ordinates from Control Frame -Accuracy Test.

Analysis :

The results obtained indicate a satisfactory degree of accuracy in the x and y co-ordinates, however the accuracy of the z-co-ordinate is nearly five times less than that of either the x or y-co-ordinates. These results are inconsistent with those of *van der Vlught and Rüther (1994)* who used the same measurement method in the development of an automated measurement system. The ranges of the z-values obtained from this test are outside the sub-millimetre limit specified for the project and require further investigation.

An additional test to analyse the accuracy of the z-co-ordinate obtained by the measurement system was performed. The test involved measuring a grid of points defined by the laser positioning system on a flat plate of glass. The glass was spray painted grey in order to eliminate the effects of reflection generating 'noise' in the images captured by the Measurement system. The glass plate although unoriented within the measurement co-ordinate system, provided a flat reference surface through which a best fit plane was plotted. It was assumed that a best fit plane would represent the actual surface of the plate. Deviations of measured points from this plane provide a practical indication of the accuracy of the Measurement system with regards to the z-co-ordinate determination. A graph illustrating the deviation of the z-co-ordinate from a best fit plane is shown in ***Figure 7. 1*** (p.85).

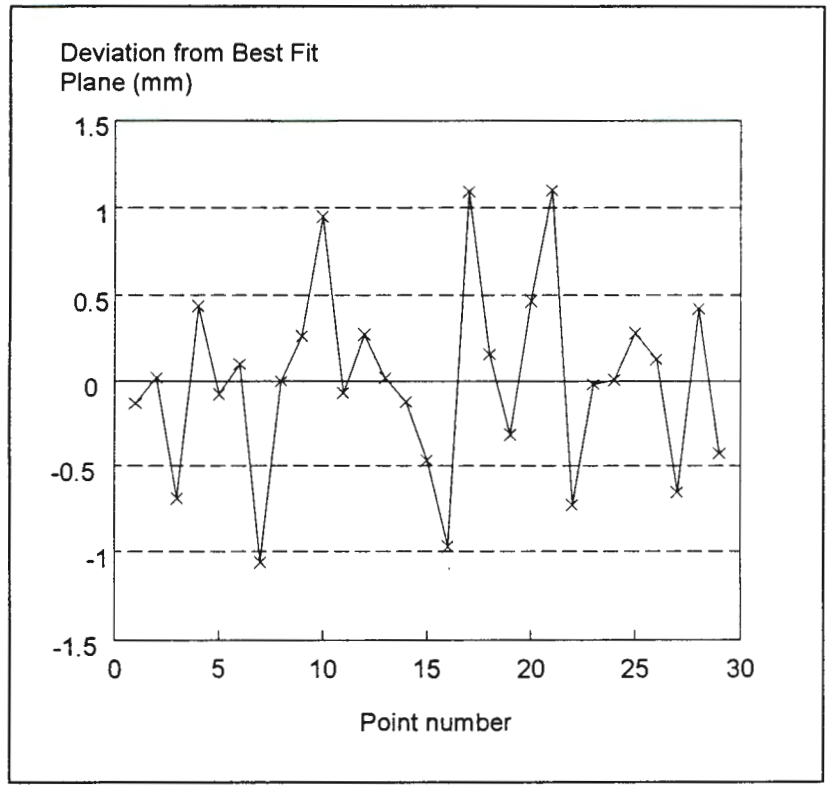

Figure 7. 1 - Plot of z-co-ordinate deviation (in mm) from best fit Plane.

Analysis :

The mean deviation of the z-co-ordinate from the best fit plane as plotted in ***Figure 7. 1***(p.85) was 0.395mm, the maximum deviation 1.100mm and the range of values 2.15mm. This test showed that the z-co-ordinate determined by the system was not of sub-millimetre accuracy as specified for the requirements of the project.

The relative geometry of the camera-object configuration was considered as a factor that could influence the accuracy of the Measurement system. The camera geometry of the *MILLMAP* system is illustrated in ***Figure 7. 2*** (p.86)

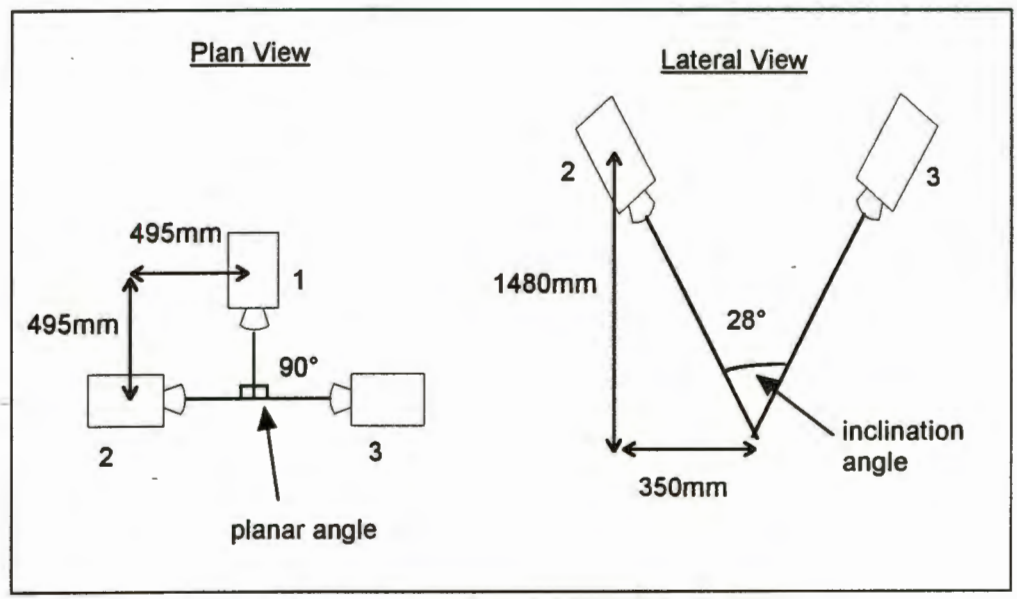

Figure 7. 2 - Camera geometry for the MILLMAP system.

The inclination angle in the lateral view shows camera 2 and 3. Identical geometry exists between camera 1 and cameras 2 and 3 respectively.

Note that the angles illustrated in ***Figure 7. 2*** are variable and not fixed. The angles are derived from a ray to the centre of the measuring region. These angles serve as a guide to the approximate geometry of the Measurement system. These angles will vary during the measurement process, depending upon the location of the laser dot in the measurement region.

Based on optimum geometry considerations (as described in *Mason, 1994)* the ideal planar configuration would place the cameras at 120° to each other (i.e. evenly distributed around the target area). The ideal inclination angle of the cameras (illustrated in the lateral view, ***Figure 7. 2***) would be 90°. The camera geometry illustrated in ***Figure 7. 2*** for the *MILLMAP* system is reliable even if it is not ideal. There will be a reduction in the accuracy of the z-co-ordinate (relative to the x,y co-ordinates) due to the reduced angle of inclination, but the magnitude of the inaccuracy for

the z-co-ordinate obtained by the Measurement system cannot be attributed to weak camera geometry.

The geometry of the *MILLMAP* system was considered to be reliable, therefore it was necessary to identify alternative factors that contributed to the inaccuracy of the Measurement system. Identification and solution of these factors would allow the accuracy requirements of the project to be satisfied. Measurement of the test objects described in section 7.2 was performed despite the inaccuracies noted in the z-co-ordinate obtained from the Measurement system. This was due to a time constraint associated with the mechanical device, which was subsequently redesigned as a 4-axis milling machine for use on another project. Unfortunately it was only in the later stages of the project when the mechanical device was no longer available (for the remeasurement of the test objects) that a solution to improve the accuracy was found. A series of simulated tests were performed as described in section 7.1.3 to predict the performance of the Measurement system using the more accurate solution.

7.1.3 Analysis of the Measurement System Accuracy.

As described in section 7.1.2. the accuracy of the z-co-ordinate obtained using the Measurement system was unacceptable for the requirements of this project. This section proposes a hypothesis to explain the poor accuracy obtained by the current measurement method. Evaluation of the hypothesis is undertaken by means of simulated tests. Finally the necessary steps to achieve the required accuracy for the *MILLMAP* system, based upon the hypothesis, are presented.

After consideration of the problem the following hypothesis was made :

- The single pixel accuracy for the determination of the target centre on the reference image causes a mis-match for elliptical target points when using rotated image geometry.

The result of mis-matching target points as suggested above, will reduce the accuracy of the space intersection when determining the object space co-ordinates of a measured point.

Simulation tests were performed to compare the results of non-rotated image geometry and rotated image geometry as well as the effects of pixel versus subpixel target point location on the reference image. Before the results of these tests are presented an overview of the theory that led to the hypothesis will be presented.

Non-rotated and Rotated Geometry

Non-rotated image geometry will be defined in this dissertation to mean "that the orientation of image geometry with respect to the object will be approximately the same for each of the images". This definition is clarified by considering the case of rotated image geometry in which the images are rotated about the z-axis of the object space co-ordinate system resulting in the situation illustrated in ***Figure 7. 3*** (p.88).

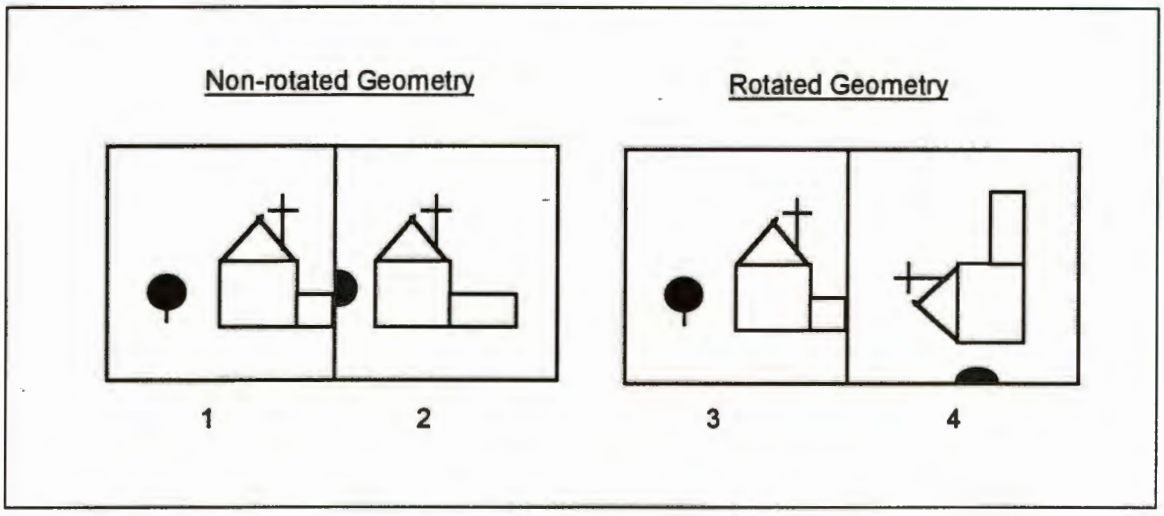

Figure 7. 3 - Schematic :Non rotated vs. Rotated image geometry.

From the schematic illustrated in ***Figure 7. 3*** it can be seen that the orientation of the object with respect to image geometry in 1 and 2 remains the same, only the position of the object in the image has changed due to the fact that the image has been captured from a different camera position. The geometry in image 4 has been rotated (due to a rotation of the camera) relative to the image geometry so that entire image appears rotated with respect to image 3.

In the case of the images captured by the *MILLMAP* system, the geometry of the images was rotated by +90° for camera 2 and -90° for camera 3 (see ***Figure 7. 2*** p.86). The epipolar search line (which was used to constrain the matching process-see Chapter two) is calculated from the collinearity equations based on image geometry. However the object geometry for the images at cameras 2 and 3 is rotated, which causes the epipolar line search to constrain the matching of the

target incorrectly with respect to the object geometry. If the image rotation is modelled correctly the epipolar line can be calculated based on the rotation and the problem associated with rotated images could be solved.

In ***Figure 7. 4*** (p.89) the elliptical nature of the target is exaggerated to clarify the concept of the problem. It is also assumed that the centre of the target on the reference image when measured to pixel accuracy does not fall in the geometric centre of the target.

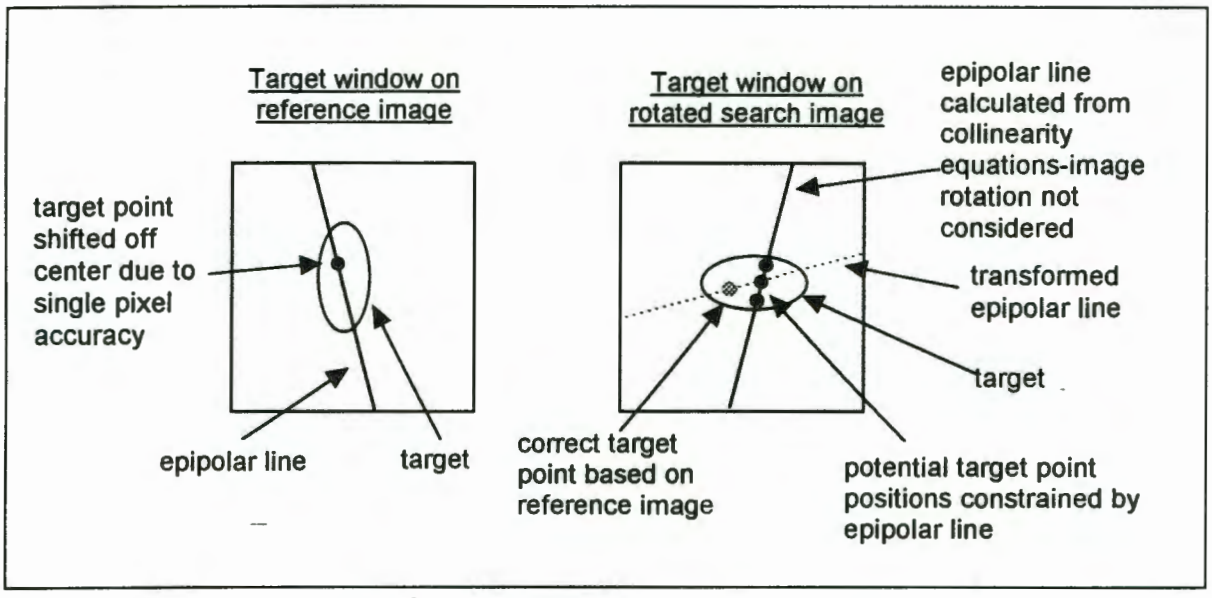

Figure 7. 4 - Effect of rotated geometry on Epipolar line search.

The epipolar line calculated from the collinearity equations (illustrated in ***Figure 7. 4***) constrains the search for a potential target point in the wrong direction. The target point finally matched is not the same point as the reference target point which introduces inaccuracy in the intersection calculation for the 'matched' points. The transformed epipolar line would constrain the target search correctly based upon the object (target) geometry as required, and not the image geometry.

Pixel versus Sub-Pixel determination of the reference target centre

The effect of the mis-matched target point using rotated geometry can be eliminated if sub-pixel accuracy is used to determine the centre of gravity of the target on the reference image. By calculating the centre of gravity on the reference target the epipolar line search, although still constraining the solution in the wrong direction, will pass through the centre of gravity on the search image allowing the correct match to be made as illustrated in ***Figure 7. 5*** (p.90).

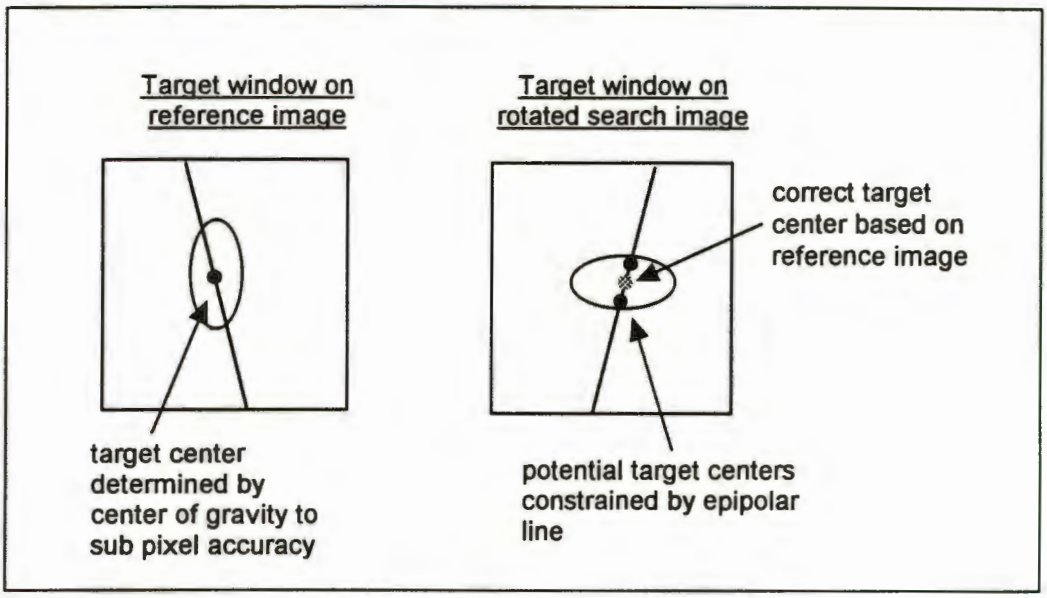

Figure 7. 5 - Sub-pixel centre of gravity determination for matching along epipolar lines.

The nature of the error introduced as a result of rotated image geometry and the location of the target centre point to pixel accuracy will only affect the matching process when:

1. The sub-pixel centre of gravity (assumed to be equivalent to the geometric centre) for the reference target differs from the single pixel centre of the reference target (i.e. pixel accuracy gives a shifted target centre as illustrated in ***Figure 7. 4*** p.89).
2. The target appearance is elliptical.

Tests to Support the Suggested Hypothesis

In order to evaluate the hypothesis suggested a series of tests were undertaken and the results compared to support the theory relating to the hypothesis.

The matching technique from the *MILLMAP* Measurement system was modified to allow the determination of target centres to sub-pixel accuracy on the reference image. Sub-pixel accuracy for the position of the reference target centre was used throughout the first test, based on the assumption that sub-pixel accuracy would improve the accuracy of the Measurement system. The first test investigated the effect of rotated image geometry on the accuracy of the measurement system.

The procedure for the first test required that three images with non-rotated geometry be captured by the Measurement system to determine the object space co-ordinates of the target points on the control frame used for calibration. A second set of three images were captured with images 2 and 3 rotated by +90° and -90° respectively, relative to image 1. The co-ordinates measured using each set of images were compared to the known co-ordinates of the control frame with the results presented in ***Table 7. 3*** (p.91).

	Non-rotated geometry			Rotated geometry		
(mm)	dX	dY	dZ	dX	dY	dZ
RMS	0.032	0.049	0.078	0.034	0.049	0.133
Max. Dev.	0.12	0.10	0.28	0.12	0.10	0.46
Range	0.17	0.18	0.42	0.17	0.18	0.65

Table 7. 3 - Accuracy of Non rotated geometry vs. rotated image geometry.

Sub-pixel accuracy for reference target centre used for both image sets.

Analysis

From ***Table 7. 3*** the effect of rotated geometry on the accuracy of the Measurement system is minimal when using sub-pixel accuracy to specify the centre of the reference target. A reduction of accuracy with respect to the z-co-ordinate, in the case of rotated image geometry, was noted. The accuracy obtained from the Measurement system using sub-pixel accuracy to determine the target centre point was within the requirements of the project. It remained to investigate the effect of single pixel accuracy with respect to the reference target centre which was the aim of the second test.

The second test compared the effect of sub-pixel accuracy to determine the reference target centre point with that of single pixel accuracy, using a rotated image configuration. The images from the first test (with rotated image geometry) were used for the test. The target centre points were determined with single pixel accuracy and the computation of object space co-ordinates carried out. The results were compared to the known co-ordinates for the control frame targets (see ***Table 7. 4*** :p.92). The discrepancy between the results obtained from sub-pixel accuracy (derived in the first test) and single pixel accuracy for defining the target centre point on the reference image were also compared.

	Sub-Pixel Target Centre			Single Pixel Target Centre		
(mm)	dX	dY	dZ	dX	dY	dZ
RMS	0.034	0.049	0.133	0.134	0.142	0.192
Max. dev	0.12	0.10	0.46	0.98	1.69	1.85
Range	0.17	0.18	0.65	1.12	1.81	2.4

Table 7. 4 -Accuracy of Sub-pixel target centring vs. single pixel target centring.

Rotated geometry configuration used for both methods.

Analysis

From ***Table 7. 4*** it is apparent that the use of single pixel accuracy to determine the target centre on the reference image reduces the measurement accuracy substantially in the case of rotated geometry. This result supports the hypothesis which stated that single pixel accuracy for the determination of the target centre on the reference image introduces an error in matching target points for rotated image geometry. The mis-matched target points reduce the accuracy obtainable from the system using rotated geometry between images. The deviation of the mis-matched target points is not systematic since it is dependent on the deviation of the target centre point (to single pixel accuracy) from the geometric target centre, which varies according to the position of the target on the reference image.

Based upon the tests described in this section (7.1.3) the hypothesis suggested has been proved as a possible explanation for the poor accuracy obtained by the Measurement system. In order to achieve sub-millimetre accuracy with the *MILLMAP* Measurement system it is proposed that :

1. The cameras be mounted to ensure non-rotated geometry exists between images, and
2. That sub-pixel accuracy is used to define the centre of the reference target.

By ensuring that these conditions are met the attainment of the sub-millimetre accuracy requirements for the project will be achieved.

7.1.4. Accuracy of the Rotation system.

The axis of rotation was defined by the measurement of a probe attached to the rotation disc using the Measurement system (see Chapter five for details regarding the measurement procedure to define the rotation axis). The accuracy with which the rotation axis is defined within the object space co-ordinate system will effect the relative accuracy between co-ordinates obtained by the measurement system whenever a rotation is applied to object during measurement. The method described in Chapter five to determine the axis of rotation does not incorporate redundant observations into the definition of the rotation axis. The axis of rotation calculated by this method cannot be analysed directly to determine its accuracy without an alternative method to define the axis. An indirect method to determine the effect of the rotation axis on the accuracy of the measurement system was investigated and is the subject of the following section.

A method incorporating redundant observations to define the rotation axis is described at the end of this section (7.1.4.).

A test was devised whereby a standard PVC cylinder of known diameter (160mm) was mounted on the rotation disc and measured by the system. Measurements were made along the length of the cylinder, which was then rotated. A mesh describing the surface of the cylinder in 3D object space co-ordinates was obtained (see ***Figure 7. 6*** p.94).

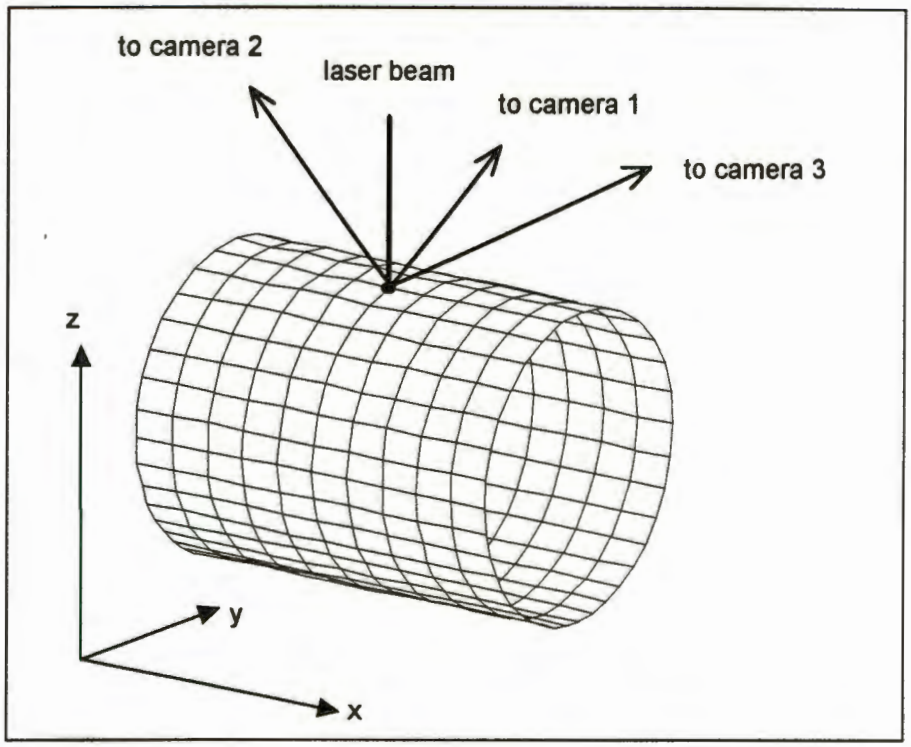

Figure 7. 6 - AutoCad mesh generation for PVC test cylinder.

Perspective View.

The x,y,z axes of the object space co-ordinate system, the laser beam position and relative position of the cameras are illustrated to aid visualisation.

Analysis :

Comparing the mean diameter obtained for the measured cylinder of 163.8mm with the known value of 160mm a discrepancy of 3.8mm is calculated. The orientation of the cylinder within the object space co-ordinate system was such that cross sections of the cylinder lie approximately on the y-z plane of object co-ordinate system describing a circle as illustrated by ***Figure 7. 7*** (p.95). The laser is projected onto the cylinder approximately in the z-direction which implies that the radius of the cylinder, and hence the effect of the rotation axis on the orientation of object space co-ordinates after rotation (see Chapter five) are dependent on the accuracy of the z-co-ordinate measured. Based on the poor accuracy originally obtained for measurement of z-co-ordinates (see section 7.1.2 and 7.1.3) it is assumed that the discrepancy of 3.8mm in measuring the diameter of the PVC cylinder can be attributed to inaccuracy associated with measurement in the z-direction. Increased accuracy in the measurement system would allow a more rigorous determination of the effect of the axis of rotation on the measurement capabilities of the system. The position of the rotation axis relative to the cylinder is illustrated in ***Figure 7. 7*** (p.95).

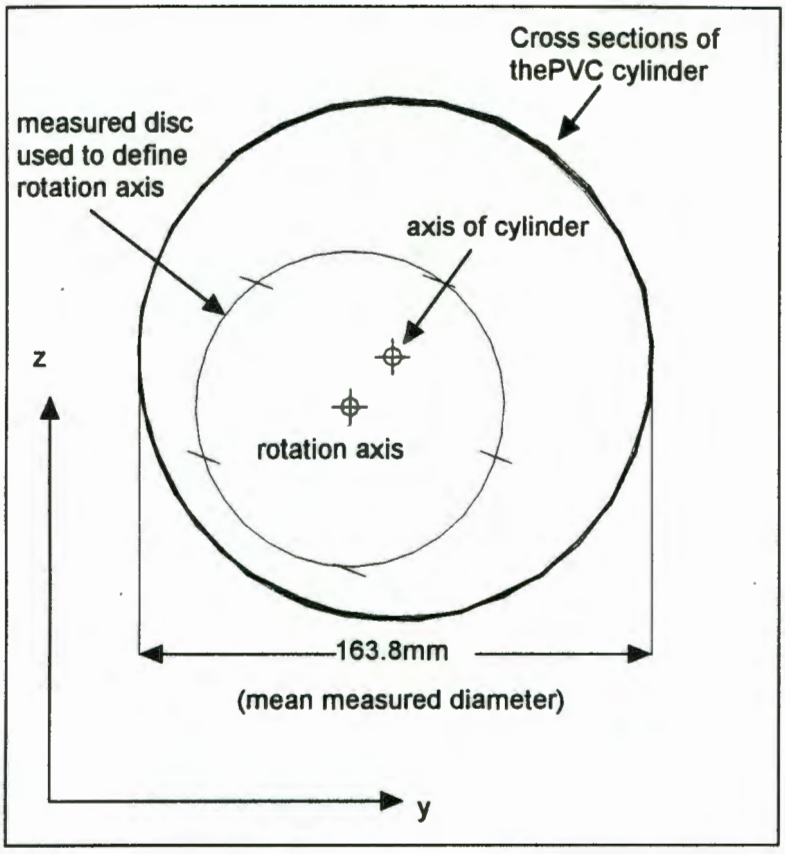

Figure 7. 7 - AutoCad plot of PVC test cylinder in y-z plane.

Cross-Sectional View.

The y,z axes of the object co-ordinate system are shown. The x axis runs into the page.

It can be seen from ***Figure 7. 7*** (p.95) that the rotation axis and the axis of the cylinder do not coincide. The position of the cylinder at various rotation angles is illustrated in ***Figure 7. 8*** (p.96) to emphasise the effect of the rotation axis not coinciding with the axis of the cylinder.

The continuity of the mesh obtained for the cylinder (see ***Figure 7. 6*** p.94) indicates that the method described in Chapter five to orient the data from the measurement system in *AutoCad* has been successful, given the accuracy with which the axis of rotation was determined. *Parbhoo (1995)* states that for 1mm resolution on the surface of an object with 300mm diameter the angular resolution of the Object positioning system must be accurate to 0.38°. Further reductions in grid resolution are achieved by repositioning the laser with the Laser positioning system. The accuracy of the angular measurement was determined by *Parbhoo (1995)* and found to be 0.042°

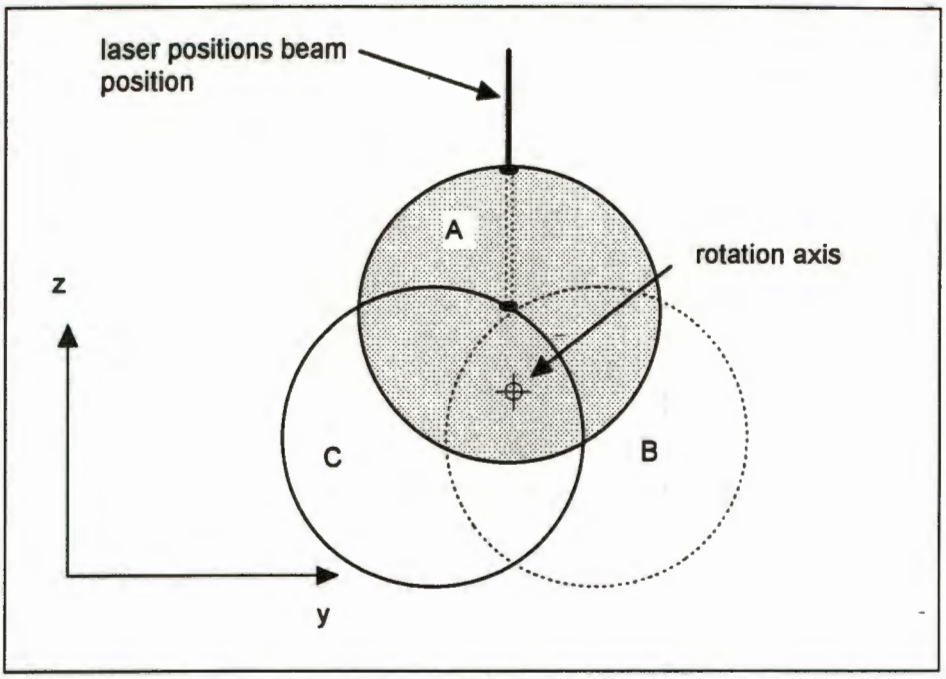

Figure 7. 8 - Rotated Cylinder positions (y-z sectional view).

The y,z axes of the object space co-ordinate system are illustrated, the x-axis runs into the page. The cylinder cross section is shown in positions A,B and C. Note lack of orthogonality between the laser and the surface of the cylinder in positions B and C .

Method to Incorporate Redundant Observations into the Definition of the Rotation Axis.

An alternative solution, using a least squares solution, to define the rotation axis incorporating redundant observations is described here. The procedure involves measuring a number of probe positions (as described in Chapter five) to define a best fit disc in the object space co-ordinate system. The probe distance from the rotation disc and radius from the centre of the rotation disc are varied. The resulting disc centres are then used for a best fit line in three dimensional space, which defines the rotation axis. The measurements required are illustrated in ***Figure 7. 9*** (p.97).

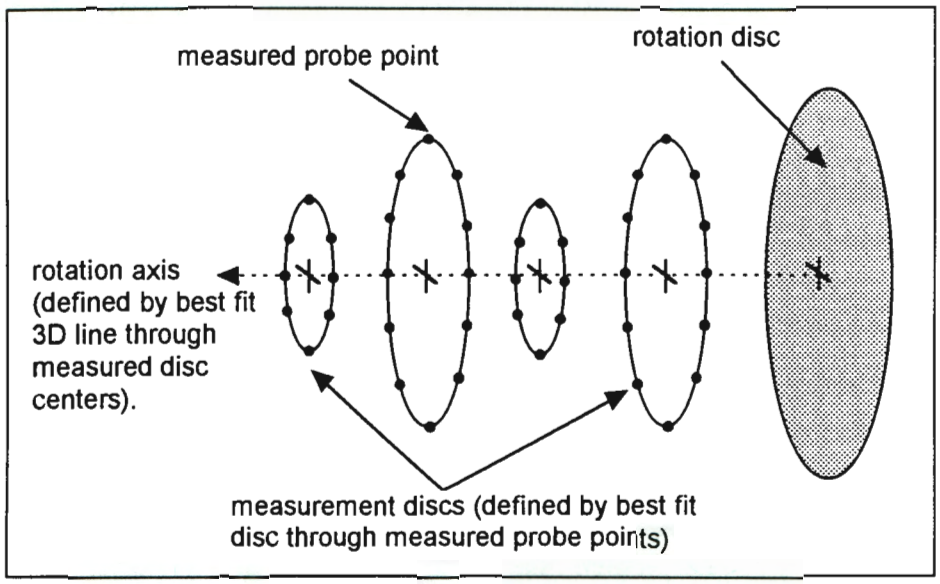

Figure 7. 9 - Redundant measurements to determine the rotation axis.

A test was carried out to compare the definition of the rotation axis using redundant observations, and the definition using only three (i.e. no redundancy) observations. The rotation axis calculated using redundant observations was derived from a best fit line through the centre of four measurement discs (each defined by a best fit circle through five measurement points). The rotation axis calculated with no redundant observations was defined by a line perpendicular to the centre of a disc fitted through three points (as described in Chapter five).

The intersection of the two lines, describing the rotation axis, were calculated for an arbitrary y-z plane in the object space co-ordinate system. A y-z plane was chosen since the direction vector describing the rotation axis is approximately parallel to the x-axis of the object space co-ordinate system. Since the lines were projected onto the same plane the x-value for the lines is not compared in ***Table 7. 5***. The direction vectors of the two lines were compared by reducing the x-component to unity, resulting in a scaling of the y and z components which are compared in ***Table 7. 5***.

(mm)	dY	dZ
Intersection with y-z plane	0.5207	0.2181
Direction vector	0.005	0.00001

Table 7. 5 - Comparison of rotation axis definitions.

Analysis

From ***Table 7. 5*** (p.97) it can be seen that there is a difference in the position of the rotation axis when defined by the two methods. The direction vectors from both methods are relatively parallel (i.e. the two lines have the same direction), which yields little difference between the y and z components of the direction vector. A discrepancy of 0.5207mm (in y) and 0.2181mm (in z) is observed when determining the position of the line where it intersects the plane. It is assumed that using redundant observations will increase the accuracy of the solution.

In the measurement of test objects (see section 7.2) the problem associated with the z-co-ordinate derived from the Measurement system (see section 7.1.3) had not been solved. As a result the accuracy of the Measurement system was outside the sub-millimetre range specified. Since the error in the Measurement system was greater than the discrepancy in defining the rotation axis, using redundant observations, a provisional definition of the rotation axis was made using no redundant observations as described in Chapter five.

7.2 Test Cases

This section examines the results obtained from measuring various test objects with the *MILLMAP* system. Each object has individual features and was selected in order to evaluate the systems performance under varying conditions. The test objects measured are listed below :

- Paper Mask.
- Mannequin Head.
- Outboard Motor Propeller.

The accuracy in measuring these objects is determined qualitatively (i.e. visually) since no alternative method was used to measure the test objects. It must be emphasised that the data collected for the test objects had inaccuracies introduced in the z-co-ordinates. The discussion of this inaccuracy has already been dealt with in sections 7.1.2 and 7.1.3. Note that throughout this section photographs of test objects have 30cm ruler in the foreground for scale comparison.

7.2.1 Paper Mask.

A paper mask (***Figure 7. 10*** : p.99) was selected as a test object to evaluate the systems performance using a dual axis scanning technique on an object with varying topography. The mask was measured using a grid type positioning procedure for the laser. A grid size of 136mm x 106mm with a grid spacing of 1.36mm in the X-direction of the motion system and 1.06mm in the Y-direction was used for measurement over the entire facial area. This grid will be referred to as GRID A. A secondary grid five times more dense (i.e. higher resolution = grid spacing of 0.27mm x 0.21mm) was also measured in a small area of the mask to illustrate the importance of mesh resolution when capturing surface data. This grid will be referred to as GRID B. The *AutoCad* mesh obtained from the measurements is shown in ***Figure 7. 11*** (p.100).

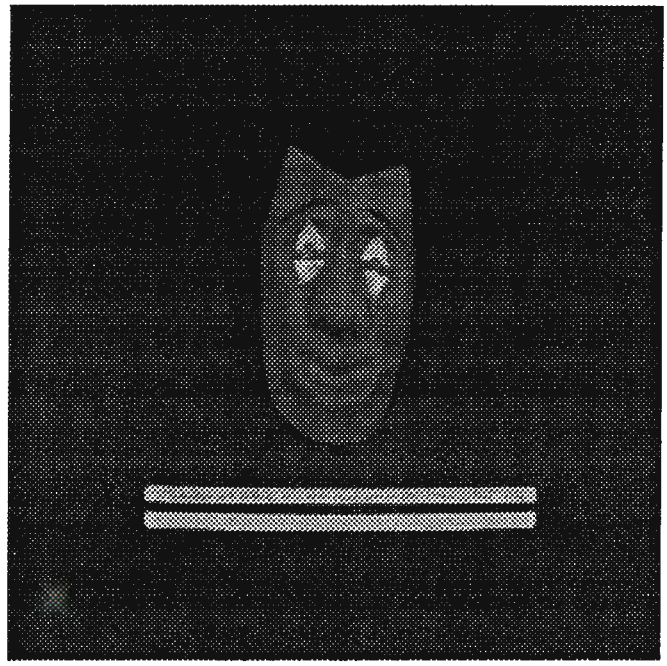

Figure 7. 10 - The Paper Mask.

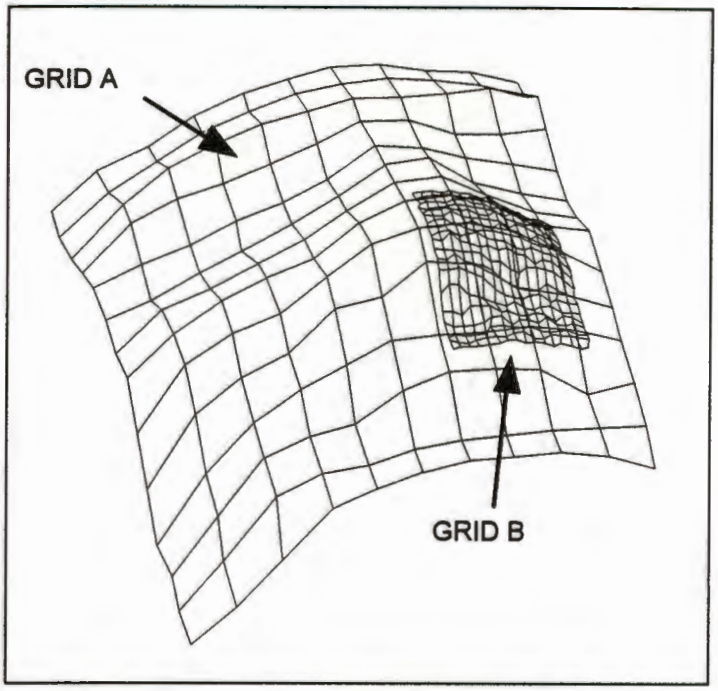

Figure 7. 11 - AutoCad Mesh of Paper Mask.

Analysis :

From ***Figure 7. 11*** (p.100) it can be seen that GRID A (with the greater grid resolution) does not effectively define the surface of the mask. GRID B (with the smaller grid resolution) defines the surface more precisely. Irregularities in z-values obtained for various locations on GRID B are explained by the inaccuracy of the measurement system in determining the z-co-ordinate (see section 7.1.2 and 7.1.3).

Practical experience showed that the topography of the object limited the measurement of the entire mask using a two axis scanning method. As the scanning laser moved towards the sides of the object (where the curvature of the mask increased) the laser dot became obscured for one or more of the CCD cameras resulting in an error message from the measurement system. The limitations of dual axis scanning in this situation are discussed in more detail in Chapter eight.

7.2.2 Mannequin Head

The Mannequin head (***Figure 7. 12*** : p. 101) was selected as a test object to evaluate the performance of the system in measuring a complicated surface of revolution. In order to map the entire object it was necessary to rotate the head through 360°. The resultant mesh generated through *AutoCad* that forms a closed surface of revolution is illustrated in ***Figure 7. 14*** (p.102). The method adopted involved scanning the head in a straight line defined by the path of the x-axis of the laser positioning system. The outer limits of the head were defined manually before the

automatic measurement procedure was executed. The lines were selected to run from the chin region to the top of the forehead (length 200mm). The grid spacing in the x-direction was 10mm resulting in 20 points being measured along each line. After each line was scanned the head was rotated by a pre-calculated amount and the line scan would be repeated. This technique ensured that the laser beam was orthogonal to the surface of the measurement object for the majority of observations.

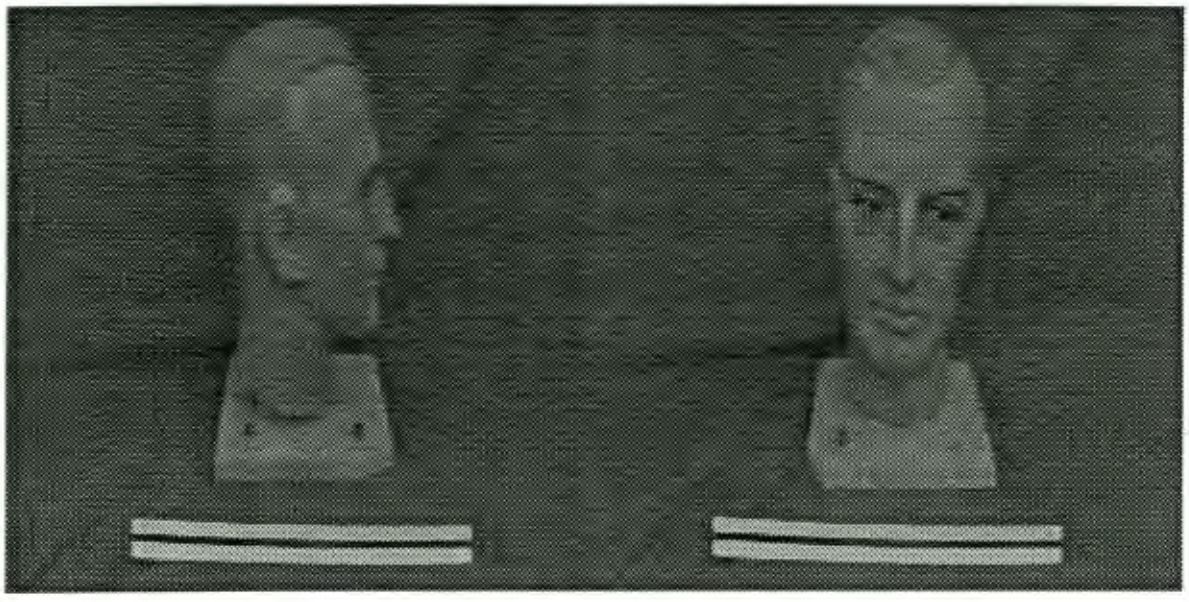

Figure 7. 12 - The Mannequin Head.

To ensure that the facial area contained a denser grid of measurement points (since this region had more topography than the back of the head) a rotation angle of 5° was used between scan lines through 45° on either side of the nose. The remaining 270° region comprising the back of the head and ears was measured using an angular rotation of 9° between scan lines see (***Figure 7. 13*** : p.101).

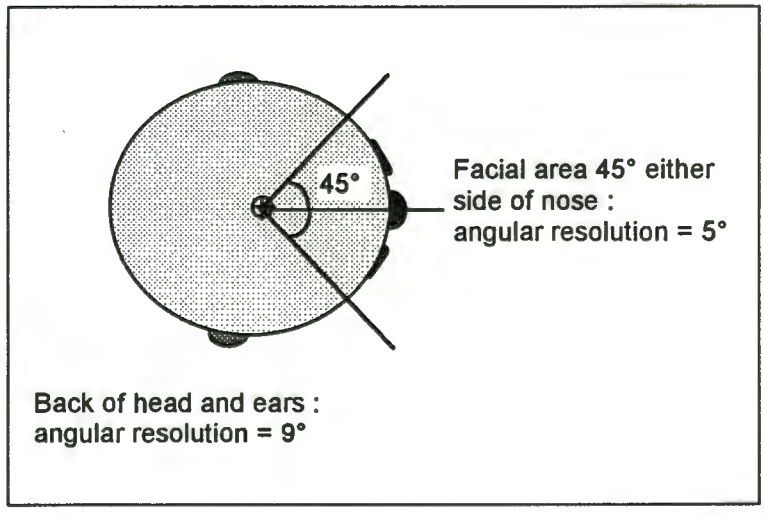

Figure 7. 13 - Variation of Angular resolution to increase mesh density.

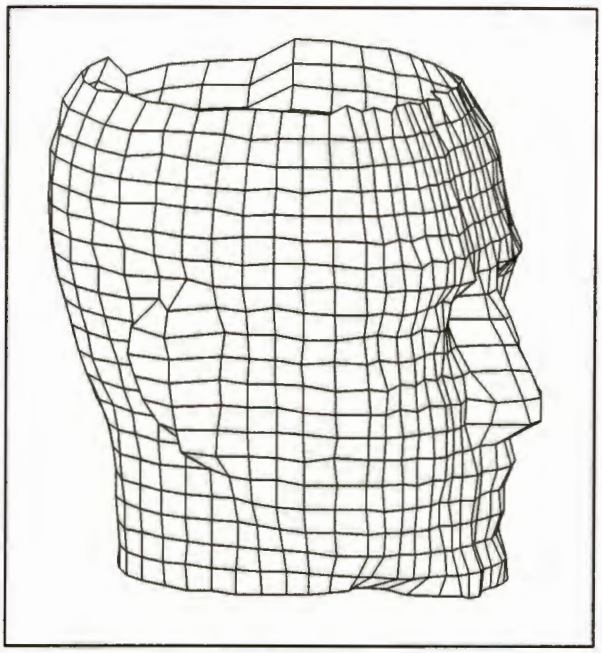

Figure 7. 14 - AutoCad mesh generated for Mannequin head.

Analysis :

As in medical applications where contour maps of a patient's face are compared to the physical face, the analysis the mesh produced for the Mannequin head was based on a visual comparison. The method used by *Pārbhoo (1995)* to mesh together three dimensional points referenced by an angular rotation between scan lines appears to have been successful with the resultant mesh closely resembling the physical object.

Practical experience in capturing the data for this mesh showed that there are two major problems associated with the automated measurement of such a complicated object.

1. The laser dot was not always visible from all three CCD cameras due to extreme topography (this was especially true around the ear region). The problem was solved by returning to the regions where automatic measurement had failed and remeasuring the problem points using only two cameras if the situation made three camera observation impossible using the fixed camera configuration.
2. Problems associated with the laser spot becoming dissipated by the translucency of the material used to construct the head were also encountered. In this situation the measurement system was unable to recognise the laser dot and the surface had to be treated (i.e. painted or covered with a thin layer of paper) in order to re-measure these points. The re-measured data was then manually patched into the data set in the appropriate position in order to generate the mesh illustrated in ***Figure 7. 14*** (p.102).

7.2.3 Outboard Motor Propeller.

The outboard motor Propeller (***Figure 7. 15*** : p.103) was chosen as a test object since it represents a discontinuous complex surface. The discontinuity arises from the edge shape of the individual blades. The measurement procedure requires that the laser scan each blade in grid pattern defined by the x and y-motion axes of the laser positioning system. The method used to define the laser path for a discontinuous object is described fully in Chapter five. Each blade of the propeller is measured in a separate procedure with the data being combined together in *AutoCad* to produce the mesh illustrated in ***Figure 7. 16*** (p.103).

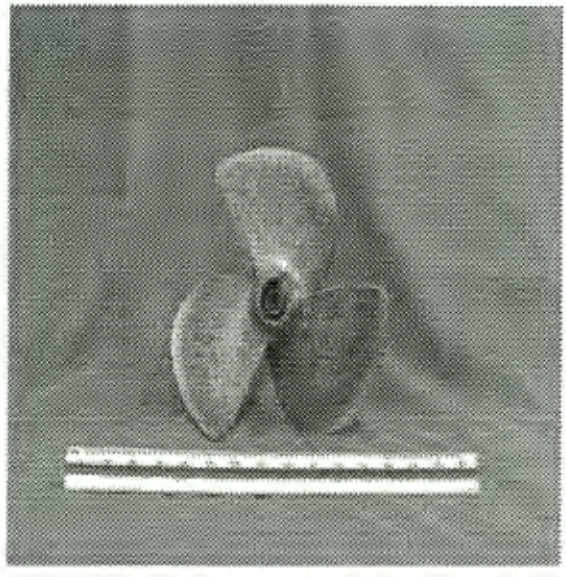

Figure 7. 15 - Outboard motor Propeller.

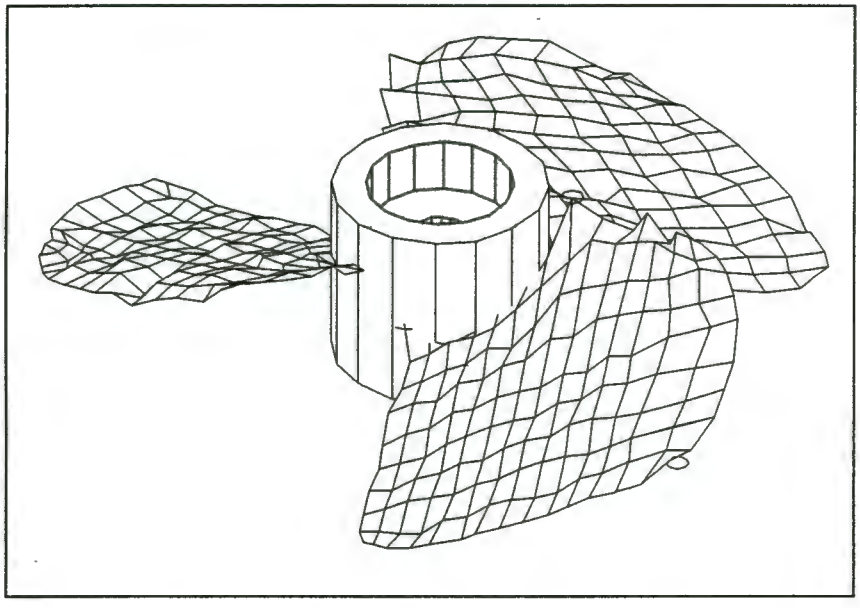

Figure 7. 16 - AutoCad mesh for Propeller.

Note that the hub has been artificially created and added to aid visualisation.

Analysis :

The discontinuous, complex nature of the propeller made it a difficult surface for the system to measure. The manual procedure used to define the measurement path (see Chapter five) was time consuming. Automation of this aspect should be investigated (see Chapter eight). Due to the topographical nature of the hub, this region could not be mapped by the system and so an artificial hub was inserted into the mesh to aid visualisation (see ***Figure 7. 16*** :p.103). Numerous errors in the z-co-ordinate can be observed distorting the mesh. These errors are attributed to the inaccuracy of the Measurement system with respect to measuring the z-co-ordinate (see section 7.1.2 and 7.1.3.). Time constraints did not permit remeasurement of this object in order to clarify the inconsistent data regarding the z-values.

Van der Vlught and Rüther (1994) report that the same propeller was measured with an accuracy of 0.11mm in the x-co-ordinates, 0.14mm in the y-co-ordinates and 0.37mm in the z-co-ordinates. It can only be assumed that application of the solution discussed in section 7.1.3. to the Measurement system would have yielded accuracy of a similar magnitude to that of *van der Vlught and Rüther (1994)* had a re-test been performed.

It should be noted that the propeller has only been scanned in one orientation. To obtain a complete mesh of the blades, the propeller would have to be rotated and the undersides of the blades scanned. The data would then be combined in *AutoCad* to provide a full three dimensional mesh of the propeller's surface.

Chapter Eight

Conclusions

From the research conducted and presented in this dissertation the following conclusions can be drawn:

1. There are applications for an automated co-ordinate measurement machine capable of mapping continuous, complex surfaces in industry. The major use for such a machine lies in quality control.

2. Existing co-ordinate measurement machines are expensive. The *MILLMAP* system offers an inexpensive alternative for co-ordinate measurement.

3. Conventional co-ordinate measurement machines have a high degree of accuracy, but rely on a contact probe to make measurements. An accurate (sub-millimetre) non-contact co-ordinate measurement machine, *MILLMAP*, has been developed. The non-contact measurement technique allows the measurement of non-rigid objects as well as fragile objects, as in the case of archaeological artefacts.

4. The non-contact measurement technique using Digital Photgrammetry to measure the position of a laser spot projected onto the surface of the object technique successfully preserves the properties of non-rigid objects and can also be used to measure rigid objects.

5. Tests proved that the determination of the laser dot centre on the reference image to sub-pixel accuracy increases the accuracy of the measurement system substantially in the case of rotated image geometry.

6. Tests proved that the criteria of non-rotated geometry between images further increases the accuracy of the measurement system.

7. Tests were performed to determine the accuracy of co-ordinates measured, using sub-pixel accuracy to define the centre of the reference target and non-rotated geometry. The results from these tests indicate that the *MILLMAP* system is capable of measuring object co-ordinates with an accuracy of 0.17mm in the x-co-ordinate, 0.18mm in the y-co-ordinate and 0.42mm in the z-co-ordinate.

8. The three dimensional mesh produced in *AutoCad* is in a format that can be used in a CADCAM environment to duplicate the measured object using a CNC milling machine.

It is important to emphasise that the initial testing of the system had to be completed within a prespecified deadline. The mechanical device was subsequently modified in order to meet the requirements for another project in the Department of Mechanical Engineering, University of Cape Town, and therefore was not available for further testing of the system. The results from the initial tests did not yield the expected measurement accuracy and this problem was investigated as described in Chapter seven. A solution to improve the accuracy of the measurement system was investigated but only implemented after the mechanical device was no longer available for testing. This meant that complete evaluation of the system using the improved measurement solution was not possible. A series of simulation tests (as described in Chapter seven) was conducted without the mechanical device. The results obtained from the simulation indicate that the potential for sub-millimetre accuracy in the measured co-ordinates is achievable with the measurement system. The results from testing the entire system, when the mechanical device was available, show that the concept of the *MILLMAP* system is feasible and the conclusions drawn indicate that the objectives of the project, as set out in Chapter one, have been met. Further recommendations for the project, based upon these conclusions are presented in Chapter nine.

Chapter Nine

Recommendations

This Chapter makes a series of recommendations based upon the limitations of the *MILLMAP* system discovered during practical testing, and the conclusions drawn in Chapter eight.

1. Effect of Rotated Geometry and Sub-pixel accuracy (for reference target point) on the Overall Accuracy of the System.

From the tests performed it was established that in order to achieve sub-millimetre accuracy specified for the project, non-rotated image geometry should be used. The rotated image geometry between the cameras of the *MILLMAP* system reduced the accuracy obtained from the matching process. In addition, the use of single pixel accuracy to define the target point (centre of the laser dot) on the reference image severely reduced the accuracy of the *MILLMAP* system with respect to the z-co-ordinate value.

Based on the simulation test results, it is recommended that non-rotated image geometry be maintained between cameras, and that sub-pixel accuracy be used when defining the target point on the reference image.

2. Open loop systems.

Chapter three described the closed and open loop system for the positioning of numerically controlled machinery. The *MILLMAP* system relies on an open loop system, which sends the laser to a specified position defined by x,y co-ordinates in the Machine co-ordinate system. The physical position of the laser is not monitored to confirm if the laser is in the correct position as defined by the machine co-ordinate system. Since the position of the laser is not used for measurement of the object, but only as a delivery system, the accuracy of the position of the laser in the machine co-ordinate system is not important.

If the x,y object space co-ordinates of the object are to be derived from the machine co-ordinates of the Laser positioning system, then an open loop system limits the accuracy that can be achieved by the system. In this case a closed loop system is recommended over the open loop system described in

the previous paragraph. A closed loop system provides a check on the physical position of the laser, and adjusts the position correctly to agree with the machine co-ordinate specified.

3. Increased Image Scale.

The entire object must be visible in the images captured by the *MILLMAP* system. This image scale permits measurement of the laser at any position on the surface of the object (as in the case of grid scanning). The resolution of the laser dot at this scale has a window 11x11 pixels. This resolution is a limitation, which decreases the accuracy in determining the sub-pixel centre of the laser dot.

By using an alternative Motion system configuration in which the laser position is fixed and the object is translated/rotated (as described in Chapter five) a reduction in the image scale is possible. It would be possible to reduce the image scale so that the laser dot fills the entire image (as opposed to the present configuration where the dot fills an 11x11 pixel window on the image). The resolution of the laser dot would then be maximised, permitting a more accurate determination of the sub-pixel centre of the laser dot. A more accurate determination of the sub-pixel centre of the laser dot would also increase the accuracy of the matching routine, since the centre point on reference and search images would lie closer to the geometric centre on the reference and search images.

If the image scale were reduced so that the target laser dot filled the entire image then the image processing requirements for images would also be reduced since recognition of the target would no longer be required. The processing time required to compute the sub-pixel centre would however be increased since this procedure would be process the entire image (512x512 pixels) as opposed to a small window (11x11 pixels).

4. Image Geometry and number of images.

The geometry between the three cameras used for the *MILLMAP* project was not ideal (90° planar intersection angle and 28° inclination angle). It is recommended that improving the camera geometry will increase the accuracy of the space intersection. The ideal camera geometry, for a three camera system, would place the cameras at 120° (planar intersection) to each other and increase the inclination angle to 90°. Investigation into the effects of camera geometry and number of images on the accuracy of the system would have to be carried out in order to evaluate the recommendation of changing the camera geometry and number of cameras.

It must be noted that the effects of occlusion with respect to object topography should be investigated when applying an inclination angle of 90° between cameras.

By capturing more than three images of the laser dot greater redundancy for the solution could be achieved. In the event of occlusion of the laser dot from one or more images, the additional images would be able to provide a solution for the position of the dot (note that a minimum of two images are required to solve the photogrammetric problem).

5. Occlusion due to Object Topography.

From practical experience using the system, it was found that certain techniques used to measure objects had limitations due to the topographic nature of the surface being measured. For example the grid scanning technique applied to the paper mask (see Chapter seven) proved to be limited by the curvature of the mask. The curvature prevented the laser dot from being visible in all three images on the periphery of the grid i.e. the topography of the mask caused the dot to become occluded by features on the mask.

The application of a rotated scanning technique to measure the mask (as used for the mannequin head -see Chapter seven) would have reduced the number of occlusions and allowed more thorough measurement of the object.

The choice of scanning technique is dependent upon the topographic nature of the object to be measured. Flat, relatively featureless objects are more suited to grid scanning, whereas objects with significant topography variations should be scanned with a rotation. In order to generate a surface of revolution it is necessary to rotate the object irrespective of the topographic nature of the object. A guideline, or automatic selection, based on object topography to determine the scanning method used for different objects is recommended.

6. Automatic Calibration.

The calibration of the *MILLMAP* system is semi-automatic, with the operator required to identify the positions of 8 control points on the calibration frame prior to calibration. Once 8 control points have been identified the remaining control points are automatically identified using the provisional DLT and the bundle adjustment proceeds. The *MILLMAP* system used a control frame that could be removed between the measurement of objects. If the camera positions were adjusted, or disturbed,

the frame was repositioned and the cameras re-calibrated. The semi-automatic recalibration of the cameras for each object limits the automation of the system.

It is recommended that the camera positions should be fixed and the location of the control frame in the object space constrained to fit in the same position for calibration. The camera and control frame positions will vary slightly due to the effects of temperature on the mountings and re-calibration will still be necessary. Provided that the camera and control frame positions can be fixed with accuracy of approximately 0.5mm, the images captured from the cameras of the control frame will have the control points located in approximately the same region of the image for successive calibration. Initial knowledge of the approximate image positions of the control points cane be used to completely automate the calibration procedure. It is recommended that a window for the position of each control point in the image (as viewed from the different cameras) is stored so that automatic identification and processing of the control points can be made. The automatic calibration of the cameras will assist the overall automation of the device which is highly desirable for industrial applications.

7. Automatic Path preparation for Discontinuous objects.

Practical experience showed that the method used to define the grid path for a discontinuous test object (outboard motor propeller -see Chapter five) was time consuming and required significant operator assistance. The need to automate this aspect of the *MILLMAP* system is highly recommended.

It is recommended that some form of edge detection be used to define the edge of the object automatically. The machine co-ordinates describing this edge must be derived from the image co-ordinates (a projective transformation is recommended to achieve this). A grid of specified resolution should then be automatically fitted to the object outline, without operator assistance. By automating the procedure described, the *MILLMAP* system will become a more robust, automated machine suitable for industrial applications.

8. Light Conditions.

The *MILLMAP* system designed operates in a darkened environment to aid in the reduction of noise, which contaminates the images complicating the identification the laser dot difficult in the images. More robust image processing routines to identify the laser dot are recommended. Alternatively a more distinct method to project a target onto the object, increasing the contrast between target and object, is recommended.

The reflective properties with regards to the surface of the measurement object created noise in some test cases, which contaminated images preventing recognition of the laser dot. It is recommended that a suitable target projection method be investigated to minimise the reflectance of the target on the measurement object's surface.

List of References

Åmdal, K. 1992. Single Camera System For Close Range Industrial Photogrammetry. *International Archives of Photogrammetry and Remote Sensing* Vol 29. No. 5. Washington DC. p.6-10.

Beyer, H..A. 1990. Calibration of CCD Cameras for Machine Vision Robotics. *Society of Photo-Optical Instrumentation Engineers.* Vol 1197. Automated Inspection and High Speed Architectures III(1990) p88-98.

Brown, D.C. 1971 Close Range camera Calibration. *Photogrammetric Engineering.* Vol. 37. No. 8. p.855-866.

Computer Graphics. 1995(a). Vol 6. No. 4. June 1995. Technique Publishers. Natal.

Computer Graphics. 1995(b). Vol 6. No. 5. July 1995. Technique Publishers. Natal.

Claus, M. 1988 Experience with InduSURF in 3D Measurement of Industrial Surfaces. *International Archives of Photogrammetry and Remote Sensing.* Vol. 27. part B5. Kyoto. p.119-129.

El-Hakim, S.F. 1985 A Photogrammetric Vision System for robots. *Photogrammetric Engineering and Remote Sensing.* Vol. 51. no 4. May 1985. p. 545-552.

El-Hakim, S.F. 1986. Real-Time Image Metrology with CCD Cameras. *Photogrammetric Engineering and Remote Sensing.* Vol. 52 no.11. November. p.1757-1766.

El-Hakim, S.F. and Barakat, M.A. 1989. A Vision - Based Co-ordinate Measuring Machine. *Optical 3-D Measurement Techniques Conference.* Vienna. p.216-228.

Forstner, W. and Gluch, E. 1987 A Fast Operator for Detection and Precise Location of Distinct Points, Corners and Centres of Circular Features. *ISPRS Intercommission Workshop.* Interlaken. p.281-305.

Frobin, W and Heirholzer, E 1982(a). Calibration and model Reconstruction in Analytical Close Range Stereophotogrammetry. Part I : Mathematical Fundamentals. *Photogrammetric Engineering and Remote Sensing.* Vol. 48 no.1 January. p.67-72.

Frobin, W and Heirholzer, E 1982(b). Calibration and model Reconstruction in Analytical Close Range Stereophotogrammetry. Part II : Special Evaluation Procedures for Rasterography and Moiré Topography. *Photogrammetric Engineering and Remote Sensing*. Vol. 48 no.2. February 1982. p.215-220.

Frobin, W. and Hierholzer, E 1983(a). Automatic Measurement of Body Surfaces Using Rastereography. Part I: Image Scan and Control Point Measurement. *Photogrammetric Engineering and Remote Sensing*. Vol. 49 no.3. March 1983. p377-384.

Frobin, W. and Hierholzer, E 1983(b). Automatic Measurement of Body Surfaces Using Rastereography. Part II: Analysis of the Rastereographic Line Pattern and 3D surface reconstruction. *Photogrammetric Engineering and Remote Sensing*. Vol. 49 no.10. October 1983. p. 1443-1452.

Godber, S.X. Robinson, M. Evans, P. 1992 Stereoscopic Vision using Line-Scan Sensors. *International Archives of Photogrammetry and Remote Sensing*. Vol 29. No. 5. Washington DC. p.618-627.

Godding, R and Luhmann, T. 1992. Calibration and Accuracy Assessment of a Multi-Sensor Online Photogrammetric system. *International Archives of Photogrammetry and Remote Sensing*. Vol 29. No. 5. Washington DC. p.24-29.

Gold, J. 1991. Programming of co-ordinate measuring machines in conjunction with CAD systems. *Carl Zeiss Industrial Metrology*. West Germany.

Gruen, A.W. and Baltsavias, E.P. 1988(a) Automatic 3-D Measurement of human faces with CCD cameras. *SPIE Vol.1030 Biostereometrics. Fifth International Meeting*. Basel, Switzerland.p.106-116.

Gruen, A.W. and Baltsavias, E.P. 1988(b) Geometrically Constrained Multiphoto Matching. *Photogrammetry Engineering and Remote Sensing*. Vol.54. no.5. May 1988. p.633-641.

Haggren, H. 1986 Real-Time Photogrammetry as Used For Machine Vision Applications. *International Archives of Photogrammetry and Remote Sensing*.Vol 26 No. 5. Ottawa. p.374-382.

Haralick R.M and Shapiro L.G. 1992. Computer And Robot Vision. *Addison-Wesley Publishing Company, Inc*. Volume I and II.

Hartl, Ph. , Wehr, A. , Pritschow, G. , Ioannides M. 1992 — 4D - Laser Scanning Followed by Internal Computer Model Generation. *International Archives of Photogrammetry and Remote Sensing* . Vol 29 Part 5. Washington D.C. p.522-527.

Herzog, K, 1982. — Zeiss Multi-Coordinate Metrology Hardware - Software - Application. *Carl Zeiss Technical Information pamphlet.* West Germany.

Karara, H.M. 1989. — Non-Topographic Photogrammetry (2ND ED). *American Society for Photogrammetry and Remote Sensing.* Virginia .

Keefe, M , Riley, D.R. 1986. — Capturing Facial Surface Information. *Photogrammetric Engineering and Remote Sensing.* Vol 52. no 9. September 1986. pp1539-1548.

Kreon Industrie. 1995. — All you need to Know About Kreon® Reverse Engineering System. *Kreon Industrie Customer Information.* Document supplied by Machine Tool Technologies. Jeppestown.

Loser, R and Luhmann, T. 1992. — The Programmable Optical 3D Masuring System POM - Applications and Performance. *International Archives of Photogrammetry and Remote Sensing.* Vol 29. No. 5. Washington DC. p.533-540.

Mason, S.O. 1994 — Expert System-Based Design of Photogrammetric Networks. *Institue for Geodesy and Photogrammetry. Swiss Federal Institute of Technology (ETH)*

McMahon, C & Browne, J. 1993. — *CADCAM - From principles to practice.* Addison-Wesley Publishing Company, INC.

Neumann, H. J., 1985. — Accuracy Specifications of Rotary Tables and particulars on their use on Coordinate Measurement Machines. *Carl Zeiss Technical Information pamphlet.* West Germany.

Parbhoo, P, 1995. — Automated Non-contact surface Mapping. Unpublished Bsc. Thesis. *Department of Mechanical Engineering.* University of Cape Town.

Petterson, A. 1992(a). — Metrology Norway System - An On-line Industrial Photogrammetric system. *International Archives of Photogrammetry and Remote Sensing.* Vol 29. No. 5. Washington DC. p.43-49.

Petterson, A. 1992(b). — Metrology Norway System - Optimum Accuracy Based on CCD Cameras. *International Archives of Photogrammetry and Remote Sensing.* Vol 29. No. 5. Washington DC. p.230- 233.

Rubinstein, M.1990. Assessing target Centering Algorithms For use in Near-Real-Time Photogrammetry. Unpublished Msc. Thesis. *Department of Surveying and Geodetic Engineering*. University of Cape Town.

Rüther, H. 1989. Near-Real-Time Photogrammetry on a Personal Computer. presented paper no. 3-2. *CONSAS*. Cape Town.

Rüther, H. 1991. Digital Photogrammetry - Introduction to a new tool for the Photogrammetrist.. ISPRS workshop. V/4 Pretoria.

Slama, C. 1980. Manual of Photogrammetry. *American Society for Photogrammetry and Semote Sensing*. fourth edition.

van der Merwe, N. 1995. Developement of an image matching software scheme using feature and area based matching techniques. Unpublished PhD. Thesis. *Department of Surveying and Geodetic Engineering*. University of Cape Town.

van der Vlught, G,and Rüther , H 1992. DIMS ©. *Image processing Software*. *Department of Surveying and Geodetic Engineering*. University of Cape Town.

van der Vlught, G, 1994. PHOTONET ©. *Bundle Adjustment Software*. *Department of Surveying and Geodetic Engineering*. University of Cape Town.

van der Vlught, G and Rüther, H, 1994 The developement of an automated surface measurement system. *International Archives of Photogrammetry and Remote Sensing*.Vol 30. No. 5. Melbourne. p.414-419.

van Niekerk, B, 1995. 3D CAD Models and Concurrent Engineering. *The South African Mecchanical Engineer. Vol 45.* November/December.

Wildschek, R. 1989. Surface Capture using Near real time photogrammetry for a computer numerically controlled milling system. Unpublished Msc. Thesis. *Department of Surveying and Geodetic Engineering*. University of Cape Town.

Wong, K.W. , Ho, W.H. 1986 Close range mapping with a solid state camera . *Photogrammetry Engineering and remote sensing*. Vol 52.no.1. January. pp.67-74.

Xue, R.G. 1992 The Image Processing for the Target Center Detection in Digital Image. Unpublished Msc. Thesis. *Department of Surveying and Geodetic Engineering*. University of Cape Town

Zeiss. 1982. Fundamental System of Zeiss CNC Multi-Coordinate Measuring Machines *Carl Zeiss Technical Information pamphlet.* West Germany.

Zeiss, 1985. Optical Probing System with Digital Image Analysis. *Carl Zeiss Product Information.* West Germany.

Zeiss, 1990(a). PSM Precision Cantilever Measuring Machines. *Carl Zeiss Product Information.* West Germany.

Zeiss, 1990(b). Coordinate Metrology - Technology and Application. *Carl Zeiss Industrial Metrology.* West Germany.

Zeiss, 1994. QUANTUM : Interactive Graphical Programming System *Carl Zeiss Industrial Metrology.* West Germany.

Zeiss, 1995. Probe Kits for CMMs with Central Dynamic Probe Head or Measuring Probe Head. *Specifications Carl Zeiss Industrial Metrology.* West Germany.